Transformations of Carboxylic Acids Derivatives Using Heterogenous Acid-base Catalysts

Md. Nurnobi Rashed

2019

Graduate School of Chemical Sciences and Engineering

Hokkaido University

Contents

Chapter 1. General Introduction

1.1 Heterogenous catalytic reactions for green chemical synthesis 2

1.2 Lewis acid-base catalyzed conversion of carboxylic acid derivatives 2

1.3 Challenges in transformations of carboxylic acids and amides 3

1.3.1 Reactivity trends of acid derivatives 3

1.3.2 Difficulties in Lewis acid catalyzed transformation of acid derivatives in presence of hard bases 4

1.3.3 Difficulties in Lewis acid catalysed transformations of amides 5

1.4 Aim of this thesis 5

1.4.1 Development of water and base tolerant Lewis acid catalyst for framework 1 6

1.4.2 Development of CeO_2 Lewis acid-base catalysis for framework 2 6

1.5 Outline of thesis 7

1.6 Concluding remarks 9

References 9

Chapter 2. Heterogeneous Catalysts for the Cyclization of Dicarboxylic Acids to Cyclic Anhydrides as Monomers for Bioplastic Production

2.1 Introduction 13

2.2 Experimental 14

2.3 Results and discussions 16

2.3.1 Catalysts screening 16

2.3.2 Pyridine adsorption on different Nb_2O_5 catalysts 18

2.3.3 Optimization of reaction's parameters 19

2.3.4 Water tolerant Nb_2O_5 catalyst 20

2.3.5 Investigation of heterogenous nature of $Nb_2O_5.nH_2O$ catalyst 21

2.3.6 Gram scale synthesis of anhydrides 22

2.3.7 NMR data of final products 23

2.4 Conclusion 24

References 25

Chapter 3. Hydrolysis of Amides and Amidation of Carboxylic Acids by Nb_2O_5 Catalyst: Insights into the Structure-activity Relationships

3.1 Introduction 28

3.2 Experimental section 29

3.3 Results and discussions 31
3.3.1 Catalyst and reaction conditions optimization for hydrolysis reaction 31
3.3.2 Characterization of surface structure and acidity of Nb_2O_5 catalysts 34
3.3.3 Correlation studies between crystallinity structure and acidity in hydrolysis of amides 36
3.3.4 Correlation between different Nb_2O_5 crystalline structure (Phases) and their activity on hydrolysis reaction 37
3.3.5 Catalytic properties and scopes of hydrolysis reaction 38
3.3.6 Catalyst and reaction conditions optimization for amidation reaction 43
3.3.7 Correlation between structure and acidity of Nb_2O_5 catalysts on amidation reaction 44
3.3.8 Catalytic properties and scopes of amidation reaction 46
3.3.9 NMR and GC/MS analysis of final products 47
3.4 Conclusion 55
References 56

Chapter 4. Esterification of Tertiary Amides by Alcohols Through C–N Bond Cleavage over CeO_2
4.1 Introduction 61
4.2 Experimental 62
4.3 Results and Discussion 65
4.3.1 Catalysts design and screening 65
4.3.2 Optimization of reaction conditions 67
4.3.3 Recycling and leaching studies of CeO_2 catalyst 68
4.3.4 Mechanistic study of alcoholysis reaction 70
4.3.5 Scopes of catalytic system 79
4.3.5 GC-MS and NMR data of products 81
4.4 Conclusion 91
References 91

Chapter 5. Direct Phenolysis Reactions of Unactivated Amides into Phenolic Esters Promoted by a Heterogeneous CeO_2 Catalyst
5.1 Introduction 97
5.2 Experimental section 99
5.3 Results and discussion 101
5.3.1 Optimization of the catalysts and reaction conditions 101
5.3.2 CeO_2 catalyzed phenolysis of amides with phenols into esters 104
5.4 Mechanistic Pathway 112

5.4.1 Effect of calcination temperature of CeO_2 catalysis 112
5.4.2 FT-IR and Kinetic studies 113
5.4.3. Plausive reaction mechanism 116
5.4.5 GC-MS and NMR analysis of reactants and products 117
5.5 Conclusions 130
References 130

Chapter 6. General Conclusions 135

Acknowledgements

Chapter 1

General Introduction

1. General Introduction

1.1 Heterogenous catalytic reactions for green chemical synthesis

To achieve alternative cleaner, environmentally friendly and sustainable processes, heterogenous catalysis is one of the priorities in chemistry.[1,2] With this objective, a standard modification is important from conventional methodologies that focus largely on chemical yield of process efficiency to one that allocates economic value to eliminating waste at source and avoiding the use of toxic and/or hazardous substances. Therefore, the use of renewable feedstocks with one-pot synthetic procedures involving single and/or multiple catalytic events permits the decrease of energy consuming steps such as separation and purification of intermediates.[3] There are various heterogenous one pot synthetic methods for green chemical synthesis. Acceptorless dehydrogenative coupling, borrowing hydrogen or hydrogen autotransfer, reductive hydrogenation, Lewis acid-base catalysis, Bronsted acid catalysis etc. are significant strategies which have been focused through the recent studies.

1.2 Lewis acid-base catalyzed conversion of carboxylic acid derivatives

Lewis acids function as catalyst which has been attracted much attention in various organic transformations[4–6] For example, hydration of alkene,[7,8] nitriles and epoxides; dehydrative condensation of alcohols and polyols;[9,10] alkylation reactions,[11] selective oxidation of hydrocarbon, amines and alcohols;[12,13] nucleophilic substitution of carboxylic acids and derivatives etc.[14–17] Therefore, numerous chemical industries are utilizing various kinds of Lewis acids to produce value-added chemicals. As the carboxyl group (-CO_2H or -COOH) is one of the most abundant functional groups in nature and they constitute the diversity in chemical compounds with versatile applications,[18–23] hence, the transformation of carboxylic acid derivatives to important chemicals using heterogenous Lewis acid-base catalysis would be a substantial area of research interest.

1.2.1 Introduction to Carboxylic acid derivatives

Carboxylic acid is an organic acid which possess the functional group (–COOH). It is analogous to the –OH functional group of alcohols and carbonyl bond (C═O) of aldehydes and ketones but entirely different in physical and chemical nature.

Carboxylic acid derivatives are the compounds in which the –OH of the carboxyl group is replaced by certain other groups. The most important of which are carboxylic acid anhydrides,

esters, amides and nitriles. They can be converted into carboxylic acids via simple acidic or basic hydrolysis.

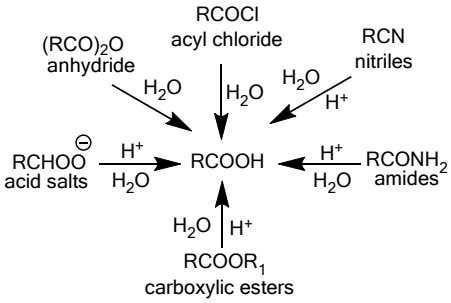

Scheme 1.1: Synthesis of carboxylic acids from its derivatives

Some important structures of acid derivatives are shown below-

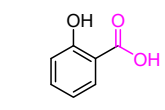

Salicylic acid
(Treatment of warts, acne, ichthyosis)

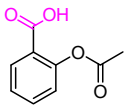

Aspirin
(NSAIDs and stroke)

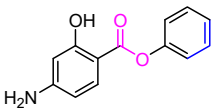

Phenyl-4-aminosalicylatesalicylate
(Tuberculosis)

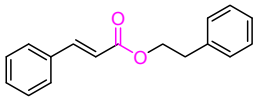

Phenethyl caffeate
(Anti-inflammatory)

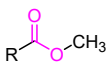

Methyl esters
(Biodiesel)

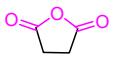

Succinic anhydride
(Monomer of bio-degradable polyesters)

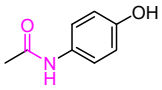

Paracetamol
(Pain & fever treatment)

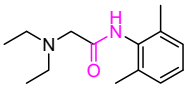

Lidocane
(Local anesthetic)

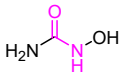

Hydroxycarbamide
(Cervical cancer, chronic myelogenous leukomia)

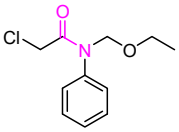

Ethachlor
(Herbicide)

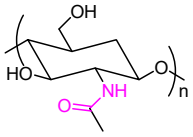

Chitin
(Natural polysaccharide derivatives)

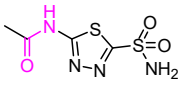

Acetazolamide
(Acute glucoma and heart treatment)

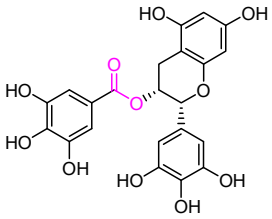

Epigallocatechin gallate (ECGC)
(Active ingrediant in green tea)

Scheme 1.2: Some important structures of carboxylic acid derivatives

1.3 Challenges in transformations of carboxylic acids and amides

1.3.1 Reactivity trends of acid derivatives

The relative reactivity of carboxylic acid derivatives toward nucleophile substitutions is related to the electronegative leaving group's ability to activate the carbonyl. The more electronegative leaving groups withdrawn electron density from the carbonyl, thereby, increasing its electrophilicity. In general, more reactive acid derivatives are converted into less reactive acid derivatives. So, this requires an understanding of which derivatives are more reactive than others.

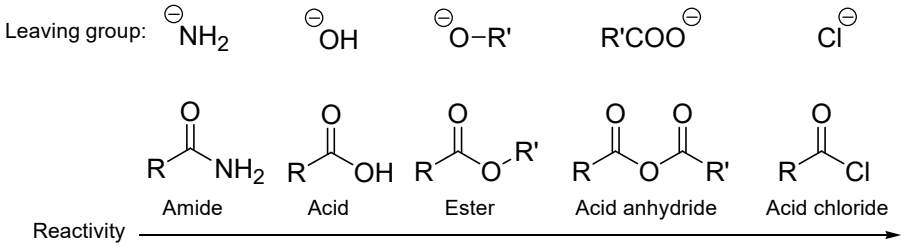

Scheme 1.3: Reactivity trends of acid derivatives towards substitution reactions

Moreover, another difficult challenge is the thermodynamic stability issue. The carboxylic groups in carboxylic acids and amides are stabilized via to resonance stabilization. They do not show the characteristic reactions of carbonyl (C=O) group as because the lone pair of electrons on oxygen and nitrogen atoms involves in delocalization into O-C-O and O-C-N bonds respectively.[24] Therefore, they are known as the least weak electrophile and it's very difficult to break down C-O and C-N bonds selectively. Hence, it requires harsh reaction conditions to transform carboxylic acids and amides.

1.3.2 Difficulties in Lewis acid catalyzed transformation of acid derivatives in presence of hard bases

It has been reported that catalysts having Lewis (LA) and/or Brønsted acid (BA) sites play key role to activate oxygen-containing functional group such as carbonyl group in carboxylic acids derivatives.[6] However, to use of conventional Lewis acids (e.g. $AlCl_3$, BF_3) catalysts, it must be used under strictly in absence of hard bases (water, amines, ammonia etc.).[25] Because, the presence of even a small amount of water and/or amines may stops the reactions. The reason of deactivation of Lewis acidity by hard bases is due to the strong co-ordination of hard bases with Lewis acidic metal centers,[16]which may prevent active sites to attack the substrates molecules.

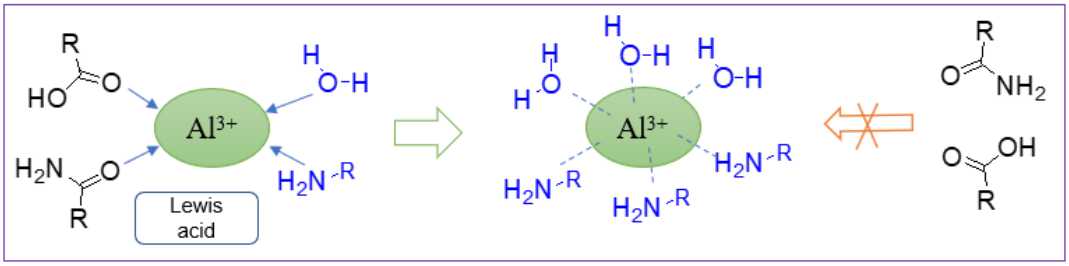

Scheme 1.4: Conventional Lewis acid deactivation in presence of hard bases

Moreover, recovery and reuse of the conventional Lewis acids are also challenging tasks. These disadvantages have restricted the use of Lewis acids in organic synthesis. Consequently, heterogeneous Lewis acid-base catalysts that are insoluble, easily separable from products, and

highly active in water as well as hard bases would be applicable for environmentally benign chemical production.

1.3.3 Difficulties in Lewis acid catalysed transformations of amides

Amides are the most stable carboxylic acid derivatives and thus requires harsh reaction conditions such as heating under strongly acidic and basic conditions or highly evolved enzymes to cleave C–N bonds.[26] The high stability and relative inertness of the amide structure across the N–C–O bond contributes this stability, having a large degree of co-planarity across the bond, allowing resonance stabilization which creates a partial double bond character.[27]

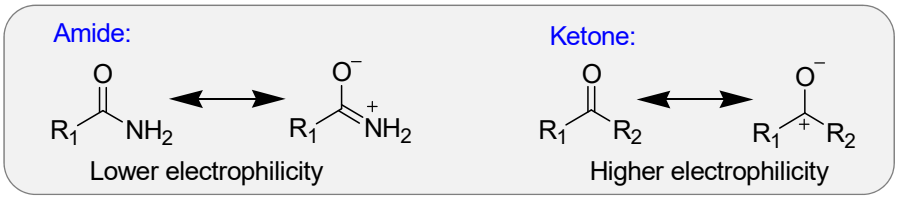

Scheme 1.5: Resonance stabilization of amide bonds

However, truly Lewis acid catalysts may not exhibit enough activity for conversion of amides through activation of C=O bonds followed by breaking of C–N bond. Hence, Lewis acid-base catalysts having balanced acid-base catalytic property is simultaneously important to overcome these problems. Therefore, an additive free and heterogenous acid-base catalytic system is aimed but challenging.

1.4 Aim of this thesis

This thesis focuses on two frameworks:

1. Development of heterogenous Lewis acid catalysts for three different transformations of carboxylic acid derivatives (acids and amides) in presence of hard bases H_2O and NH_3
   - ✓ Cyclization of dicarboxylic acids to cyclic anhydrides
   - ✓ Hydrolysis of amides to carboxylic acids
   - ✓ Amidation of carboxylic acids with NH_3 to amides
2. Development of heterogenous Lewis acid-base catalysts and investigation of acid-base co-operative mechanism in two esterification reactions of most stable carboxylic acid derivatives i.e. amides-
   - ✓ Alcoholysis of tertiary unactivated amides to alcoholic esters

✓ Phenolysis of unactivated amides to phenolic esters

1.4.1 Development of water and base tolerant Lewis acid catalyst for framework 1.

The concept of water tolerant Lewis acid catalysts first reported by Kobayashi and co-workers.[28] He showed that $Sc(OTf)_3$, $Y(OTf)_3$, $Ln(OTf)_3$ and $Yb(OTf)_3$ can act as homogenous Lewis acid catalyst in water-containing solvents. Later, $Nb_2O_5.nH_2O$ is reported as water tolerant heterogenous Lewis acid catalysts for various reactions.[6,14] It has been revealed by Prof Hara and co-workers[25] that coordinatively unsaturated Nb^{5+} can activate oxygen-containing functional group of substrates even in presence of hard bases like as water or amines. Recent studies of our research group have been demonstrated that Nb_2O_5 acts as a water and base tolerant Lewis acid catalyst[6,14] for various amidation reactions of carboxylic acids, anhydrides and esters in presence of various amines.

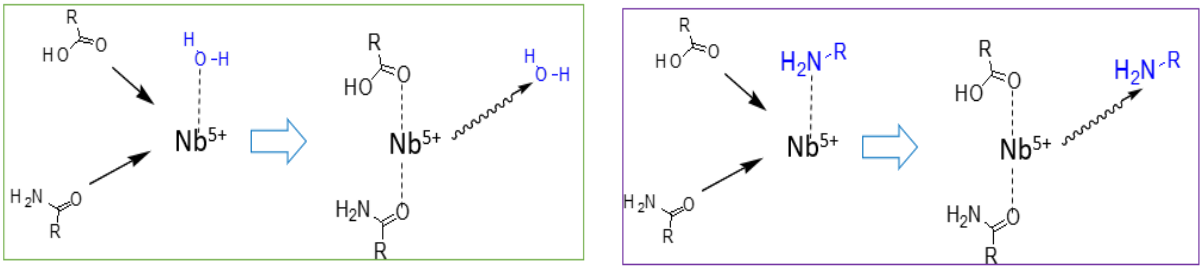

Scheme 1.6: Water tolerant (left side) and base tolerant (right side) Nb_2O_5 catalysts[14]

Therefore, to utilize this concept of acid and base tolerant $Nb_2O_5.nH_2O$ and Nb_2O_5 catalysis, some other type of reactions like as dehydration/condensation, hydrolysis and amidation reactions are explored. Similarly, structure and activity relationship of Nb_2O_5 catalysis have been done to have a rational design of Nb-based metal oxide catalysts for various reactions.

1.4.2 Development of CeO_2 Lewis acid-base catalysis for framework 2

There has been a long-standing challenge in solvolysis reaction of the most thermodynamically stable amide's C–N bond. Recently, catalytic amide C–N bond activation via deconstruction of amides has been performed using Ni and Pd catalysts.[26,29] However, these homogenous catalytic systems can activate only *N*-activated (*N*-Boc, Ts etc.) tertiary amides in presence of stoichiometric amount of ligands.

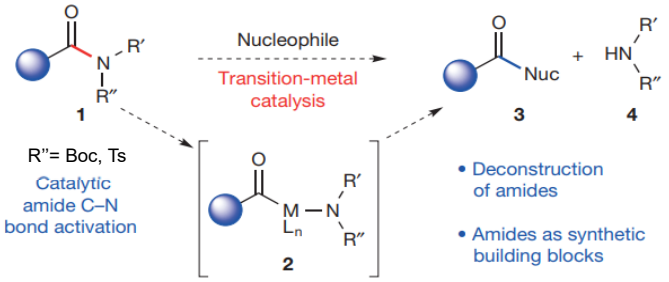

Scheme 1.7: Amide C–N bonds activation by transition metal catalysis[26]

In contrast, CeO_2 has been reported as heterogenous acid-base catalyst for various transformation of amides.[30–32]Therefore, the author hypothesized the utilization of CeO_2 acid-base property in much more challenging reactions for esterification reaction of unactivated tertiary amides with alcohols and phenolysis reaction of unactivated amides.

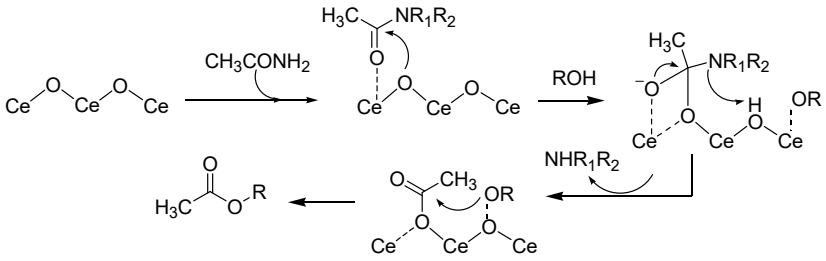

Scheme 1.8: CeO_2 Lewis acid-base catalytic interplay for direct activation and conversion of amides[33]

1.5 Outline of thesis

This thesis efforts on direct transformation of carboxylic acid derivatives (acid and amides) by using two heterogeneous catalysts 1) water and base tolerant different Nb_2O_5 catalysts and 2) Lewis acid-base CeO_2 catalyst. Five types of reaction systems are developed for transformation of acid derivatives with a wide substrate scope.

Chapter 2 presents a development of heterogeneous Lewis acid catalyst for direct intramolecular dehydration of dicarboxylic acids, which has been unprecedented previously by conventional heterogeneous catalysts. I screened various water tolerant heterogeneous and homogeneous catalysts for this cyclization reaction. The result showed that a commercial niobic acid, $Nb_2O_5{\cdot}nH_2O$, gave the highest yield of the corresponding cyclic anhydride. Various dicarboxylic acids, which can be produced from biorefinery process, are transformed to the corresponding cyclic anhydrides as monomers for polyesters. The proposed catalytic system was applicable for gram-scale synthesis of anhydrides up to 96% isolated yields. Moreover, catalyst reusability and leaching study indicate that $Nb_2O_5{\cdot}nH_2O$ possesses high durability for

the reaction. In industry, cyclic anhydrides, as key intermediates of carbon-neutral and biodegradable polyesters, are currently produced from biomass-derived dicarboxylic acids by a high-cost multistep process. The simple synthetic method of cyclic anhydride developed in this work can simplify the current high-cost synthetic route to renewable polyesters.

Chapter 3 highlights the structure-activity relationship of Nb_2O_5 catalysis for two challenging reactions:1) hydrolysis of amides to carboxylic acids and 2) amidation of carboxylic acids with NH_3. The number of Lewis acid (LA) sites of Nb_2O_5 catalysts and interaction between LA sites and carbonyl group of amides decreased with the calcination temperature. Low temperature calcined Nb_2O_5 (TT and/or T-Nb_2O_5 phases) were more reactive than that of high temperature calcined M- and/or H-Nb_2O_5 phases. The catalytic performance is attributed to the preferential activation of carbonyl group (soft base) by surface Nb(V) LA sites even in presence of hard bases (H_2O and NH_3). Detailed structure-activity relationship investigation for the present reactions was performed toward a rational design of catalysts.

Chapter 4 shows that CeO_2 catalyzes esterification reaction of tertiary amides by alcohols, which has been unprecedented previously by conventional heterogeneous catalysts. CeO_2 was found to promote ester forming alcoholysis reactions via direct cleavage of amide's C–N bonds. The catalytic method was operationally simple, recyclable, and it did not require any additives. *In situ* FT-IR and temperature programmed desorption using probe molecules demonstrated that both acidic and basic sites of CeO_2 were important for the reaction. Based on DFT and in situ FT-IR studies, I propose a possible reaction mechanism, in which nucleophilic attack of surface oxygen of CeO_2 to the carbonyl group of the acetamide adsorbed on Ce (IV) LA site is the rate limiting step.

Chapter 5 describes that more challenging reaction, phenolysis of amides, can be achieved by CeO_2. Catalyst screening study showed that CeO_2 was the best catalyst for the reaction. Various functionalized amides and phenols were converted to the corresponding phenolic esters. Results of kinetic studies afforded mechanistic insights; the cooperation of the acid-base functions of the CeO_2 catalyst is of importance for the efficient progression of the C–N bond breaking process. Consequently, CeO_2 showed the best catalytic performance among the catalysts explored.

Chapter 6 demonstrates general conclusions of the thesis. Chapters 2, 3 conclude that a solid Lewis acid, Nb_2O_5, effectively catalyzes three challenging reactions of carboxyl acids derivatives: 1) direct intramolecular dehydration of dicarboxylic acids, 2) hydrolysis of amides to carboxylic acids, 3) amidation of carboxylic acids with NH_3. The key feature in these catalytic systems is the activation of carbonyl group (soft base) even in presence of hard bases

(H_2O and NH_3). Chapters 4, 5 conclude that CeO_2 promotes two catalytic transformation of amides, 1) esterification reaction of tertiary amides by alcohols and 2) phenolysis of amides, which have been unprecedented by previous heterogeneous catalysts. The key feature in these catalytic systems is cooperation of Ce (IV) Lewis acid sites (for coordination of carbonyl oxygen) and adjacent basic oxygen (nucleophilic oxygen).

1.6 Concluding remarks

I have developed Nb-based oxide catalysts for direct transformation of carboxylic acids and amides which is effective even in presence of hard bases (NH_3 and H_2O) in the reaction mixtures. The transformations are 1) $Nb_2O_5{\cdot}nH_2O$ catalyzed cyclization of dicarboxylic acids to cyclic anhydrides; 2) Nb_2O_5 catalyzed hydrolysis of amides and amidation of carboxylic acids with NH_3. Similarly, structure and activity relationship has also been revealed for later reactions. Furthermore, CeO_2 acid-base catalysis has been established for the two different types of transformations of most stable acid derivatives, amides into a) alcoholic and b) phenolic esters. Here, the catalytic interplay of Lewis acid-base sites of CeO_2 catalyst is being found as the key controller of these reactions.

References

[1] I. T. Horváth, P. T. Anastas, *Chem. Rev.* **2007**, *107*, 2169–2173.

[2] M. J. Climent, A. Corma, S. Iborra, *Chem. Rev.* **2011**, *111*, 1072–1133.

[3] I. Arends, R. Sheldon, U. Hanefeld, *Green Chemistry and Catalysis*, **2007**.

[4] A. G. Davies, *Appl. Organomet. Chem.* **2002**, *16*, 65–65.

[5] S. Kobayashi, *European J. Org. Chem.* **1999**, *1999*, 15–27.

[6] S. M. A. H. Siddiki, M. N. Rashed, M. A. Ali, T. Toyao, P. Hirunsit, M. Ehara, K. Shimizu, *ChemCatChem* **2019**, *11*, 383–396.

[7] A. J. M. Van Dijk, R. Duchateau, E. J. M. Hensen, J. Meuldijk, C. E. Koning, *Chem. - A Eur. J.* **2007**, *13*, 7673–7681.

[8] S. Okazaki, H. Harada, *Chem. Lett.* **1988**, *17*, 1313–1316.

[9] Q. Sun, Y. Fu, H. Yang, A. Auroux, J. Shen, *J. Mol. Catal. A Chem.* **2007**, *275*, 183–193.

[10] A. Takagaki, D. Lu, J. N. Kondo, M. Hara, S. Hayashi, K. Domen, *Chem. Mater.* **2005**, *17*, 2487–2489.

[11] K. Nakajima, T. Fukui, H. Kato, M. Kitano, J. N. Kondo, S. Hayashi, M. Hara, *Chem. Mater.* **2010**, *22*, 3332–3339.

[12] S. Furukawa, Y. Ohno, T. Shishido, K. Teramura, T. Tanaka, *ACS Catal.* **2011**, *1*, 1150–

1153.

[13] S. Furukawa, T. Shishido, K. Teramura, T. Tanaka, *ChemPhysChem* **2014**, *15*, 2665–2667.

[14] M. A. Ali, S. M. A. H. Siddiki, W. Onodera, K. Kon, K. Shimizu, *ChemCatChem* **2015**, *7*, 3555–3561.

[15] S. Paul, Y. Zhu, C. Romain, R. Brooks, P. K. Saini, C. K. Williams, *Chem. Commun.* **2015**, *51*, 6459–6479.

[16] P. Hirunsit, T. Toyao, S. M. A. H. Siddiki, K. Shimizu, M. Ehara, *ChemPhysChem* **2018**, *19*, 2848–2857.

[17] M. N. Rashed, S. M. A. H. Siddiki, M. A. Ali, S. K. Moromi, A. S. Touchy, K. Kon, T. Toyao, K. Shimizu, *Green Chem.* **2017**, *19*, 3238–3242.

[18] K. Subramanian, S. L. Yedage, B. M. Bhanage, *Adv. Synth. Catal.* **2018**, *360*, 2511–2521.

[19] Y. Tu, L. Yuan, T. Wang, C. Wang, J. Ke, J. Zhao, *J. Org. Chem.* **2017**, *82*, 4970–4976.

[20] T. Deguchi, H.-L. Xin, H. Morimoto, T. Ohshima, *ACS Catal.* **2017**, *7*, 3157–3161.

[21] P. Gautam, P. Kathe, B. M. Bhanage, *Green Chem.* **2017**, *19*, 823–830.

[22] S. D. Roughley, A. M. Jordan, *J. Med. Chem.* **2011**, *54*, 3451–3479.

[23] D. J. C. Constable, P. J. Dunn, J. D. Hayler, G. R. Humphrey, J. L. Leazer, Jr., R. J. Linderman, K. Lorenz, J. Manley, B. A. Pearlman, A. Wells, et al., *Green Chem.* **2007**, *9*, 411–420.

[24] T. Kamachi, S. M. A. H. Siddiki, Y. Morita, M. N. Rashed, K. Kon, T. Toyao, K. Shimizu, K. Yoshizawa, *Catal. Today* **2018**, *303*, 256–262.

[25] K. Nakajima, Y. Baba, R. Noma, M. Kitano, J. N. Kondo, S. Hayashi, M. Hara, *J. Am. Chem. Soc.* **2011**, *133*, 4224–4227.

[26] L. Hie, N. F. Fine Nathel, T. K. Shah, E. L. Baker, X. Hong, Y.-F. Yang, P. Liu, K. N. Houk, N. K. Garg, *Nature* **2015**, *524*, 79–83.

[27] J. I. Mujika, J. M. Mercero, X. Lopez, *J. Am. Chem. Soc.* **2005**, *127*, 4445–4453.

[28] S. Kobayashi, K. Manabe, *Acc. Chem. Res.* **2002**, *35*, 209–217.

[29] G. Meng, P. Lei, M. Szostak, *Org. Lett.* **2017**, *19*, 2158–2161.

[30] M. Tamura, K. Shimizu, A. Satsuma, *Chem. Lett.* **2012**, *41*, 1397–1405.

[31] S. M. A. H. Siddiki, A. S. Touchy, M. Tamura, K. Shimizu, *RSC Adv.* **2014**, *4*, 35803–35807.

[32] T. Toyao, M. Nurnobi Rashed, Y. Morita, T. Kamachi, S. M. A. Hakim Siddiki, M. A. Ali, A. S. Touchy, K. Kon, Z. Maeno, K. Yoshizawa, et al., *ChemCatChem* **2019**, *11*, 449–456.

[33] T. Kamachi, S. M. A. H. Siddiki, Y. Morita, M. N. Rashed, K. Kon, T. Toyao, K. Shimizu, K. Yoshizawa, *Catal. Today* **2018**, *303*, 256–262.

Chapter 2

Heterogeneous catalysts for the cyclization of dicarboxylic acids to cyclic anhydrides as monomers for bioplastic production

2.1 Introduction

There is a growing demand to develop a new methodology for substitution of petroleum refinery to biorefinery, that is, production of chemicals with carbon-neutral and biorenewable resources.[1–8] To establish the biorefinery process, it is important to develop a new catalytic process for the selective transformation of biomass–derived feedstocks to platform chemicals. Dicarboxylic acids are regarded as one of the key platform chemicals, because they are available in a minimum number of steps from biorefinery carbohydrate streams.[2–9] For example, succinic acid is one of the top bioplatform chemicals as it is available from the bioconversion of glucose.[2,8,9] Recently, considerable progress has been achieved towards commercialization of fermentative production of succinic acid.[9] Among the derivatives of dicarboxylic acids, recent attentions have focused on cyclic anhydrides as monomers for the production of biorenewable aliphatic polyesters.[10] Aliphatic polyesters, which can be produced by ring-opening copolymerization of epoxides with cyclic anhydrides,[10–13] are important alternatives to petroleum-based polyesters, because they can be produced from renewable feedstocks and disposed of with minimal environmental impact.

The aromatic carboxylic dianhydrides are synthesized also by thermal dehydration of tetracarboxylic acids at extremely high reaction temperatures (220-270 °C),[14] which limits industrial application. Generally, cyclic anhydrides are prepared by dehydration of dicarboxylic acids with excess amount of dehydrating agents (**Scheme 1**) such as an acid chloride, benzenesulfonyl chloride, ketene, acetic anhydride and phosphorous pentoxide.[15,16]

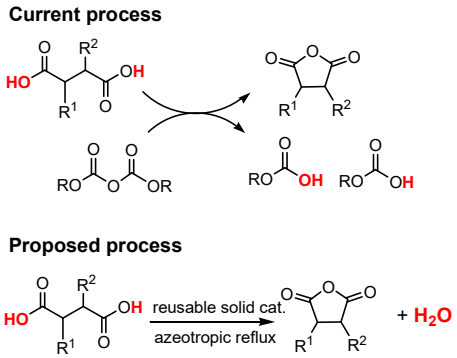

Scheme 2.1: Current and proposed process for production of cyclic anhydride from dicarboxylic acids.

The method suffers from the use of toxic reagents, limited scope, low atom-efficiency and difficulty in the complete removal of the dehydrating agent from the products. Recently, Thomas and co-workers[16] have reported direct high-yielding synthesis of cyclic anhydrides from dicarboxylic acids by small amount of $MgCl_2$ as Lewis acid catalyst at 40 °C without azeotropic reflux conditions. However, the method has low atom-efficiency requiring significant excess amount (50 equiv.) of di-tert-butyl dicarbonate as a dehydrating agent, which

suffers from co-production of large amount of wastes. Catalytic intramolecular condensation of dicarboxylic acids is the most atom-efficient route to cyclic anhydrides since it generates water as the only byproduct. However, to our knowledge, only one method by Ishihara et al.,[17,18] succeeded in the catalytic self-condensation of dicarboxylic acids under mild conditions. They have used a homogeneous catalyst, an arylboronic acid bearing two bulky (N,N-dialkylamino)methyl groups at the 2,6-positions, which has drawbacks of limited substrate scope and difficulties in the catalyst synthesis.

Potentially, the reaction is catalyzed by Lewis acid, but co-presence of water as byproduct can suppress Lewis acidity by hindering coordination. Inspired by recent reports that some homogeneous[19] and heterogeneous[20–22] Lewis acid catalysts act as water-tolerant Lewis acid catalysts, we have recently reported that Nb_2O_5 acts as a water- and base-tolerant Lewis acid catalyst for various dehydrative condensation reactions such as direct imidation of dicarboxylic acids with amines and direct amidation of carboxylic acids with amines.[23,24] We report herein that hydrates of amorphous Nb_2O_5, generally named niobic acid or $Nb_2O_5{\cdot}nH_2O$, is an effective and reusable catalyst for the intramolecular dehydrative condensation of di- and tetracarboxylic acids. Catalytic results show wide applicability of the synthetic method, and control experiments show that Lewis acid site of the catalyst is catalytically important for the reaction. It is important to note that a commercial $Nb_2O_5{\cdot}nH_2O$ (HY-3400), as received from a supplier (CBMM), can be utilized for the reactions without any pretreatments.

2.2 Experimental

Commercially available organic compounds (from Tokyo Chemical Industry, WAKO or Sigma-Aldrich) were used without further purification. GC (Shimadzu GC-2014) and GCMS (Shimadzu GCMS-QP2010) analyses were carried out with Ultra ALLOY$^+$-1 capillary column (Frontier Laboratories Ltd.) with N_2 and He as the carrier. All reactions were carried out in oven-dried glassware under an inert atmosphere of nitrogen. Analytical TLC was performed on a Merck 60 F254 silica gel (0.25 mm thickness). Column chromatography was performed with silica gel 60 (spherical, 63-210 μm, Kanto Chemical Co. Ltd.). Molecular sieves 4Å (MS4Å) was dehydrated at 100 °C.

2.2.1 Preparation of the catalysts

Niobic acid ($Nb_2O_5{\cdot}nH_2O$, HY-340) was kindly supplied by CBMM. Nb_2O_5 was prepared by calcination of the niobic acid at 500 °C for 3 h. According to the previous method,[26] Na^+ -

exchanged $Nb_2O_5 \cdot nH_2O$ (Na^+-$Nb_2O_5 \cdot nH_2O$) was prepared by stirring 1.0 g of $Nb_2O_5 \cdot nH_2O$ in 400 mL of 1 M NaCl solution at 60 °C for 52 h. The pH was adjusted to 11.0−11.4 by adding 0.05 M NaOH solution. Then, the sample was washed repeatedly with distilled water, followed by drying in an oven at 100 ° C for 12 h. TiO_2 (JRC-TIO-4), CeO_2 (JRC-CEO-3), amorphous SiO_2-Al_2O_3 (JRC-SAL-2, Al_2O_3 content = 13.75 wt%, surface area = 560 m^2 g^{-1}) were supplied from Catalysis Society of Japan. SiO_2 (Q-10, 300 m^2 g^{-1}) was supplied from Fuji Silysia Chemical Ltd. ZrO_2, ZnO, SnO_2, MoO_3, Ta_2O_5 and CaO were prepared by calcination (500 °C, 3 h) of the hydrous oxides: $ZrO_2 \cdot nH_2O$, $ZnO \cdot nH_2O$ (Kishida Chemical), H_2SnO_2 (Kojundo Chemical Laboratory Co., Ltd.), H_2MoO_4 (Kanto Chemical), $Ca(OH)_2$ (Kanto Chemical) and $Ta_2O_5 \cdot nH_2O$ (Mitsuwa Chemicals). Al_2O_3 was prepared by calcination of γ-AlOOH (Catapal B Alumina purchased from Sasol) for 3 h at 900 °C. Sulfonic resins (Amberlyst-15 and Nafion-SiO_2 composite) were purchased from Sigma-Aldrich. The BET surface area of the oxide (**Table 1**) was measured by N_2 adsorption at -196 ºC using BELCAT (MicrotracBEL). Scandium(III) trifluoromethanesulfonate [$Sc(OTf)_3$], $In(OTf)_3$, $Hf(OTf)_4$, $MgCl_2$, sulfuric acid (H_2SO_4) and p-toluenesulfonic acid (PTSA) were purchased from Sigma-Aldrich or WAKO.

2.2.2 FT-IR studies of pyridine adsorption measurement

IR (infrared) study of pyridine adsorption on the catalysts was performed using JASCO FT/IR-4200 spectrometer equipped with an MCT detector using a flow-type IR cell connected to a flow reaction system. The IR disc of the sample (40 mg, 20 mm) was first dehydrated under He flow at 200 or 300 °C, and then a background spectrum was taken under He flow at 200 °C. Then, pyridine (0.3 mmol g-1) was introduced to the sample, followed by purging by He for 600 s, and by IR measurement of adsorbed pyridine at 200 °C.

2.2.3 Typical reaction procedure

The heterogeneous catalysts were used for catalytic reactions without dehydration treatments. Typically, dicarboxylic acids (1 mmol) in 2 mL o-xylene with 50 mg of catalysts and a magnetic stirrer bar were added to a reaction vessel (Pyrex cylinder) with a reflux condenser, and the mixture was heated to reflux under N_2 with stirring (400 rpm). For azeotropic removal of water, a funnel containing 4Å molecular sieves (MS4Å, 0.2 g) wrapped in a filter paper (Advantech, No. 4A) was fixed at the upper part of the cylinder surmounted by a cooling part (reflux condenser) as shown in **Figure 2.1**.

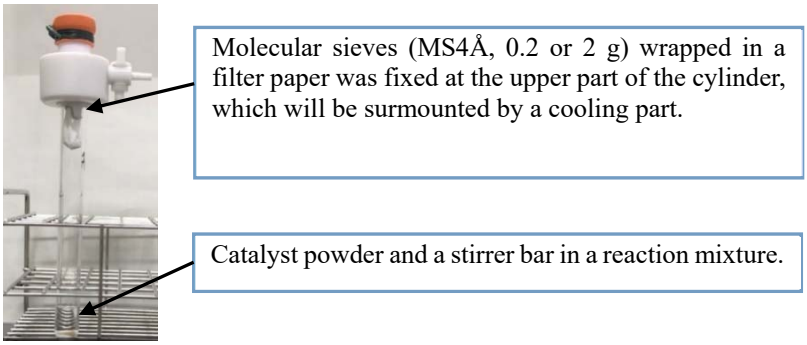

Figure 2.1: Typical reaction set up for anhydride formation reaction.

Yields were determined by ^{1}H NMR using DMSO-d_6 as an internal standard as follows. After completion of the reaction, 2-propanol (4 mL) and acetone (3 mL) was added to the mixture, and the catalyst was separated by centrifugation and filtration, followed by washing the catalyst with acetone (6 mL). The solution was evaporated to give crude mixture, which was analyzed by ^{1}H NMR and ^{13}C NMR. The Nb content in the reaction mixture was determined by an inductively coupled plasma (ICP-AES) method (ICPE-9000, Shimadzu). The gram-scale reactions of dicarboxylic acids to cyclic anhydrides (Table 3) were carried out as follows using 2 g of MS4Å for azeotropic water removal. After the reaction, followed by addition of 10 mL 2-propanol and 10 mL acetone to the mixture, the catalyst was removed by filtration. Evaporation of the mixture at 60 °C gave a solid, which was recrystallized using mixture of ethylacetate (5 mL) and hexane (3 mL) to get pure anhydride. The anhydrides were identified by ^{1}H NMR and ^{13}C NMR.

2.2.4 NMR analysis procedure

^{1}H and ^{13}C NMR spectra for anhydrides of **Table 3** were assigned and reproduced to the corresponding literature. ^{1}H and ^{13}C NMR spectra were recorded using at ambient temperature on JEOL-ECX 600 operating at 600.17 and 150.92 MHz, respectively with tetramethylsilane as an internal standard. All chemical shifts (δ) are reported in ppm and coupling constants (*J*) in Hz. All chemical shifts are reported relative to tetramethylsilane and *d*-solvent peaks 40.42 ppm for dimethyl sulfoxide-d_6 and 77.00 ppm chloroform-d. Abbreviations used in the NMR experiments: s, singlet; d, doublet; dd, doublet of doublets, t, triplet; m, multiplet.

2.3 Results and discussion

2.3.1 Catalyst screening

We carried out catalyst screening adopting the intramolecular condensation of succinic acid (**1a**) to succinic anhydride (**2a**) as a model reaction. **Table 1** lists the yields of **2a** for the

condensation of **1a** (1 mmol) in 2 mL *o*-xylene under azeotropic reflux conditions for 5 h in the presence of 50 mg of the catalysts. Note that the thermal reaction in the absence of catalyst showed no conversion of **1a** (entry 1).

Table 1 Catalyst screening for cyclization of succinic acid (**1a**).

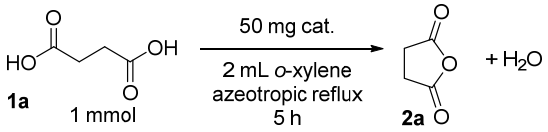

Entry	Catalyst	S_{BET} [a] (m^2g^{-1})	**2a** yield (%)[b]
1	blank	-	0
2	$Nb_2O_5{\cdot}nH_2O$	118	99
3	Na^+-$Nb_2O_5{\cdot}nH_2O$	42	89
4	Nb_2O_5	54	82
5	TiO_2	47	52
6	SnO_2	25	9
7	ZnO	12	7
8	ZrO_2	73	5
9	Al_2O_3	124	4
10	CaO	22	4
11	CeO_2	81	4
12	Ta_2O_5	12	2
13	MoO_3	3	1
14	Nafion-SiO_2	-	44
15	Amberlyst-15	-	68
16	H_2SO_4	-	0
17	PTSA	-	0
18	$Sc(OTf)_3$	-	0
19	$In(OTf)_3$	-	0
20	$Hf(OTf)_4$	-	0
21	$MgCl_2$	-	0

[a]Specific surface area of the catalyst determined by N_2 adsorption at -196 °C; [b]Yields were determined by the integration of ^{1}H NMR.

We tested the reaction using 22 types of catalysts including heterogeneous catalysts (entries 2-15) and homogeneous acid catalysts (entries 16-21). Among simple metal oxides tested

(entries 4-13), Nb_2O_5 showed the highest yield (82%) of **2a**, and a Lewis acidic solid, TiO_2[25,26] was secondary most effective (52% yield). As received $Nb_2O_5{\cdot}nH_2O$ (uncalcined precursor of Nb_2O_5) showed higher yield (99%) than Nb_2O_5. Na^+-$Nb_2O_5{\cdot}nH_2O$ showed a relatively high yield (89%).

Combined with the IR results that Na^+-$Nb_2O_5{\cdot}nH_2O$ is mostly Lewis acidic and the number of Lewis acid sites of $Nb_2O_5{\cdot}nH_2O$ is larger than those of Na^+-$Nb_2O_5{\cdot}nH_2O$ and Nb_2O_5, the catalytic results suggest that Lewis acid sites are catalytically relevant sites for the reaction by the niobium oxides. Commercially available Brønsted acidic resins, *Nafion-SiO_2* composite (entry 16) and Amberlyst-15 (entry 17) showed moderate yields of 44 and 68%, respectively. Conventional homogeneous Brønsted acids (entries 18, 19), H_2SO_4 and p-toluenesulfonic acid (PTSA), and homogeneous Lewis acids (entries 20-23), including $Sc(OTf)_3$, $In(OTf)_3$, $Hf(OTf)_4$ and $MgCl_2$, gave 0% yields of the anhydride. Heterogeneous Brønsted acids, Nafion-SiO_2 and Amberlyst-15 (entries 14, 15), showed moderate yields (44, 68%), but the yields were lower than that of $Nb_2O_5{\cdot}nH_2O$ (99%). Summarizing the results in **Table 1**, it is concluded that $Nb_2O_5{\cdot}nH_2O$ is the most effective catalyst for the cyclization of succinic acid to succinic anhydride.

2.3.2 Pyridine adsorption on different Nb_2O_5 catalysts

IR spectra (ring-stretching region) of pyridine adsorbed on niobium oxides are shown in **Figure 2.2.** As reported in the previous IR studies on the similar system,[20,23–25,27] strong bands at 1445 cm^{-1} due to the coordinatively bound pyridine on a Lewis acid site are observed for $Nb_2O_5{\cdot}nH_2O$, Nb_2O_5 and Na^+-exchanged $Nb_2O_5{\cdot}nH_2O$ (Na^+-$Nb_2O_5{\cdot}nH_2O$).[27] Previously, we determined the averaged integrated molar extinction coefficient (1.73 cm μmol^{-1}) of the adsorbed pyridine on Lewis acid sites on various metal oxides.[25] Using this coefficient combined with the area intensities of the bands at 1445 cm^{-1}, the numbers of Lewis acid sites on $Nb_2O_5{\cdot}nH_2O$, Nb_2O_5 and Na^+-$Nb_2O_5{\cdot}nH_2O$ were calculated to be 98 $\mu mol\ g^{-1}$, 58 $\mu mol\ g^{-1}$ and 53 $\mu mol\ g^{-1}$, respectively. A band at 1540 cm^{-1} due to pyridinium ion (PyH^+) is also observed for $Nb_2O_5{\cdot}nH_2O$, while the band is nearly absent in the spectrum of Na^+-$Nb_2O_5{\cdot}nH_2O$. Thus, $Nb_2O_5{\cdot}nH_2O$ has both Lewis and Brønsted acid sites, whereas Na^+-$Nb_2O_5{\cdot}nH_2O$ is mostly Lewis acidic.[27]

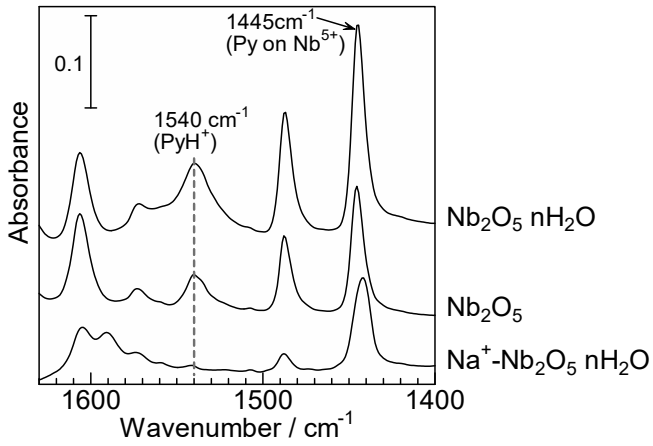

Figure 2.2: IR spectra of pyridine on niobium oxides at 200 ºC.

2.3.3 Optimization of reaction parameters

Effect of solvents

The effect of reaction conditions on the yield of **2a** for the standard reaction of **1a** under reflux conditions in different solvent are shown in **Table 2**. Among the three solvents tested, the yield increased with increase in the boiling point of the solvent as follows: *o*-xylene > *n*-octane > toluene.

Table 2: Cyclization of **1a** to **2a** by $Nb_2O_5 \cdot nH_2O$ (50 mg) for 5 h.

Entry	Solvent	MS4Å [a]	**2a** yield
1	*o*-xylene	0.2 g	99
2	*o*-xylene	0 g	90
3	*n*-octane	0.2 g	58
4	*n*-octane	0 g	40
5	toluene	0.2 g	39
6	toluene	0 g	29

[a]Weight of MS4Å inside the reflux condenser. [b] Determined by ^{1}H NMR.

The presence of molecular sieves 4Å (MS4Å) at the upper part of the reactor increased the yields of **2a**, indicating the importance of azeotropic removal of water as reported by Ishihara et al.,[17,18] Summarizing the optimization study, use of $Nb_2O_5 \cdot nH_2O$ under azeotropic reflux in *o*-xylene is the best conditions.

Time course of reaction

Figure 2.3 compares time-yield profiles for the standard reaction of **1a** by three heterogeneous Lewis acid catalysts and a homogeneous Lewis acid catalyst. The reaction rate estimated from the initial slope of the curve changed in the following order: $Nb_2O_5{\cdot}nH_2O$ > TiO_2 > Al_2O_3 > $Sc(OTf)_3$.

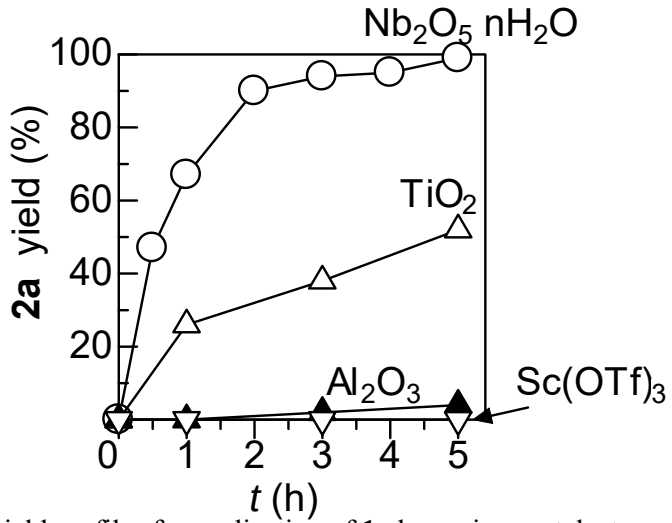

Figure 2.3: Time-yield profiles for cyclization of **1a** by various catalysts under azeotropic reflux in *o*-xylene.

In our previous studies,[23,24] we have shown that Lewis acid activation of carbonyl group of carboxylic acids by metal oxides increases in the order of Nb_2O_5 > TiO_2 > Al_2O_3. Hence, the high catalytic activity of $Nb_2O_5{\cdot}nH_2O$ can be due to the activation of carbonyl group by the surface Nb^{5+} Lewis acid sites of $Nb_2O_5{\cdot}nH_2O$. A possible mechanism for the present catalytic system involves the initial activation of carbonyl groups of dicarboxylic acid by the Nb^{5+} Lewis acid site. The electrophilic carbonyl group undergoes intermolecular nucleophilic attack by the OH group of **1a**.

2.3.4 Water tolerant Nb_2O_5 catalyst

Another advantage of $Nb_2O_5{\cdot}nH_2O$ is water-tolerance.[20] **Figure 2.4** compares the yields of **2a** for cyclization of **1a** by $Nb_2O_5{\cdot}nH_2O$ and TiO_2 in the absence and presence of 0.2 g of MS4Å inside reflux condenser used for azeotropic water removal. For both catalysts, the presence of MS4Å increased the yields, but the increase in the yield was larger for TiO_2. This suggests that $Nb_2O_5{\cdot}nH_2O$ is more water-tolerant than TiO_2, which can be an additional reason of the high catalytic activity of $Nb_2O_5{\cdot}nH_2O$.

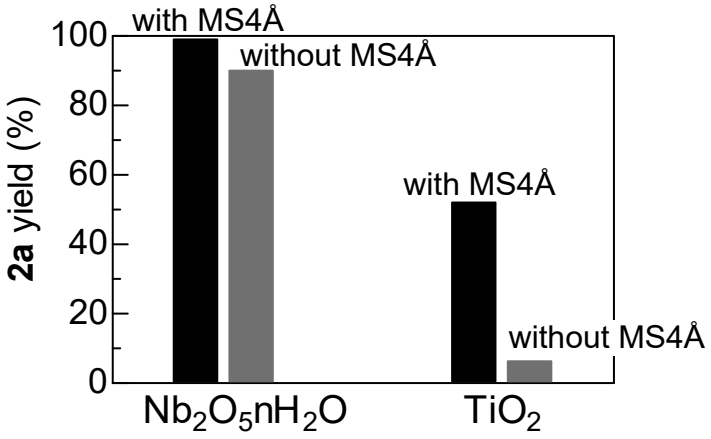

Figure 2.4: Yields of **2a** for cyclization of **1a** (5 h) in the absence and presence of 0.2 g of MS4Å inside the reflux condenser.

2.3.5 Investigation of heterogenous nature of $Nb_2O_5.nH_2O$ catalyst

We studied catalyst reusability for the standard reaction of **1a** to **2a** by $Nb_2O_5 \cdot nH_2O$ under the conditions shown in **Table 1** (entry 2). After the first cycle, the catalyst was separated from the mixture by centrifugation, followed by washing with acetone, and by drying at 90 °C for 3 h. The catalyst was reused three times (**Figure 2.5**).

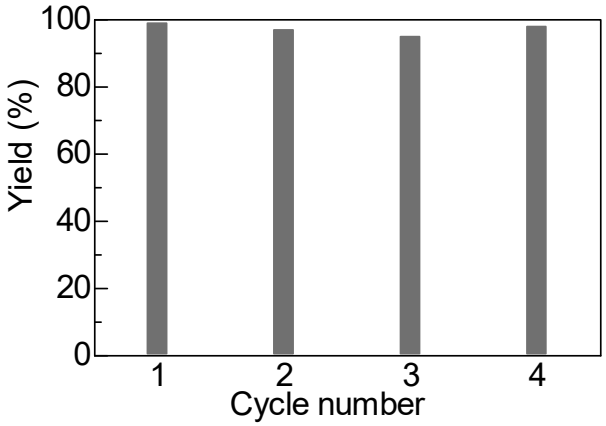

Figure 2.5: Reuse of $Nb_2O_5 \cdot nH_2O$ (50 mg) for cyclization of **1a** (1 mmol) to **2a** under azeotropic reflux in 2 mL *o*-xylene (5 h).

ICP-AES analysis of the solution after the first cycle showed that the contents of Nb in the solution was only 0.8 ppm, corresponding to 0.004% of Nb in the 50 mg catalyst. We also checked the hot filtration test. The reaction was completely terminated by a removal of the catalyst from the reaction mixture after 15 min (28% yield); further heating of the filtrate for 5 h under the reflux condition did not increase the yield. These results indicate that the present method is a heterogeneous reusable catalytic system.

2.3.6 Gram scale synthesis of anhydride

The present method was generally applicable to gram-scale intramolecular condensation of various dicarboxylic acids to the corresponding cyclic anhydrides (**Table 3**).

Table 3 Gram scale cyclization of various dicarboxylic acids.[a]

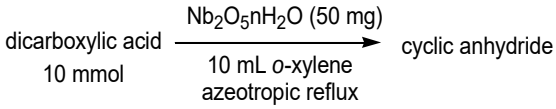

Entry	Substrates	Products	*t*/ h	*T*/ °C	Yield/ %
1	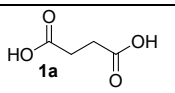	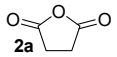	24	160	96
2[b]	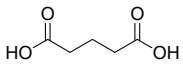	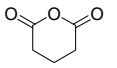	60	200	91
3[b]	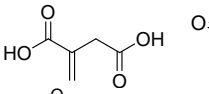	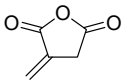	36	200	92
4	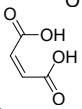	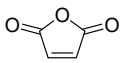	72	160	90
5	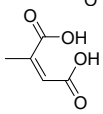	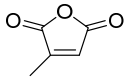	72	160	94
6	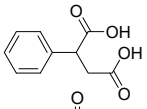	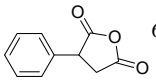	60	160	95
7	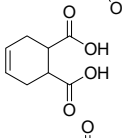	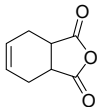	60	160	96
8	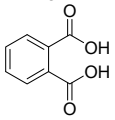	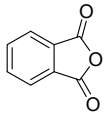	60	160	94
9	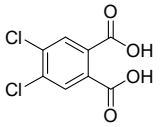	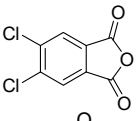	72	160	95
10	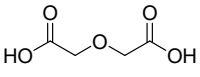	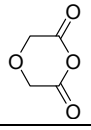	72	160	86

[a] Yields of isolated products were reported. [b] In 10 mL mesitylene.

Succinic acid (entry 1), glutaric acid (entry 2), itaconic acid (entry 3), maleic acid (entry 4), citraconic acid (entry 5), phenyl-succinic acid (entry 6), cis-4-cyclohexene-1,2-dicarboxylic acid (entry 7), phthalic acid (entry 8), 4,5-dichlorophthalic acid (entry 9), and diglycolic acid

(entry 10) underwent cyclization to give the corresponding cyclic anhydrides with high isolated yields (85-96%).

The results indicate that the present catalytic method is generally applicable to condensation of dicarboxylic acids to cyclic anhydride with wide functional group tolerance. Some of the dicarboxylic acids in **Table 3** can be produced from biorefinery process, and many of the anhydrides in Table 3 are commonly applied to the synthesis of polyesters by ring-opening copolymerization with epoxides.[10–13]

2.3.7 NMR data of final products

Dihydro-furan-2,5-dione:[16]

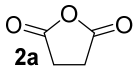

^{1}H NMR (600.17 MHz, DMSO-d_6): δ 2.93 (s, 4H); ^{13}C NMR (150.92 MHz, DMSO-d_6): δ 174.01 (C×2), 29.68 (C×2).

Dihydro-pyran-2,6-dione:[16]

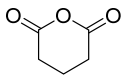

^{1}H NMR (600.17 MHz, $CDCl_3$, TMS): δ 2.75 (t, *J* = 6.61 Hz, 4H), 2.05-2.01 (m, 2H); ^{13}C NMR (150.92 MHz, $CDCl_3$, TMS): δ 166.51 (C×2), 29.91 (C×2), 16.29.

3-Methylene-dihydro-furan-2,5-dione:[16]

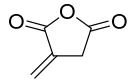

^{1}H NMR (600.17 MHz, CDCl3, TMS): δ 6.48 (t like, J = 2.52 Hz, 1H), 5.93 (t like, J = 2.52 Hz, 1H), 3.63 (t, J = 4.98 Hz, 2H); 13C NMR (150.92 MHz, CDCl3, TMS): δ 167.71, 164.46, 130.30, 126.63, 33.59.

Furan-2,5-dione:[16]

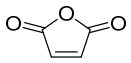

^{1}H NMR (600.17 MHz, DMSO-d6): δ 6.67 (s, 2H); 13C NMR (150.92 MHz, DMSO-d6): δ 166.88 (C×2), 134.92 (C×2).

3-Methyl-furan-2,5-dione:[16]

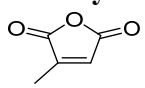

^{1}H NMR (600.17 MHz, DMSO-d_6): δ 7.10 (d like s, 1H), 2.12 (s, 3H); ^{13}C NMR (150.92 MHz, DMSO-d_6): δ 167.71, 165.90, 150.35, 130.63, 12.04.

3-Phenyl-dihydro-furan-2,5-dione:[16]

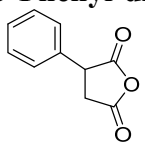

^{1}H NMR (600.17 MHz, $CDCl_3$, TMS): δ 7.39 (t, *J* = 6.90 Hz, 2H), 7.34 (t, *J* = 7.56 Hz, 1H), 7.24 (d, *J* = 6.90 Hz, 2H), 4.32 (m, 1H), 3.42 (dd, *J* = 18.87, 10.32 Hz, 1H), 3.07 (dd, *J* = 18.87, 6.84 Hz, 1H); ^{13}C NMR (150.92 MHz, $CDCl_3$, TMS): δ 171.71, 169.62, 134.56, 129.36 (C×2), 128.55, 127.24 (C×2), 46.39, 36.49.

3a,4,7,7a-Tetrahydro-isobenzofuran-1,3-dione:[10]

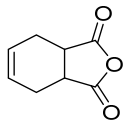

^{1}H NMR (600.17 MHz, DMSO-d_6): δ 5.99 (t, *J* = 1.38 Hz, 2H), 3.55 (t, *J* = 2.04 Hz, 2H), 2.43 (d, *J* = 15.31 Hz, 2H), 2.29 (d, *J* = 15.31 Hz, 2H); ^{13}C NMR (150.92 MHz, DMSO-d_6): δ 176.59 (C×2), 128.85 (C×2), 40.44 (C×2), 24.06 (C×2).

Isobenzofuran-1,3-dione:[16]

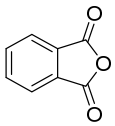

^{1}H NMR (600.17 MHz, DMSO-d_6): δ 8.13-8.12 (m, 2H), 8.06-8.04 (m, 2H); ^{13}C NMR (150.92 MHz, DMSO-d_6): δ 164.09 (C×2), 137.09 (C×2), 132.14 (C×2), 126.25 (C×2).

5,6-Dichloro-isobenzofuran-1,3-dione:[28]

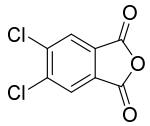

^{1}H NMR (600.17 MHz, DMSO-d_6): δ 8.52 (s, 2H); ^{13}C NMR (150.92 MHz, DMSO-d_6): δ 161.97 (C×2), 139.72 (C×2), 131.96 (C×2), 127.76 (C×2).

[1,4] Dioxane-2,6-dione:[10]

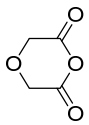

^{1}H NMR (600.17 MHz, DMSO-d_6): δ 4.13 (s, 4H); ^{13}C NMR (150.92 MHz, DMSO-d_6): δ 172.16 (C×2), 68.07 (C×2).

2.4 Conclusions

In conclusion, we have presented a versatile and sustainable method for direct cyclization of

dicarboxylic acids to the corresponding cyclic anhydride using $Nb_2O_5 \cdot nH_2O$ as a reusable, inexpensive and commercially available heterogeneous catalyst. This simple method shows high yields for the cyclization of various dicarboxylic acids which can be produced from biorefinery process. This method can simplify current high-cost synthesis routes to renewable polyesters.

References

[1] P. Van Wouwe, M. Dusselier, E. Vanleeuw, B. Sels, *ChemSusChem* **2016**, *9*, 907–921.

[2] I. Delidovich, P. J. C. Hausoul, L. Deng, R. Pfützenreuter, M. Rose, R. Palkovits, *Chem. Rev.* **2016**, *116*, 1540–1599.

[3] I. Bechthold, K. Bretz, S. Kabasci, R. Kopitzky, A. Springer, *Chem. Eng. Technol.* **2008**, *31*, 647–654.

[4] C. Delhomme, D. Weuster-Botz, F. E. Kühn, *Green Chem.* **2009**, *11*, 13–26.

[5] P. Gallezot, *Chem. Soc. Rev.* **2012**, *41*, 1538–1558.

[6] J. J. Bozell, G. R. Petersen, *Green Chem.* **2010**, *12*, 539.

[7] A. Corma Canos, S. Iborra, A. Velty, *Chem. Rev.* **2007**, *107*, 2411–2502.

[8] H. Danner, R. Braun, *Chem. Soc. Rev.* **1999**, *28*, 395–405.

[9] M. L. A. Jansen, W. M. van Gulik, *Curr. Opin. Biotechnol.* **2014**, *30*, 190–197.

[10] S. Paul, Y. Zhu, C. Romain, R. Brooks, P. K. Saini, C. K. Williams, *Chem. Commun.* **2015**, *51*, 6459–6479.

[11] N. J. Van Zee, G. W. Coates, *Angew. Chemie - Int. Ed.* **2015**, *54*, 2665–2668.

[12] N. J. Van Zee, M. J. Sanford, G. W. Coates, *J. Am. Chem. Soc.* **2016**, *138*, 2755–2761.

[13] C. Robert, F. De Montigny, C. M. Thomas, *Nat. Commun.* **2011**, *2*, 1–6.

[14] D. Davidson, P. Newman, *J. Am. Chem. Soc.* **1952**, *74*, 1515–1516.

[15] *R. Sustmann; in Comprehensive Organic Synthesis, Ed. B. M. Trost, I Fleming and Winterfeldt, Pregamon, Oxford, 1991, Vol. 6, Pp. 301-321*, **n.d.**

[16] C. Robert, F. De Montigny, C. M. Thomas, *ACS Catal.* **2014**, *4*, 3586–3589.

[17] H. Mukherjee, N. T. McDougal, S. C. Virgil, B. M. Stoltz, *Org. Lett.* **2011**, *13*, 825–827.

[18] A. Sakakura, R. Yamashita, T. Ohkubo, M. Akakura, K. Ishihara, *Aust. J. Chem.* **2011**, *64*, 1458.

[19] S. Kobayashi, K. Manabe, *Acc. Chem. Res.* **2002**, *35*, 209–217.

[20] K. Nakajima, Y. Baba, R. Noma, M. Kitano, J. N. Kondo, S. Hayashi, M. Hara, *J. Am. Chem. Soc.* **2011**, *133*, 4224–4227.

[21] Y. Wang, F. Wang, Q. Song, Q. Xin, S. Xu, J. Xu, *J. Am. Chem. Soc.* **2013**, *135*, 1506–

1515.

[22] E. V. Beletskiy, X. Hou, Z. Shen, J. R. Gallagher, J. T. Miller, Y. Wu, T. Li, M. C. Kung, H. H. Kung, *J. Am. Chem. Soc.* **2016**, *138*, 4294–4297.

[23] M. A. Ali, S. M. A. H. Siddiki, K. Kon, J. Hasegawa, K. Shimizu, *Chem. - A Eur. J.* **2014**, *20*, 14256–14260.

[24] M. A. Ali, S. M. A. H. Siddiki, W. Onodera, K. Kon, K. Shimizu, *ChemCatChem* **2015**, *7*, 3555–3561.

[25] M. Tamura, K. I. Shimizu, A. Satsuma, *Appl. Catal. A Gen.* **2012**, *433–434*, 135–145.

[26] R. Noma, K. Nakajima, K. Kamata, M. Kitano, S. Hayashi, M. Hara, *J. Phys. Chem. C* **2015**, *119*, 17117–17125.

[27] G. S. Foo, D. Wei, D. S. Sholl, C. Sievers, *ACS Catal.* **2014**, *4*, 3180–3192.

[28] D. E. Beck, W. Lv, M. Abdelmalak, C. B. Plescia, K. Agama, C. Marchand, Y. Pommier, M. Cushman, *Bioorganic Med. Chem.* **2016**, *24*, 1469–1479.

Chapter 3

Hydrolysis of Amides and Amidation of Carboxylic Acids by Nb_2O_5 Catalysts: Insights into the Structure-Activity Relationships

3.1 Introduction

Niobium pentoxide exists in various stoichiometric (NbO, NbO_2 and Nb_2O_5), nonstoichiometric, metastable and mixed phases based on method of its preparation. [1–6] The conglomerations of structures and compositions in Nb_2O_5 provide spectacular physicochemical properties enabling extensive catalytic applications.[2,7–13] It is well-studied that phase transformation of different polymorphic niobium oxides arise as a function of heat treatment and amorphous niobium oxide crystallizes to common crystal phases including pseudohexagonal (TT-Nb_2O_5), orthorhombic (T-Nb_2O_5), tetragonal (M-Nb_2O_5) and monoclinic (H-Nb_2O_5).[2,6,7,14–18] The correlation between the crystalline phases and their catalytic activity in various reactions are of great interest to understand.

Generally, all polymorphs of Nb_2O_5 composed of distorted octahedra (NbO_6) and this distortion differs on octahedra connection by edges or corners and others connection possibilities are crystallographic shear and mixing of different linkage regions.[12–14,19] A deviation from regular coordination number of 6 is generated due to the presence of impurities and oxygen defect.[20] The Nb-atom in TT-Nb_2O_5 is along with four (NbO_4), five (NbO_5) and six-fold (NBO_6) coordination on ab-plane and an Nb-O-Nb-O chain structure exists along the c-axis.[14,21,22] However, T-Nb_2O_5 consists of distorted octahedra or pentagonal bipyramidal sites via edge- or corner-sharing in the ab-plane and by corner sharing along with the c-axis, where Nb-atom exists with six (NbO_6) and seven-fold (NbO_7) coordination[14,22,23] Thermodynamically most stable H-Nb_2O_5 phase containing corner sharing NbO_6 octahedra with adjacent block linked by edge sharing with a shift of half unit cell dimension along with the c-axis. Meanwhile, the M-Nb_2O_5 phase framed of corner-sharing octahedra which are linked by edge-sharing octahedra.[2,3,7,24] Surface acidity of different polymorphs of Nb_2O_5 are identical and this plays an important role to correlate the concentration and strength of acid sites with surface morphology to reveal the mechanistic pathway of different catalytic process.

Niobic acid is a well-established water tolerant solid acid catalyst[25–28]for many of acid-catalyzed reactions with high reactivity and selectivity including dehydrative condensation,[6,29–34] hydration,[35,36] oxidation/dehydrogenation,[37–40]Friedel-Crafts alkylation,[41] nucleophilic substitution reactions[5,42,43] Classical Lewis acid catalysts along with $AlCl_3$, BF_3 suffer from the decomposition in water.[26,29,44] Metal triflates $Sc(OTf)_3$ and $Yb(OTf)_3$ exhibit as excellent water-tolerant homogenous Lewis acid catalysts to activate carbonyl compounds.[45–47] Recent studies reported that Nb_2O_5 surface catalyzes nucleophilic substitution reactions of acids, esters, anhydrides, amides in presence of H_2O, alcohol, amines even-though they have greater affinity towards Lewis acids rather than acid derivatives[5,30,43]

Such unusual property of niobium oxide reasoned that coordinatively superficial Nb^{5+} cation acts as active Lewis acid sites and that can activate oxygen-containing functional groups even in presence of water.[26,29] Further, the origin Lewis acid in Nb_2O_5 and activation of carboxylic acid derivatives in presence of hard base is already demonstrated by Shimizu and co-workers.[25]

Amides and carboxylic acids are being considered as poor electrophiles and less reactive towards nucleophilic substitution reactions[48–53] and very few heterogeneous catalytic methods are reported for alcoholysis of amides and amidation of carboxylic acids and its derivatives with amines[43,51] However, hydrolysis of amides and amidation of carboxylic acids with NH_3 (g) using solid catalyst have not been explored that much yet. Enzymatic hydrolysis of amides are classical methods to synthesize corresponding acids.[54–56] Microwave irradiated hydrolysis of amides demonstrated by employing silica assisted phthalic anhydride[57] and potassium fluoride doped alumina[58] respectively. However, these methods suffer in direct use of H_2O, low atom efficiency, limited scopes and catalytic reusability.

Herein, we have exhibited different Nb_2O_5 polymorphs (amorphous and/or crystalline phases) as a heterogenous catalyst for direct hydrolysis of amides with water and amidation of carboxylic acids with ammonia gas. The main focus of our studies is on how the structural changes of different Nb_2O_5 phases control the Lewis acidity and catalytic activity for these reactions of amides and acids respectively. We found that low temperature calcined Nb_2O_5 phases (TT and/or T-Nb_2O_5) are more reactive towards these reactions compared to the Nb_2O_5 phases created at high temperature calcination (M and/or H-Nb_2O_5). It is observed that surface area and Lewis acid sites of Nb_2O_5 is the key factor for this reaction where orthorhombic phase (T-Nb_2O_5) catalyze the hydrolysis reaction predominantly.

3.2. Experimental section

3.2.1 Materials. Commercially available organic and inorganic compounds were purchased from TCI (Tokyo Chemical Industry) and Sigma Aldrich Chemical Industry, Wako Pure Chemical Industries, Kishida Chemical, or Mitsuwa Chemicals) were used without further purifications. The GC (Shimadzu GC-14B) and GCMS (Shimadzu GCMS-QP2010) analyses were carried out with Ultra ALLOY capillary column UA^+-1 (Frontier Laboratories Ltd.) using nitrogen and He as the carrier gas. ^1H and ^{13}C NMR spectra were recorded using at ambient temperature on JEOL-ECX 600 and 400 operating at 600.17, 150.92 MHz and at 395.88, 99.54 MHz respectively with Dimethylsulfoxide (DMSO) as an internal standard.

3.2.2 Catalyst Preparation. Different Nb_2O_5 ware prepared by calcination of $Nb_2O_5 \cdot nH_2O$ (HY-340, provided by CBMM, Brazil) at 200 °C, 500 °C, 700 °C, 1000 °C for 3h in air prior to use. Specially TT-Nb_2O_5 and T- Nb_2O_5 was supplied from prof. Ueda and his group.[6] CeO_2 was supplied from Daiichi Kigenso Kagaku Kogyo Co., Ltd (Type A) was calcined at 600 °C for 3 h. TiO_2 (JRC-TIO-8) and MgO (JRC-MGO-3) were supplied by the Catalysis Society of Japan. γ-Al_2O_3 was prepared by calcination of γ-AlOOH (Catapal B Alumina, Sasol) at 900 °C for 3 h. SiO_2 (Q-10) was supplied by Fuji Silysia Chemical Ltd. ZnO was prepared by calcination (T = 500 °C, t = 3 h) of a hydroxide of Zn (Kishida Chemical). ZrO_2 was prepared by calcining Zr hydroxide at 773 K for 3 h that was made via hydrolysis of $Y(NO_3)_3.6H_2O$, $ZrO(NO_3)_2 \cdot 2H_2O$ with an aqueous NH_4OH solution. SnO_2 was prepared from H_2SnO_3 (Kojundo Chemical Laboratory Co., Ltd.) by calcination at T =500 °C for t = 3 h. CaO was prepared by calcination (T = 500 °C, t = 3 h) of $Ca(OH)_2$ (Kanto Chemical). La_2O_3, Sulfated ZrO_2, $Ce(NO_3)_4$, *p*-Toluenesulfonic acid were supplied by Wako Pure Chemical Industries, Japan. $Sc(OTf)_3$ (>98%) and $C_3CeF_9O_9S_3$ were obtained from TCI Co. Ltd., $Zr(SO_4).4H_2O$ and $Ce_3(PO_4)_4$ (min. 99%) were supplied from Alfa Aesar, Ward hill, China. Montmorillo-nite K10 clay (mont. K10), and sulfonic regin Nafion-SiO_2 composite were purchased from Sigma-Aldrich.

3.2.3 Catalyst Characterization. X-ray diffraction (XRD; Rigaku MiniFlex) patterns of the powdered catalysts were recorded with a Rigaku MiniFlex II/AP diffractometer using Cu-Kα (λ= 1.5418 Å) radiation to identify the samples crystallinity. Diffractograms were collected at incident angles from 2θ = 10 to 70° with a step size of 0.0167°. To get specific surface area of the catalysts, N_2 adsorption-desorption measurements were carried out by using AUTOSORB 6AG (Yuasa Ionics Co.). Inductively coupled plasma-atomic emission spectroscopy (ICP-AES) analysis was undertaken by using a SHIMADZU ICPE-9000 instrument to investigate the heterogeneous nature of niobia catalyst.

3.2.4 FT-IR Studies. *In situ* FT-IR spectra were recorded at 120 °C by using a JASCO FT/IR-4200 with an MCT (Mercury-Cadmium-Telluride) detector. Niobia sample (40 mg) was pressed to obtain a self-supporting pellet (ϕ = 2 cm). The obtained pellet was placed in the quartz IR cell with CaF_2 windows connected to a conventional gas flow system. Prior to the measurement, the sample pellet was heated under He flow (20 cm^3 min^{-1}) at 300 °C for 0.5 h. After cooling to 120 °C under the He flow, 1 μL of acetamide were injected to the sample individually through a line which was preheated at ca. 200 °C to vaporize them. Spectra were

measured accumulating 15 scans at a resolution of 4 cm^{-1}. A reference spectrum taken at 120 °C under He flow was subtracted from each spectrum.

3.2.5 Pyridine adsorption measurement. The adsorptions of pyridine were performed with JASCO FT/IR-4200 spectrometer equipped with an MCT detector at room temperature. All spectra were normalized to 40 mg wafers. For each spectrum, 15 scans were recorded at a resolution of 4 cm^{-1}. Each sample was pressed into a self-supported wafer. The sample was activated at 200 °C for 0.5 h under purging of He gas at constant flowrate and then cooled down to room temperature. A background spectrum was collected. The consecutive quantities of 1 μL of pyridine was introduced. At the end of each adsorption experiment, a pressure of 0.1 mbar was established in the cell to reach saturation followed by evacuation by purging He gas at 300 ºC to remove physically adsorbed species. The amount of adsorbed probe molecule was determined by using the integrated area of bands typical of the coordinated (Lewis) or protonated (Brønsted) forms at 1445 and 1540 cm^{-1} respectively. The molar absorption coefficients given by M Tamura et al.[59] was used.

3.2.6 Typical Procedure for the Catalytic Reactions. Amide **1** (1 mmol), water (5 mmol), *n*-dodecane (0.2 mmol) and a magnetic stirrer bar were added to the tube followed by filling N_2 through the septum inlet. Catalyst (50 mg) was used as the standard amount for the reaction. The yields of products were determined by using GC with *n*-dodecane as the internal standard. GC-sensitivities were estimated using commercial compounds or isolated products. In substrate scope studies, products were isolated by using column chromatography on silica gel 60 (spherical, 40–100 μm, Kanto Chemical Co. Ltd.) using hexane/ethyl acetate (10:1 to 16:1, v/v) as the eluting solvent, followed by analyses by ^{1}H and ^{13}C NMR spectroscopy in combination with GC-MS equipped with the same column as that used for GC-FID analyses. For recycling experiments, after each catalytic cycle, 2-propanol (3 mL) was added into the reaction mixture. The catalyst was separated by using centrifugation and washed for twice with acetone (3 mL) followed by water (3 mL). The catalyst was then dried at 110 °C for 5 h and used.

3.3 Results and discussion

3.3.1 Catalyst and reaction conditions optimization for hydrolysis reaction

Table 1. Catalyst screening for hydrolysis of acetamide to acetic acid.

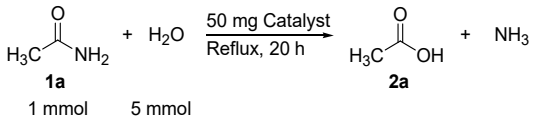

Entry	Catalyst	Yield (%)[a]
1	none	0
2	Nb_2O_5	97
3	Na^+- Nb_2O_5	78
4	CeO_2	45
5	ZrO_2	53
6	TiO_2	15
7	SnO_2	8
8	SiO_2	4
9	ZnO	7
10	Al_2O_3	6
11	CaO	3
12	MgO	1
13	Hβ-20	0
14	MFI-20	0
15	HY 5.5	0
16	Fe-mont	12
17	Mont. K10	10
18	Nafion-SiO_2	14
19	La_2O_3	17
20	Sulfated ZrO_2	27
21	$Sc(OTf)_3$	47
22	$Ce(NO_3)_4$	31
23	$Ce_3(PO_4)_4$	35
24	$Zr(SO_4).4H_2O$	25
25	$C_3CeF_9O_9S_3$	21
26	*p*-toluenesulfonic acid (PTSA)	trace
27	H_2SO_4	3

[a] GC yield.

First, we examined catalyst screening for direct synthesis of acetic acid from acetamide (**1a,** 1.0 mmol) and water (5 mmol) under solvent-free reflux condition at N_2 atmosphere. Our experimental findings are outlined in **Table 1**. Hydrolysis reaction did not take place without any catalyst (Table 1, entry 1).

Among various heterogenous Lewis acid catalysts tested, Nb_2O_5 (calcinated at 500 ^{0}C for 3 h) gave the maximum 97% yield of acetic acid within 20 h (Table 1, entries 2-7). However, the other basic and amphoteric catalysts showed very lower activity towards hydrolysis reaction and giving maximum 7% of yield of the product (Table 1, entries 8-12). For some solid Brønsted acid catalysts such as HB-20, MFI-20, HY5.5 zeolites (Table 1, entries 13-15), no product formation was observed which indicating that only Bronsted acid sites could not be able to perform hydrolysis reaction. Some other minerals and composite materials showed reactivity with up to 14% yield (Table 1, entries 16-18). In contrast, amongst some homogeneous Lewis acid catalysts tried (Table 1, entries 19-25) $Sc(OTf)_3$ gave maximum 47% yield of the product. In addition, some homogenous Brønsted acid catalysts were found less sensitive towards hydrolysis reaction and obtained <5% of acetic acid.

Table 2. Optimization of the reaction conditions for hydrolysis of acetamide to acetic acid.

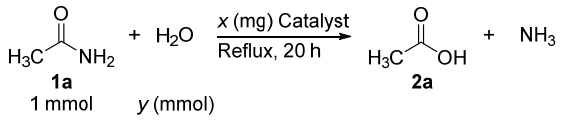

Entry	(*x* mg) Nb_2O_5	(*y* mmol) water	Yield (%)[a]
1	20	10	52
2	30	10	70
3	40	10	83
4	50	10	96
5	60	10	97
6	50	5	97
7	50	4	88
8	50	3	68
8	50	2	47

[a] GC yield.

Using the most effective Nb_2O_5 catalyst, we performed a study to finalize the optimum conditions required for the reaction using acetamide hydrolysis as the model reaction. We observed that for 1.0 mmol of acetamide maximum 50 mg of catalyst was required to get about

97% of product using 10 mmol of water (**Table 2**, entries 1-5). Subsequently, investigation of the results arising from reactions enhanced by decreasing the amount of water on the reaction system and we observed maximum 5 mmol of water was required for hydrolysis of 1 mmol of amides (Table 2, entries 6-8) within 20 h.

3.3.2 Characterization of surface structure and acidity of Nb_2O_5 catalysts

After getting the most favorable catalyst and reaction conditions, we focused on the investigation of crystalline structure and catalytic activity for various Nb_2O_5 catalysts towards hydrolysis reaction. Using various state-of-the-art analytic techniques, a new insight into structure-activity correlations on the hydrolysis of amide bond over different Nb_2O_5 catalysts were achieved.

Initially, crystallographic study on different structure of Nb_2O_5 catalysts were analyzed by conventional X-ray powder diffraction pattern obtained from X-ray diffraction (XRD).

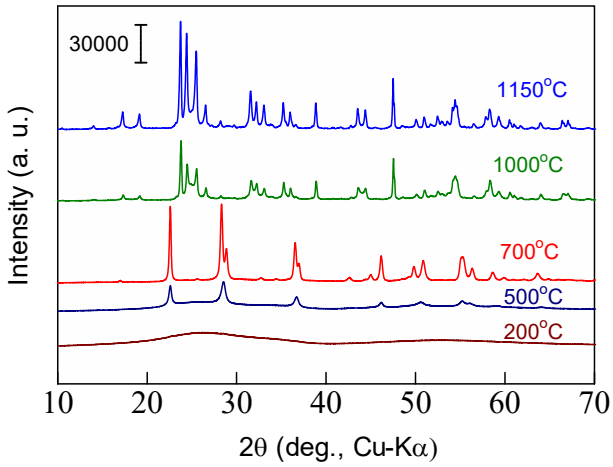

Figure 3.1. XRD pattern of different Nb_2O_5 catalysts calcined at different temperature

Figure 3.1 shows XRD patterns of Nb_2O_5 catalysts where various X-ray powder pattern was obtained with increasing the calcination temperature. The result specified several crystal forms of Nb_2O_5 polymorphs might be obtained. Depending on calcination temperature, the Nb_2O_5 polymorphs were subdivided into several phases such as pseudo-hexagonal (TT), orthorhombic (T), tetragonal (M), monoclinic (B) and monoclinic (H).[11] At lower temperature calcination temperature (200 ^{0}C), catalyst was totally amorphous. The mixture of pseudo-hexagonal (TT) and orthorhombic (T) phases were formed at 500 ^{0}C calcination where the only crystalline orthorhombic (T) phase was observed at 700 ^{0}C calcination.[13] Basically, these TT and T phases are very similar in structure. However, the only difference is the presence of legitimate defect of oxygen atom in TT phase which makes it less crystalline than T-phase. That's why a broadening of XRD peaks at $2\theta = 29^0$ and $2\theta = 37^0$ (Cu Kα radiation) were obtained in TT phase.

In contrast, splitting of the same peaks occurred in case of T phase due to the formation of (180) and (181) planes respectively.[5] So, T-Nb_2O_5 stabilized by closely spaced Nb atoms having separate and equivalent sites where as TT-Nb_2O_5 stabilized by impurities such as OH^-, Cl^-, or oxygen vacancies.[60] Moreover, at high temperature (1000 ^{0}C) calcinations, XRD patterns contains some diffuse and several sharp peaks. These results considerably resembling that of the formation of Nb_2O_5 tetragonal (M) and monoclinic (B) phases respectively. However, monoclinic (H) phase crystallizes at 1150 ^{0}C calcination.[61] Therefore, TT phase is the least stable phase, while H phase is the most thermodynamically stable one.[5] Overall, temperature-dependent crystal system of Nb_2O_5 catalysts were obtained.

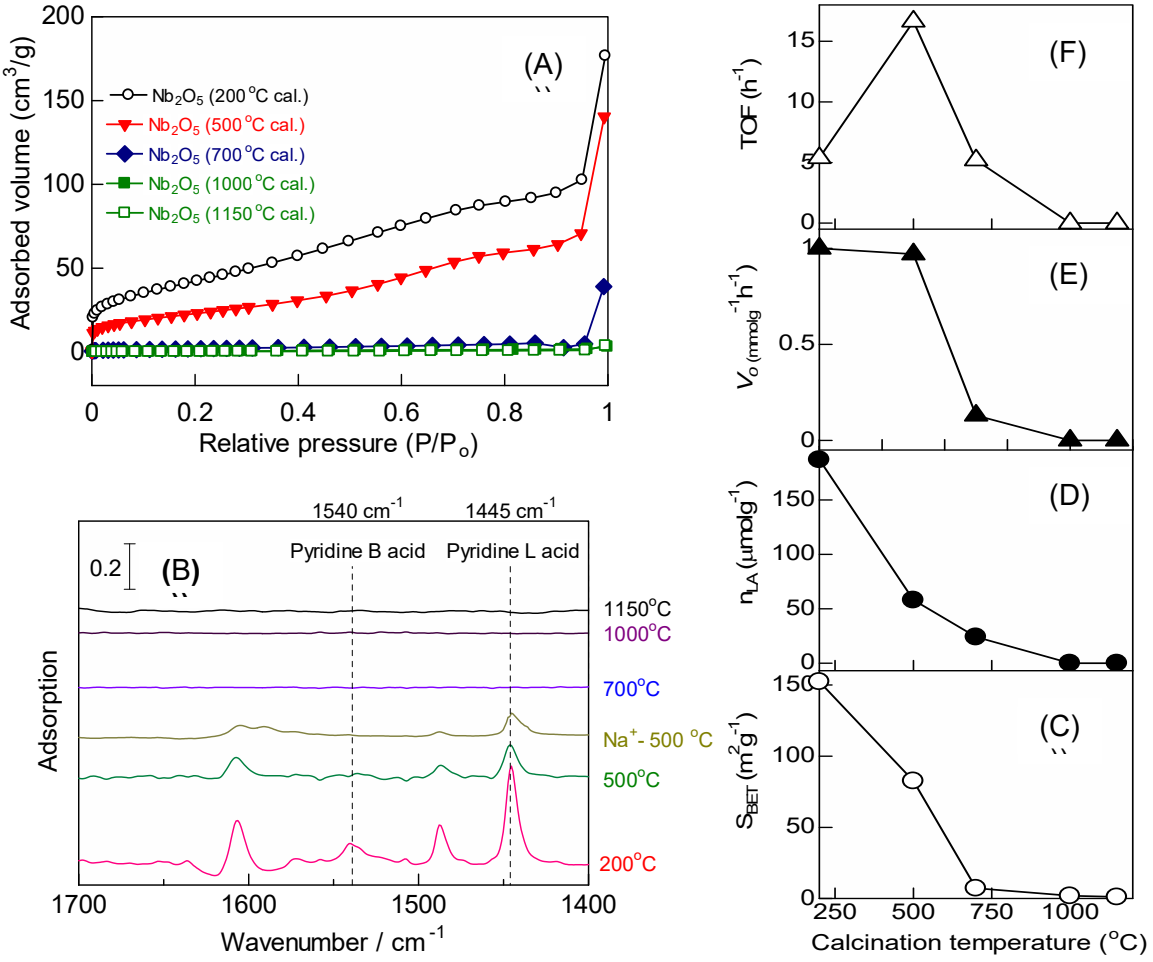

Figure 3.2. (A) N_2 adsorption isotherm and (B) IR spectra of pyridine adsorption on different Nb_2O_5 catalysts at 200 °C; (C) Surface area (D) number of LA sites were estimated by N_2 and pyridine adsorption experiments respectively. Moreover, initial rate (E) and Turn over frequency (TOF) per surface Lewis acid sites (F) for hydrolysis of acetamide by using different Nb_2O_5 catalysts calcined at different temperature are shown.

Next, N_2 adsorption experiment was performed to determine the specific surface areas of different Nb_2O_5 polymorphs. N_2 adsorption isotherm are shown in Figure 3.2 (A). Brunauer-Emmett-Teller (BET) method was used to obtain the specific surface areas. It was found that

surface area of niobium oxides decreased while the calcination temperature consequently increased (Figure 3.2 (C)). After that, acid properties of Nb_2O_5 catalysts were investigated.

Conventional pyridine adsorption experiment followed by IR spectroscopy were used to quantify the Lewis and Brønsted acid sites. IR spectra of pyridine adsorption are shown in Figure 3.2 (B). The adoption bands at 1445 cm^{-1} and 1540 cm^{-1} are due to adsorption of pyridine on superficial Nb^{5+} cation as Lewis acidic sites and H^+ cation from Brønsted acid sites of Nb_2O_5 catalysts respectively. Subsequently, the numbers of Lewis and Brønsted acid sites on different Nb_2O_5 were calculated from the area intensities of the bands at 1445 cm^{-1} and 1540 cm^{-1}. The average integrated molar extinction coefficient 1.73 cm μmol^{-1} and 1.23 cm μmol^{-1} were used respectively in Lewis and Brønsted acid sites calculations.[59] We observed that with increasing the calcination temperature the amount of acid sites gradually decreased (Figure 3.2 (D)). After calcination at 1000 ^{0}C or more, acid sites were almost lost on niobium oxides.

3.3.3 Correlation studies between crystallinity structure and acidity in hydrolysis of amides

To understand how crystallinity changes the acidity which affects the hydrolysis reaction, initial rate and turn over frequency (TOF) was checked over different calcination temperature (Figure 3.2 (E) and (3.2 (F)). With increasing calcination temperature, surface area and acid sites were decreased. Hence, the initial rate of hydrolysis was decreased accordingly (Figure 3E).

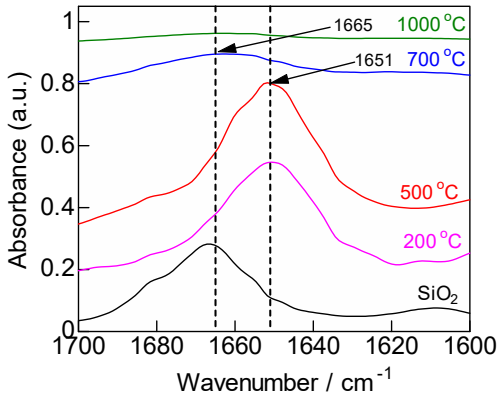

Figure 3.3. FT-IR spectra of adsorbed acetamide species on SiO_2 and different Nb_2O_5 catalysts

In addition, a volcano type relationship was found at Nb_2O_5 prepared by 500 °C calcination that showed the highest turnover frequency (TOF) towards the hydrolysis reaction. Therefore, least crystalline Nb_2O_5 containing moderate no of Lewis acid sites are effective for this hydrolysis reaction. Moreover, from *in-situ* IR, we found that the C═O stretching band of adsorbed acetamide on 500 °C calcinated Nb_2O_5 was at lower wavenumber (1651 cm^{-1}) compared to 700 °C or higher calcinated one Figure 4. These results confirm that the acid sites

of low crystalline Nb_2O_5 can activate the adsorbed acetamide more efficiently than high crystalline ones which can lead the better catalytic performance.

Additionally, a comparative study was also performed to investigate the role of Lewis and Brønsted acid sites of Nb_2O_5 among the other heterogenous and homogenous Brønsted acid catalysts on hydrolysis reaction. So, Na^+-exchanged Nb_2O_5 was prepared where the Brønsted acid sites were successfully replaced by Na^+ ion and the number of Lewis acid was lower than that of Nb_2O_5. Additionally, Nb_2O_5 catalyst was found as a water tolerant Lewis acid catalyst because the IR spectrum of adsorbed pyridine followed by re-hydration did not essentially changed.[5,43]The result is shown in Figure 3.4.

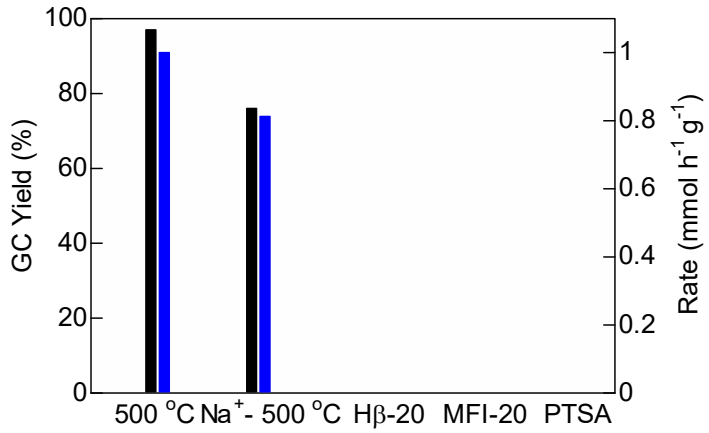

Figure 3.4. Comparison of the role of Lewis and Brønsted acid sites of catalysts on hydrolysis of acetamide

Here, it is obtained that Na^+-exchanged Nb_2O_5,[30] an almost Lewis acidic catalyst gives a compatible rate and yield of product acetic acid with Nb_2O_5. Therefore, it might be concluded that hydrolysis reaction predominantly catalyzes by the LA sites of Nb_2O_5 whereas the truly Brønsted acid sites of the other catalysts are entirely inactive.

3.3.4 Correlation between different Nb_2O_5 crystalline structure (Phases) and their activity on hydrolysis reaction

It has been reported that TT and T-phase Nb_2O_5 are greatly used in catalysis due to their high surface area as well as number of Lewis and Brønsted acid sites.[5]

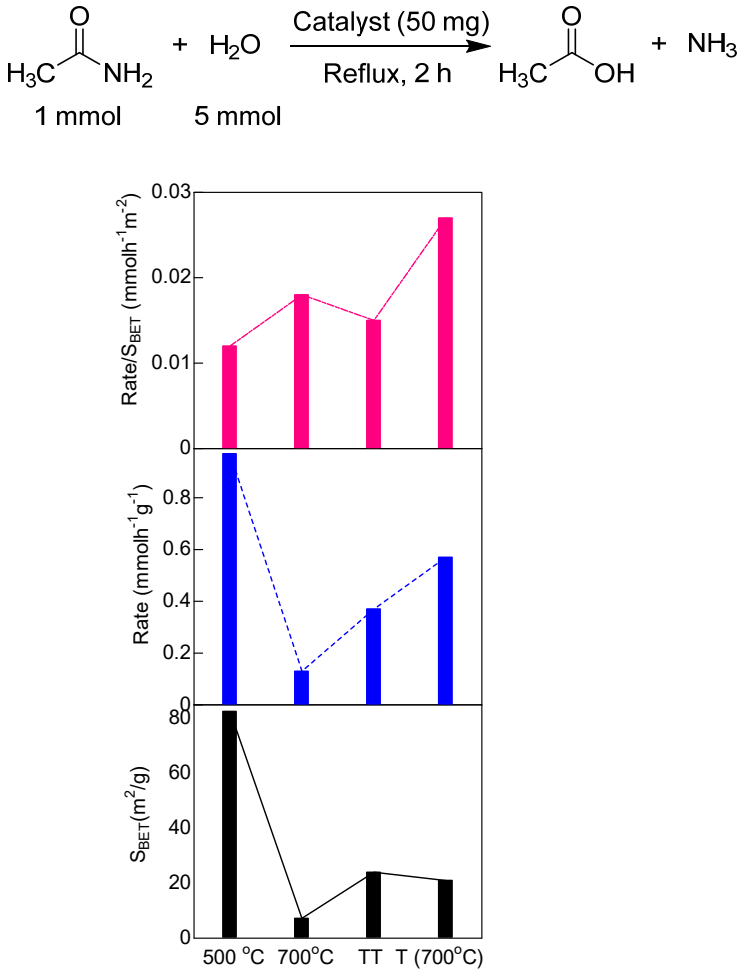

Figure 3.5. Comparison of effectiveness of different Nb2O5 catalysts in hydrolysis reaction.

..To understand the role of different Nb_2O_5 phases on amide hydrolysis reaction, a comparative study between 500 ºC, 700 ºC, TT- Nb_2O_5, T- Nb_2O_5[6] were explored which is shown in Figure 3.5, where the TT (S_{BET}: 24 m^2/g) and T- Nb_2O_5 (S_{BET}: 21 m^2/g) were supplied by prof Ueda, Kanagawa University, Japan. It is found that T- Nb_2O_5 possess higher initial reaction rate for acetamide hydrolysis reaction than TT- Nb_2O_5 (Figure 6C) with the highest normalized reaction rate as well (Figure 6C). Therefore, it has been proved that the role of T-phase of Nb_2O_5 is more significant than TT-phase for this reaction even the no of Lewis acid sites and surface area plays an important role.

3.3.5 Catalytic properties and scopes of hydrolysis reaction

Time course of the reaction was performed to explore the full catalytic cycle (Figure 3.6) under standard reaction condition. From the concentration/time plot of reactive components it was found that the reaction time 20 h was enough to obtain the highest conversion and selectivity of the product. No by-product was observed until completion of the reaction.

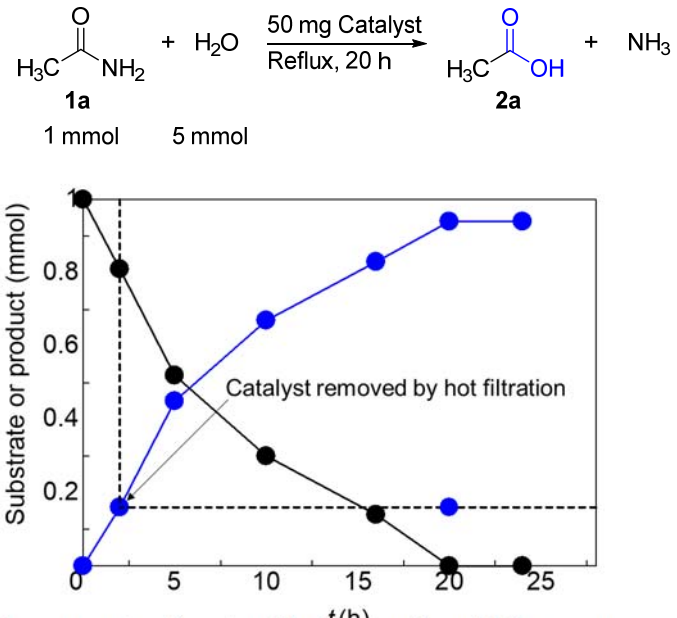

Figure 3.6. Plots of the amounts of acetamide **1a**, acetic acid **2a** versus reaction time over Nb_2O_5 catalysts, acetamide (1 mmol), water (5 mmol) were refluxed under standard reaction condition Table 2 entry 7.

Next, leaching test was carried out to check the heterogeneous nature of Nb_2O_5. For this purpose, after 2 h of the reaction (18% yield), the solid catalyst was separated by simply filtration and then continued the reaction without any catalyst until 20 h. We observed that the product yield was not increase after removal of catalyst. The result confirmed that no leaching of the catalyst was occurred, and the reaction was stopped in absence of catalyst as well (Figure 7). Additionally, the amount of Nb_2O_5 present in the filtrate was confirmed by ICP-AES analysis. The amount was below of the detection limit.

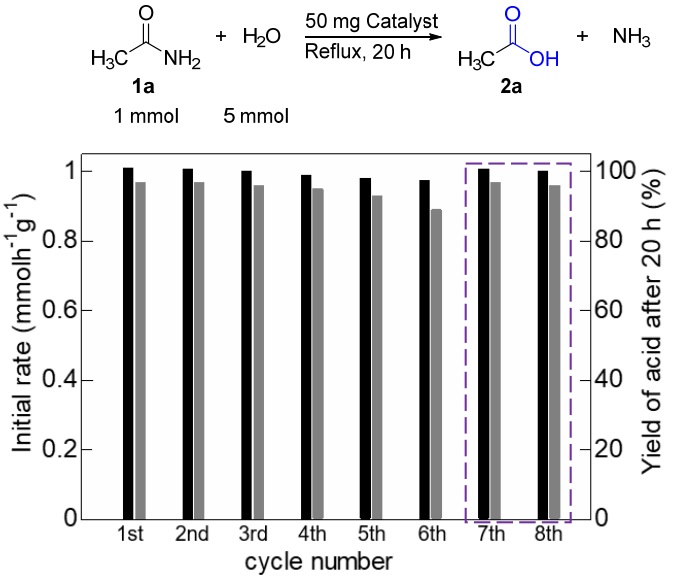

Figure 3.7. Catalyst reuse for the hydrolysis of acetamide **1a** to acetic acid **2a** promoted by Nb_2O_5 catalyst under the standard conditions shown in Table 1 (entry 2; (gray bars)) initial rates of **2a** formation and (black bars) **2a** yields after 20 h. After sixth cycle catalyst was calcined at 500 °C for 3 h and then used in 7th and 8th cycle (dotted box).

Then we studied the reusability of our catalytic system through the standard reaction condition of **1a** to **2a** (Figure 3.7). The initial reaction rate as well as the yield after each cycle were determined. There was no significant change in case of both reaction rate and yield. After each cycle, the catalyst was separated from the mixture by centrifugation. After that catalyst was washed with isopropyl alcohol (2 mL) and acetone (2 mL) for twice and drying at 110 °C for 5 h and then used for next cycle. The catalyst Nb_2O_5 was reusable at least 6 times without any significant change in the catalytic performance. However, after the 6th cycle the catalytic performance was regained by the recalcination at 500 °C for 3 h in the air (Figure 8).

After finalizing optimized reaction conditions, the applicability of the catalytic system was explored by checking the substrate scopes using various amide substrates. Our method was applicable for a wide range of aliphatic and aromatic amide substrates.

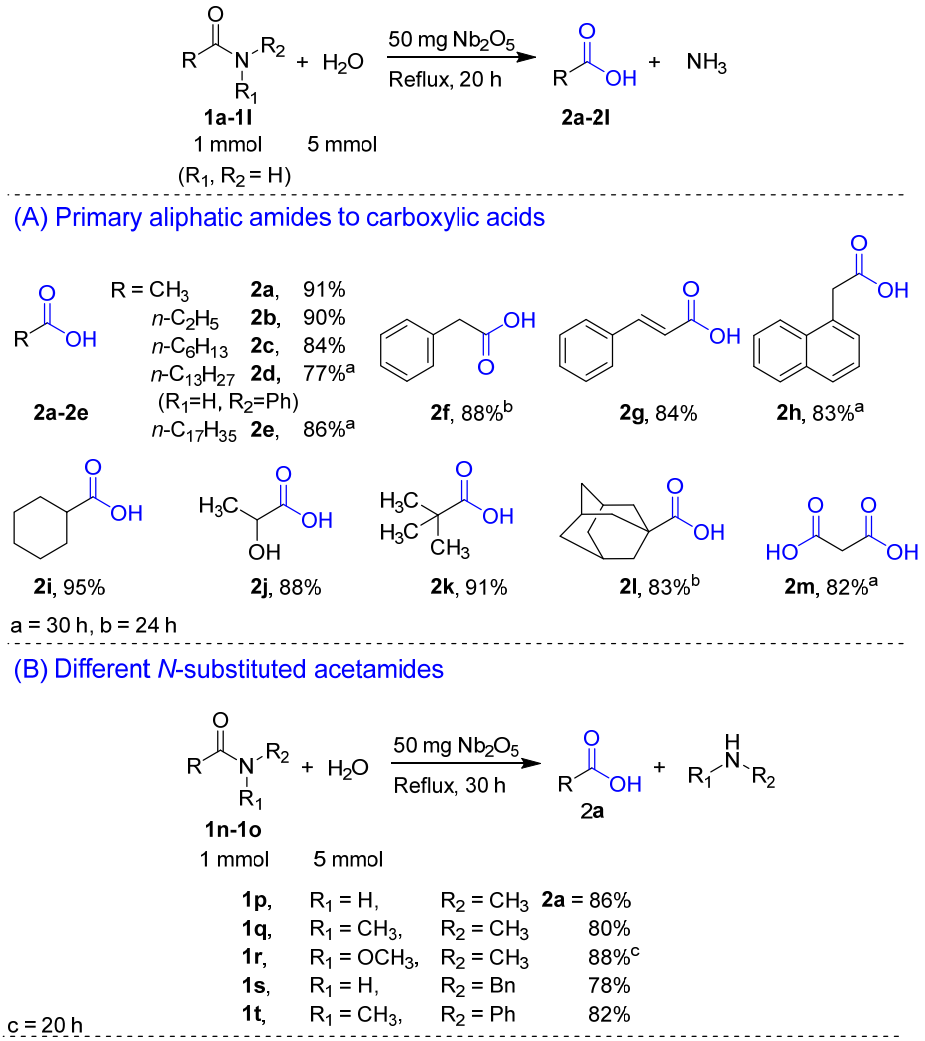

Scheme 1. Hydrolysis of different aliphatic amides to the corresponding carboxylic acids. Isolated yields are shown.

As shown in Scheme 1**,** several aliphatic amides having various functionalities were screened. Linear amides containing small and long carbon chain (1a-1e), benzylic (1f, 1h) and allylic

(1g) amides underwent hydrolysis to their corresponding acids with excellent isolated yields (83-91%). Amides containing cyclohexyl-substituted tertiary α-carbon (1i), α-stereocenter (1j) and sterically hindered quaternary (pivaloyl and adamantyl) amides (1k, 1l) were converted to the respective acids with 83-95% of isolated yields. Moreover, the present catalytic system can successfully transform malonamide (1m) to malonic acid (2m, 82% isolated yield) indicating the practicability of converting two amides to two acids in same reaction pot. Different secondary and tertiary aliphatic amides (1n-1o) were also tolerated and gave equivalent acids with high isolated yields (82-86%). Although, our catalytic system required longer reaction time for secondary and tertiary unactivated aliphatic amides, but it exhibited good performance to the *N*-MeO activated amide giving high isolated yield (88%) within 20 h.

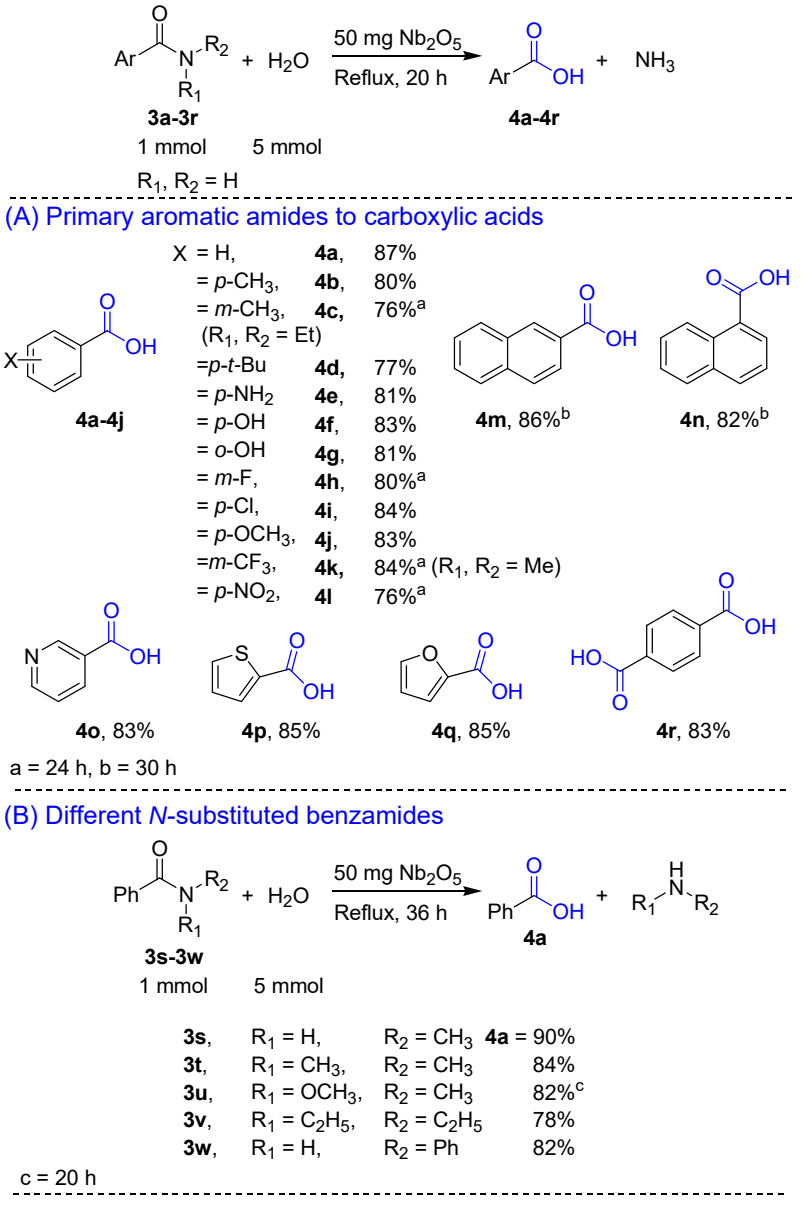

Scheme 2. Hydrolysis of different aromatic amides to the corresponding carboxylic acids. Isolated yields are shown.

In Scheme 2 the reaction scopes of hydrolysis reactions for different aromatic amides are shown. Here we observed that a series of electron-donating (3a-3g) and withdrawing (3h-3l) substituents containing aromatic amides were converted to their corresponding acids in good to high isolated yields (4a-4l, 76-87%). We were also pleased to find that sterically hindered tertiary amides particularly N,N-Diethyl-3-methyl-benzamide (3c) and N,N-Dimethyl-3-trifluoromethyl-benzamide (3k) were good tolerable towards our proposed catalytic system. Similarly, naphthyl-substituted amides (3m, 3n) and N, O and S heteroatom containing amides (3o-3q) were also underwent this hydrolysis reactions over our present catalytic system giving good isolated yields (> 80%). Besides, two amides containing aromatic substituent like as terephthalamide (3r) was also hydrolyzed into terephthalic acid (4r, 83%) successfully.

Further, we investigated the catalytic applicability of our present catalytic system over different *N*-substituted secondary and tertiary aromatic amides. We found that secondary and tertiary aromatic amides were successfully transformed into their corresponding carboxylic acids (4s-4w, 78-90% isolated yield, 36 h) where *N*-methoxy activated amide (3u) hydrolyzed readily than other unactivated amides (3s-3w).

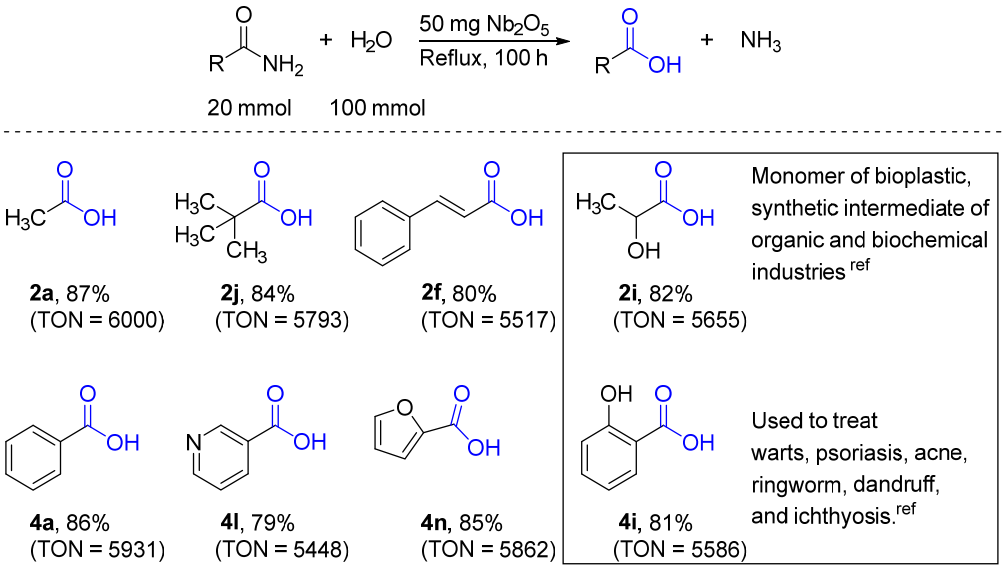

Scheme 3. Gram scale hydrolysis of amides to synthesize different carboxylic acids including lactic acid **2d** and salicylic acid **4i**. GC yields are shown.

We flourished gram scale reactions of several amides (20 mmol) and water **1b** (100 mmol) for carboxylic acid synthesis using only 50 mg of the catalyst in 100h h. It was observed that our present method was highly applicable for large scale synthesis of carboxylic acids with high turnover number (TON).

3.3.6 Catalyst and reaction conditions optimization for amidation reaction

First, catalyst screening for direct amidation reaction of acetamide (**2a,** 1.0 mmol) and NH_3 (g) (4.8 mmol) was performed using various Lewis acid catalysts under solvent-free reflux condition at N_2 atmosphere (**Table 3)**. No amidation reaction was observed place without any catalyst (Table 1, entry 1). Like the hydrolysis reactions, among various Lewis acid catalysts, Nb_2O_5 (500 ºC calcined for 3 h, CBMM) was the best catalyst for this amidation reaction which gave 98% of acetamide within 15 h (Table 3, entry 2-7). To finalize the optimum conditions required for amidation reaction with Nb_2O_5 catalyst, we found that 4.8 mmol NH_3 was required to get 98% yield of amide using 50 mg catalysts within 15 h **(Table 4**, Entry 1-6). Moreover, it was observed that with decreasing the reaction temperature, the yield of acetamide formation reaction was decreasing (Table 6, Entry 5-6) and the required optimum temperature for this amidation reaction was 100 ºC (Table 6, Entry 2). Finally, we investigated the effect of different NH_3 sources for amidation reaction. We observed that gaseous NH_3 was effective for this reaction than aqueous NH_3 (Figure 3.8)

Table 3. Catalyst screening for amidation of acetic acid with ammonia to produce acetamide.

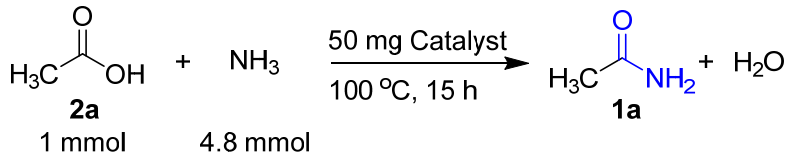

2a 1 mmol 4.8 mmol **1a**

Entry	Catalyst	Yield (%)[a]
1	none	0
2	Nb_2O_5	98
3	CeO_2	55
4	ZrO_2	61
5	TiO_2	42
6	Al_2O_3	51
7	SnO_2	34

[a] GC yield

Table 4. Optimization of the reaction conditions for amidation of acetic acid to acetamide.

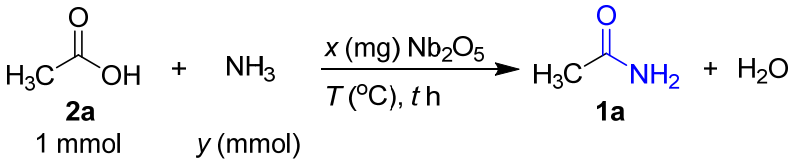

Entry	*x*(mg) Nb_2O_5	*y* (mmol) NH_3	*T* (°C)	*t* (h)	Yield (%)[a]
1	50	4.8	100	20	98
2	50	4.8	100	15	98
3	50	4.8	100	10	87
4	50	3.6	100	15	91
5	50	4.8	80	15	68
6	50	4.8	90	15	83

[a] GC yield

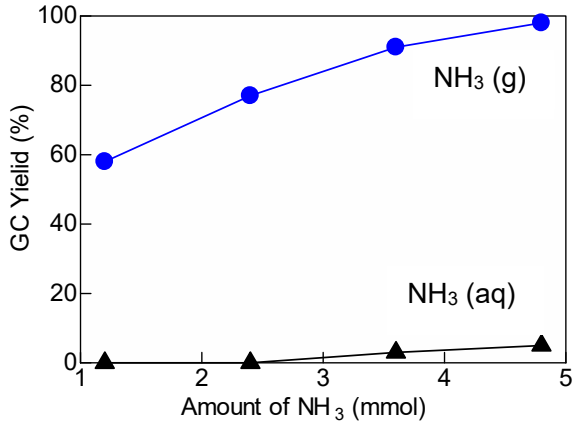

Figure 3.8. Optimization of NH_3 sources for amidation of acetic acid to acetamide over Nb_2O_5 catalyst calcinated at 500 °C; Condition: acetic acid (1 mmol), reaction temperature 100 °C, reaction time 15 h.

3.3.7 Correlation between structure and acidity of Nb_2O_5 catalysts on amidation reaction

To understand how Nb_2O_5 structures and their acidity controls the amidation reaction, initial rate and turn over frequency (TOF) was checked over different calcination temperature (Figure 3.9A and 3.9B) under standard reaction condition within 2 h, where the 500 °C calcined Nb_2O_5 showed the maximum catalytic performance. However, the other calcined catalyst (>500 °C calcination) was totally inactive This result indicates that amidation reaction by NH_3 (g) is mostly phase independent reaction although it might have strong dependency on Lewis acid

sites of Nb_2O_5. Similarly, we found that purely TT and T phase containing Nb_2O_5 was entirely inactive for this amidation reaction (Figure 3.10).

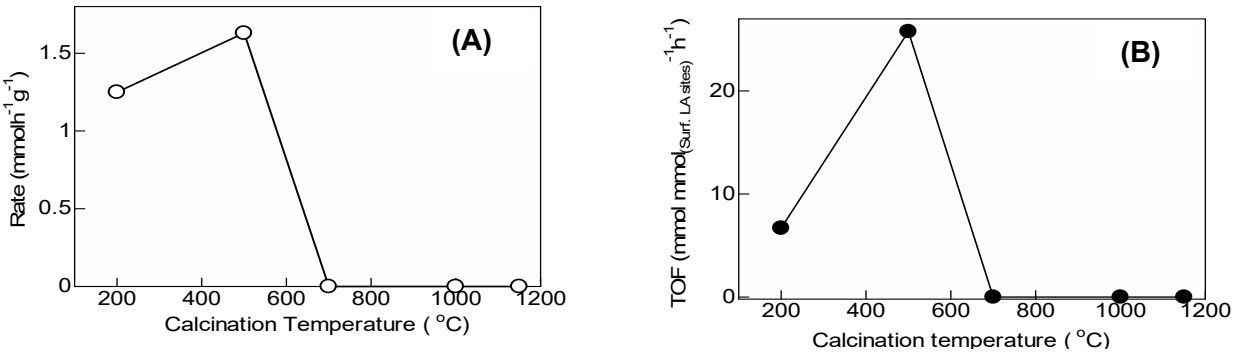

Figure 3.9. Initial rate (A) and Turn over frequency (TOF) per surface Lewis acid sites (B) for amidation of acetic acid with ammonia gas by using different Nb_2O_5 catalysts calcined at different temperature

.

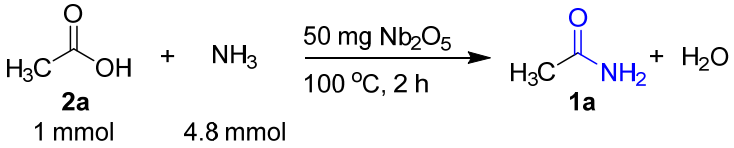

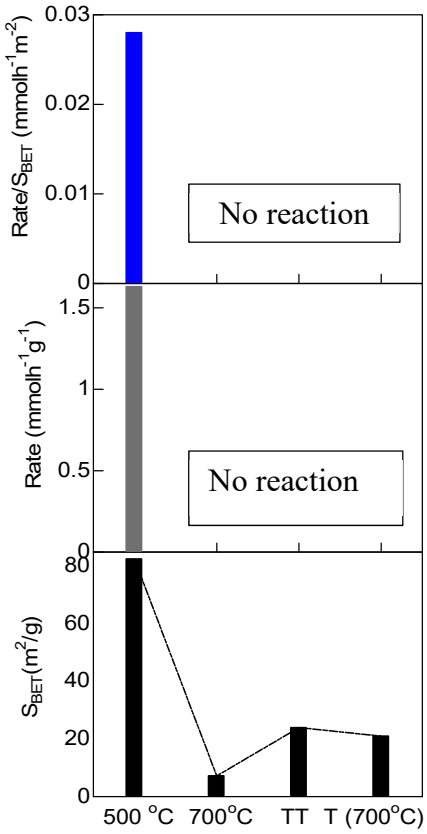

Figure 3.10. A comparative study of different Nb_2O_5 catalysts for amidation of acetic acid with ammonia.

3.3.8 Catalytic properties and scopes of amidation reaction

Using the standard reaction conditions (acid 1.0 mmol, NH_3 (g) 4.8 mmol, catalyst (50 mg), reaction temperature 100 °C) we investigated the time course of the reaction to explore the full catalytic cycle (Figure 12). From the concentration/time plot of reactive components it was found that the reaction time 15 h was enough to obtain the highest conversion and selectivity of the product. No by-product was observed until completion of the reaction.

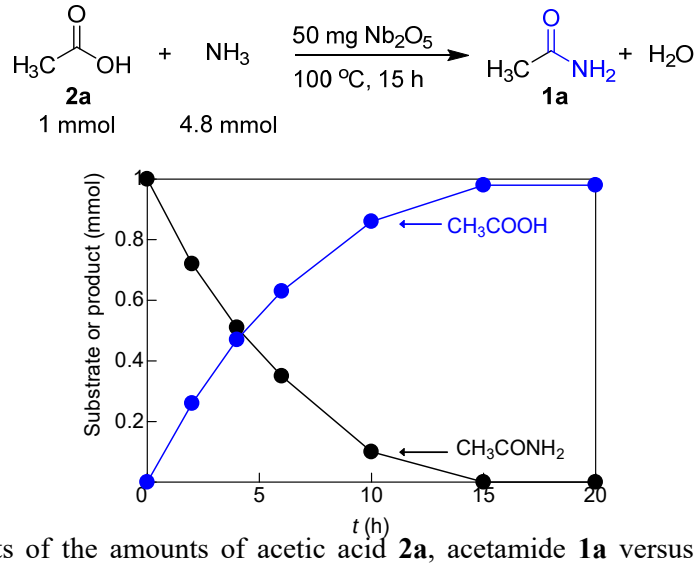

Figure 12. Plots of the amounts of acetic acid **2a**, acetamide **1a** versus reaction time over Nb_2O_5 catalysts under standard reaction condition Table 4 entry 2.

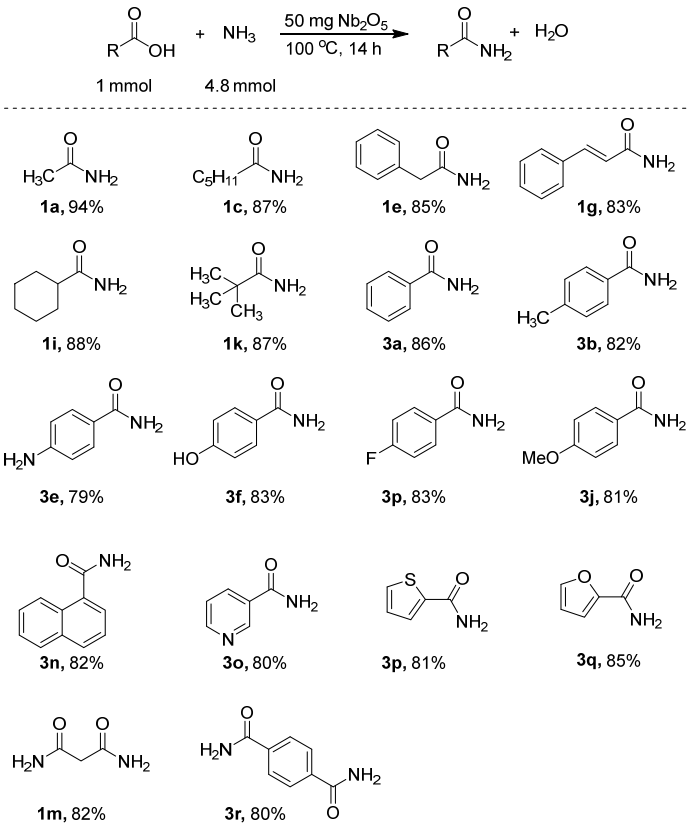

Scheme 4. Nb_2O_5-catalyzed amidation of different carboxylic acids to the corresponding amides. Isolated yields are shown.

After finalizing optimized reaction conditions, the substrate scopes using various aliphatic and aromatic carboxylic acids were explored. In Scheme 4**,** several aliphatic and aromatic acids having various functionalities were screened. Linear (1a, 1c), benzylic (1e), allylic (1g), cyclic (1i), pivaloyl (1k) and aromatic acids containing electron donating (3a, 3b, 3e, 3f) and withdrawing groups (3p, 3j) and naphthyl acid (3n) undertook amidation to their corresponding amides with excellent isolated yields (79-94%). Heteroatoms like N, S and O-containing acids also transformed into their corresponding amides (3o, 3p, 3q) successfully with good isolated yield. Moreover, our present catalytic system synthesizes both aliphatic and aromatic diamides (1m, 3r) from diacids efficiently.

3.3.9 NMR and GC/MS analysis of final products

^1H and ^{13}C NMR spectra of the products were assigned and reproduced to the corresponding literature. ^1H and ^{13}C NMR spectra were recorded using at ambient temperature on *J*EOL-ECX 600 operating at 600.17 MHz and 150.92 MHz and JEOL-ECX 400-2 operating at 399.78 MHz and 100.52 MHz respectively with tetramethylsilane as an internal standard. Abbreviations used in the NMR experiments: s, singlet; d, doublet; t, triplet; q, quartet; m, multiplet. GC-MS spectra were taken by SHIMADZU QP2010.

Acetic acid:[1]

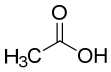

^1H NMR (600.17 MHz, DMSO-d6): δ 11.94 (s, 1H), 1.89 (s, 3H); ^{13}C NMR (150.92 MHz, DMSO-d6) δ 172.18, 21.12; GC-MS m/e: 60.05.

Propionic Acid:[63]

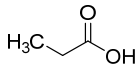

^1H NMR (600.17 MHz, DMSO-d6): δ 11.95 (s, 1H), 2.22-2.18 (m, 2H), 0.98 (t, *J* =7.56 Hz , 3H); ^{13}C NMR (150.92 MHz, DMSO-d6) δ 175.27, 26.94, 9.13; GC-MS m/e: 74.05.

Hexanoic Acid:[50]

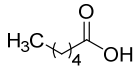

^{1}H NMR (600.17 MHz, DMSO-d6): δ 11.96 (s, 1H), 2.18 (t, *J* =7.56 Hz ,2H), 1.51-1.42 (m, 2H), 1.32-1.19 (m, 4H), 0.85 (t, *J* =7.08 Hz, 3H); ^{13}C NMR (150.92 MHz, DMSO-d6) δ 174.52, 33.65, 30.81, 24.21, 21.87, 13.84; GC-MS m/e: 116.15.

Tetradecanoic Acid:[50]

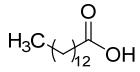

^{1}H NMR (600.17 MHz, DMSO-d6): δ 11.96 (s, 1H), 2.17 (t, *J* =7.56 Hz ,2H), 1.48-1.42 (m, 2H), 1.29-1.19 (m, 20H), 0.85 (t, *J* =7.05 Hz, 3H); ^{13}C NMR (150.92 MHz, DMSO-d6) δ 174.50, 33.67, 31.31, 30.81, 29.03 (C×2), 28.92 , 28.75, 28.72 (C×2), 28.56, 24.50, 22.11, 13.96; GC-MS m/e: 228.35.

Heptadecanoic Acid:[64]

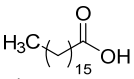

^{1}H NMR (600.17 MHz, DMSO-d6): δ 11.68 (s, 1H), 2.18 (t, *J* =7.56 Hz ,2H), 1.54-1.49 (m, 2H), 1.34-1.19 (m, 28H), 0.86 (t, *J* =6.87 Hz, 3H); ^{13}C NMR (150.92 MHz, DMSO-d6) δ 173.85, 33.40, 30.90, 30.80, 28.61 (C×2), 28.49 (C×2), 28.31 (C×2), 28.26 (C×2), 28.21 (C×2), 24.17, 21.65, 13.42; GC-MS m/e: 270.45.

Phenyl Acetic acid:[65]

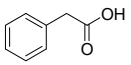

^{1}H NMR (600.17 MHz, DMSO-d6): δ 11.32 (s, 1H), 7.30 (t, *J* =7.44 Hz ,2H), 7.27-7.21 (m, 3H), 3.56 (s, 2H); ^{13}C NMR (150.92 MHz, DMSO-d6) δ 172.75, 135.06, 129.40 (C×2), 128.26 (C×2), 126.61, 40.72; GC-MS m/e: 136.15.

3-Phenyl -acrylic Acid:[50]

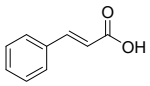

^{1}H NMR (600.17 MHz, DMSO-d6): δ 11.46 (s, 1H), 7.65 (t, *J* =8.22 Hz ,2H), 7.62 (t, *J* =8.12 Hz ,1H), 7.40-7.361 (m, 3H), 6.54 (t, *J* =8.012 Hz ,1H); ^{13}C NMR (150.92 MHz, DMSO-d6) δ 167.80, 144.09, 134.39, 130.32, 129.02 (C×2), 128.31 (C×2), 119.38; GC-MS m/e: 148.15.

Naphthalene-2-yl-acetic acid:[66]

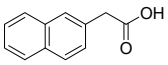

^{1}H NMR (600.17 MHz, DMSO-d6): δ 12.43 (s, 1H), 7.97 (d, *J* =8.10 Hz, 1H), 7.92 (d, *J* =8.04 Hz, 1H), 7.84 (d, *J* =8.04 Hz, 1H), 7.58-7.351 (m, 2H), 7.48-7.34 (m, 2H), 4.04 (s, 2H); ^{13}C NMR (150.92 MHz, DMSO-d6) δ 172.78, 133.34, 131.89, 131.69, 128.46, 128.01, 127.40,

126.18, 125.72, 125.54, 124.04, 38.50; GC-MS m/e: 186.20.

Cyclohexanecarboxylic acid:[66]

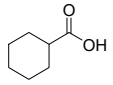

^{1}H NMR (600.17 MHz, DMSO-d6): δ 11.94 (s, 1H), 2.20-2.15 (m, 1H), 1.82-1.76 (m, 2H), 1.68-1.62 (m, 2H), 1.59-1.531 (m, 2H), 1.33-1.14 (m, 5H); ^{13}C NMR (150.92 MHz, DMSO-d6) δ 176.75, 42.28, 28.73, 25.52 (C×2), 25.01 (C×2); GC-MS m/e: 128.15.

2-hydroxypropionic Acid:[63]

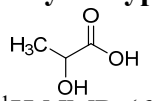

^{1}H NMR (600.17 MHz, DMSO-d6): δ 12.51 (s, 1H), 5.13 (d, *J* =8.64 Hz, 1H), 4.04-4.01(m, 1H), 1.19 (d, *J* =6.91 Hz, 3H); ^{13}C NMR (150.92 MHz, DMSO-d6) δ 176.41, 65.83, 20.51; GC-MS m/e: 90.08.

Propionic Acid:[63]

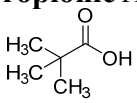

^{1}H NMR (600.17 MHz, DMSO-d6): δ 12.01 (s, 1H), 1.10 (s, 9H); ^{13}C NMR (150.92 MHz, DMSO-d6) δ 179.37, 37.92, 27.01 (C×3); GC-MS m/e102.15.

Malonic Acid:[63]

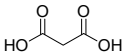

^{1}H NMR (600.17 MHz, DMSO-d6): δ 12.60 (br s, 2H), 3.23 (s, 2H); ^{13}C NMR (150.92 MHz, DMSO-d6) δ 168.50 (C×2), 41.99; GC-MS m/e104.05.

Adamantane -1-carboxylic acid:[67]

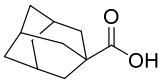

^{1}H NMR (600.17 MHz, DMSO-d6): δ 11.97 (s, 1H), 1.94 (br s, 9H), 1.78 (s, 6H), 1.68-1.62 (m, 5H); ^{13}C NMR (150.92 MHz, DMSO-d6) δ 178.44, 38.49 (C×4), 36.04 (C×3), 30.71 (C×2), 27.38; GC-MS m/e180.25.

Benzoic acid:[64]

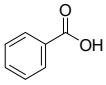

^{1}H NMR (600.17 MHz, DMSO-d6): δ 12.96 (s, 1H), 7.94 (d, *J* =8.04 Hz, 2H), 7.61 (t, *J* =6.87 Hz, 2H), 7.49 (t, *J* =6.87 Hz ,2H); ^{13}C NMR (150.92 MHz, DMSO-d6) δ 167.50, 133.02,

130.93, 129.44 (C×2), 128.73 (C×2); GC-MS m/e: 122.10.

4-methyl benzoic acid:[64]

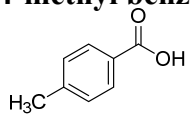

^{1}H NMR (600.17 MHz, DMSO-d6): δ 12.79 (s, 1H), 7.83 (d, *J* =7.68 Hz, 2H), 7.26 (d, *J* =7.68 Hz, 2H), 2.34 (s, 3H); ^{13}C NMR (150.92 MHz, DMSO-d6) δ 167.41, 143.08, 129.41, 129.17, 128.12 (C×2), 21.17; GC-MS m/e: 136.15.

3-methyl benzoic acid:[64]

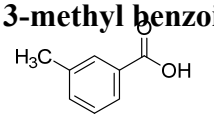

^{1}H NMR (600.17 MHz, DMSO-d6): δ 10.83 (s, 1H), 8.28 (d, *J* =8.22 Hz, 2H), 7.94 (d, *J* =8.14 Hz, 2H), 1.73 (s, 9H); ^{13}C NMR (150.92 MHz, DMSO-d6) δ 167.42, 137.90, 133.46, 130.74, 129.74, 128.46, 126.46, 20.82; GC-MS m/e: 136.15.

4-*tert*- butyl benzoic acid:[64]

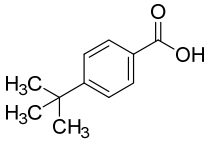

^{1}H NMR (600.17 MHz, DMSO-d6): δ 12.87 (s, 1H), 7. 7.61 (d, *J* =8.10 Hz, 2H), 6.53 (d, *J* =8.10 Hz, 2H), 5.86 (br s, 2H); ^{13}C NMR (150.92 MHz, DMSO-d6) δ 166.27, 155.21, 130.37 (C×2), 127.83, 125.82 (C×2), 35.23, 31.44 (C×3); GC-MS m/e: 178.25.

4-amino benzoic acid:[64]

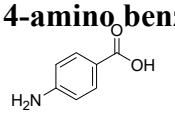

^{1}H NMR (600.17 MHz, DMSO-d6): δ 11.96 (br s, 1H), 7.79-7.71 (m, 2H), 7.42 (d, *J* =7.32 Hz, 1H), 7.39-7.34 (m, 1H), 2.35 (s, 3H); ^{13}C NMR (150.92 MHz, DMSO-d6) δ 166.59, 153.21, 131.31 (C×2), 116.93, 112.63 (C×2); GC-MS m/e: 137.15.

2-hydroxy benzoic acid:[64]

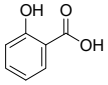

^{1}H NMR (600.17 MHz, DMSO-d6): δ 14.00 (br s, 1H), 11.30 (br s, 1H), 7.78 (d, *J* =6.85 Hz, 1H), 7.52-7.48 (m, 1H), 6.96-7.91 (m, 2H); ^{13}C NMR (150.92 MHz, DMSO-d6) δ 171.95, 161.14, 135.69, 130.28, 119.21, 117.11, 112.66; GC-MS m/e: 137.10.

3-fluro benzoic acid:[64]

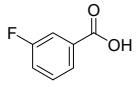

^{1}H NMR (600.17 MHz, DMSO-d6): δ 13.29 (br s, 1H), 7.77 (d, *J* =7.08 Hz, 1H), 7.64 (d, *J* =8.22 Hz, 1H), 7.57-7.51 (m, 1H), 7.46 (t, *J* =7.56 Hz, 1H); ^{13}C NMR (150.92 MHz, DMSO-d6) δ 166.25, 162.02 (d, *J* =244.20 Hz) 133.30 (d, *J* =6.03Hz), 130.82 (d, *J* =6.03 Hz), 125. 48, 119.89 (d, *J* =20.23 Hz), 115.79 (d, *J* =22.63 Hz); GC-MS m/e: 140.10.

4-methoxy benzoic acid:[64]

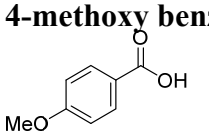

^{1}H NMR (600.17 MHz, DMSO-d6): δ 12.62 (s, 1H), 7.85 (d, *J* =8.75 Hz, 2H), 7.00 (d, *J* =8.75 Hz, 2H), 3.82 (s, 3H); ^{13}C NMR (150.92 MHz, DMSO-d6) δ 167.01, 162.85, 131.36 (C×2), 122.83, 113.82 (C×2), 55.45; GC-MS m/e: 152.15.

4-methoxy benzoic acid:[64]

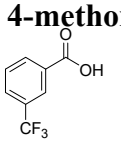

^{1}H NMR (600.17 MHz, DMSO-d6): δ 13.54 (s, 1H), 8.21 (d, *J* =7.02 Hz, 1H), 8.16 (s, 1H), 7.97 (d, *J* =8.10 Hz, 1H), 7.74 (d, *J* =7.56 Hz, 1H), 3.82 (s, 3H); ^{13}C NMR (150.92 MHz, DMSO-d6) δ 166.06, 133.23, 132.04, 130.07, 129.46(d, *J* =24.14 Hz), 129.35 (d, *J* =4.33 Hz), 125.54 (d, *J* =4.33 Hz), 123.83 (d, *J* =271.65 Hz); GC-MS m/e: 190.10

4-nitro benzoic acid:[64]

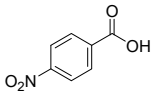

^{1}H NMR (600.17 MHz, DMSO-d6): δ 13.66 (s, 1H), 8.30 (d, *J* =7.98 Hz, 1H), 8.15 (d, *J* =7.98 Hz, 1H); ^{13}C NMR (150.92 MHz, DMSO-d6) δ 166.83, 150.05, 136.38, 130.72 (C×2), 123.74 (C×2); GC-MS m/e: 167.10.

Naphthalen-2-carboxylic acid:[68]

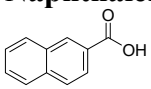

^{1}H NMR (600.17 MHz, DMSO-d6): δ 13.10 (br s, 1H), 8.61 (s, 1H), 8.10 (d, *J* =7.98 Hz, 1H), 8.01-7.94 (m, 3 H), 7.64 (t, *J* =7.44 Hz, 1H), 7.59 (d, *J* =7.44 Hz, 1H), 7.57 (t, *J* =7.56 Hz, 1H),; ^{13}C NMR (150.92 MHz, DMSO-d6) δ 167.49, 134.96, 132.18, 130.56, 129.31, 128.35, 128.20, 128.10 (C×2), 127.68 (C×2), 126.84, 125.20; GC-MS m/e: 172.15.

Naphthalen-1-carboxylic acid:[68]

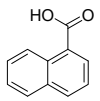

^{1}H NMR (600.17 MHz, DMSO-d6): δ 13.15 (br s, 1H), 8.85 (d, *J* =7.98 Hz, 1H), 8.14 (d, *J* =6.90 Hz, 2H), 8.01 (d, *J* =6.84 Hz, 1H), 7.63 (t, *J* =7.22 Hz, 1H), 7.58 (d, *J* =7.82 Hz, 2H); ^{13}C NMR (150.92 MHz, DMSO-d6) δ 168.66, 133.47, 132.95, 130.68, 129.87, 128.62, 127.52, 126.20, 124.89; GC-MS m/e: 172.15.

Nicotinic acid:[64]

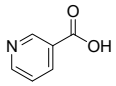

^{1}H NMR (600.17 MHz, DMSO-d6): δ 13.43 (br s, 1H), 8.77 (d, *J* =7.56 Hz, 1H), 8.25 (d, *J* =8.04 Hz, 1H), 7.52 (t, *J* =8.04 Hz, 1H); ^{13}C NMR (150.92 MHz, DMSO-d6) δ 166.34, 153.32, 150.29, 137.02, 126.63, 123.85; GC-MS m/e: 123.10.

Thiophene-2-carboxylic acid:[68]

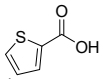

^{1}H NMR (600.17 MHz, DMSO-d6): δ 13.04 (br s, 1H), 7.90-7.86 (m, 1H), 7.72 (d, *J* =7.02 Hz, 1H), 7.18 (t, *J* =6.54 Hz, 1H); ^{13}C NMR (150.92 MHz, DMSO-d6) δ 162.94, 134.67, 133.30, 133.25, 128.25; GC-MS m/e: 128.15.

Terephthalic acid:[64]

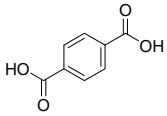

^{1}H NMR (600.17 MHz, DMSO-d6): δ 13.29 (br s, 2H), 8.05 (s, 4H); ^{13}C NMR (150.92 MHz, DMSO-d6) δ 166.74 (C×2), 134.50(C×2), 129.53 (C×4); GC-MS m/e: 166.15.

Acetamide:[68]

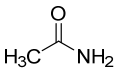

^{1}H NMR (600.17 MHz, DMSO-d6): δ 7.30 (s, 1H), 6.71 (s, 1H), 1.752 (s, 3H); ^{13}C NMR (150.92 MHz, DMSO-d6) δ 171.66, 22.54; GC-MS m/e: 59.05.

Hexanoic acid amide:[50]

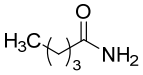

^{1}H NMR (600.17 MHz, DMSO-d6): δ 7.22(s, 1H), 6.68 (s, 1H), 2.01 (t, *J* =7.22 Hz ,2H), 1.50-1.44 (m, 2H), 1.29-1.19 (m, 4H), 0.85 (t, *J* =7.44 Hz, 3H); ^{13}C NMR (150.92 MHz, DMSO-d6) δ 174.38, 35.10, 30.98, 24.82, 21.93, 13.89; GC-MS m/e: 115.15.

2-Phenyl Acetamide:[65]

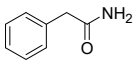

^{1}H NMR (600.17 MHz, DMSO-d6): δ 7.47 (s, 1H), 7.29 (t, *J* =7.44 Hz ,2H), 7.26 (d, *J* =6.84 Hz ,2H), 7.21 (t, *J* =7.22 Hz ,1H), 6.88 (s, 1H), 3.36 (s, 2H); ^{13}C NMR (150.92 MHz, DMSO-d6) δ 172.24, 135.53, 129.08 (C×2), 128.16 (C×2), 126.27, 42.28; GC-MS m/e: 135.15.

3-Phenyl-acrylic Acid:[50]

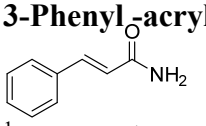

^{1}H NMR (600.17 MHz, DMSO-d6): δ 7.47(s, 1H), 7.71 (d, *J* =8.94 Hz , 2H), 7.66 (t, *J* =7.56 Hz ,1H), 7.40-7.36 (m, 3H), 6.64 (s ,1H); ^{13}C NMR (150.92 MHz, DMSO-d6) δ 166.73, 144.09, 139.21, 134.89, 129.47, 128.94, 127.56, 122.34; GC-MS m/e: 135.15.

Cyclohexane carboxylic acid amide:[66]

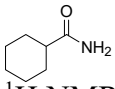

^{1}H NMR (600.17 MHz, DMSO-d6): δ 7.14 (s, 1H), 6.62. (s, 1H), 2.06-2.01 (m, 1H), 1.68 (d, *J* =8.32 Hz , 2H), 1.59 (d, *J* =8.22 Hz , 2H), 1.32-1.10 (m, 5H); ^{13}C NMR (150.92 MHz, DMSO-d6) δ 177.33, 43.69, 29.18, 25.54 (C×2), 25.33 (C×2); GC-MS m/e: 127.15.

2,2-dimethylPropionamide:[63]

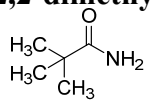

^{1}H NMR (600.17 MHz, DMSO-d6): δ 7.01(s, 1H), 6.69 (s, 1H), 1.06 (s, 9H); ^{13}C NMR (150.92 MHz, DMSO-d6) δ 179.91, 37.79, 27.52 (C×3); GC-MS m/e101.15.

Benzamide:[64]

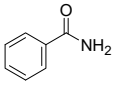

^{1}H NMR (600.17 MHz, DMSO-d6): δ 7.99 (s, 1H), 7.88 (d, *J* =6.90 Hz, 2H), 7.50 (t, *J* =6.44 Hz, 1H), 7.44 (t, *J* =7.44 Hz ,2H), 7.39 (s, 1H) ; ^{13}C NMR (150.92 MHz, DMSO-d6) δ 167.97, 134.29, 131.26, 128.24 (C×2), 127.50 (C×2); GC-MS m/e: 121.15.

4-methyl benzamide:[64]

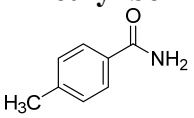

^{1}H NMR (600.17 MHz, DMSO-d6): δ 7.77 (s, 1H), 7.76 (d, *J* = 8.04 Hz, 2H), 7.26 (s, 1H), 7.23 (d, *J* =8.04 Hz, 2H), 2.33 (s, 3H); ^{13}C NMR (150.92 MHz, DMSO-d6) δ 167.78, 141.06, 131.48, 128.73, 127.51 (C×2), 20.96; GC-MS m/e: 135.15.

4-amino benzamide:[64]

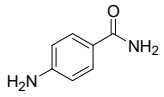

^{1}H NMR (600.17 MHz, DMSO-d6): δ 7.58 (t, *J* = 6.87 Hz, 2H), 7.53 (s, 1H), 6.86 (s, 1H), 6.51 (t, *J* =6.87 Hz, 2H), 5.60 (s, 2H); ^{13}C NMR (150.92 MHz, DMSO-d6) δ 168.14, 151.70, 129.16 (C×2), 120.96, 112.50 (C×2); GC-MS m/e: 136.15.

3-fluro benzamide:[64]

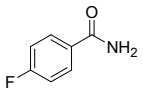

^{1}H NMR (600.17 MHz, DMSO-d6): δ 8.01 (s, 1H), 7.94 (t, *J* =7.44 Hz, 2H), 7.41 (s, 1H), 7.26 (t, *J* =4.88 Hz, 2H); ^{13}C NMR (150.92 MHz, DMSO-d6) δ 166.25, 162.02 (d, *J* =244.20 Hz) 133.30 (d, *J* =6.03Hz), 130.82 (d, *J* =6.03 Hz), 125. 48, 119.89 (d, *J* =20.23 Hz), 115.79 (d, *J* =22.63 Hz); GC-MS m/e: 139.15.

4-methoxy benzamide:[64]

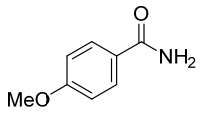

^{1}H NMR (600.17 MHz, DMSO-d6): δ 7.85 (d, *J* =9.18 Hz, 3H), 7.18 (s, 1H), 6.96 (d, *J* =9.12 Hz, 2H), 3.79 (s, 3H); ^{13}C NMR (150.92 MHz, DMSO-d6) δ 167.42, 161.58, 129.36 (C×2), 126.50, 113.39 (C×2), 55.32; GC-MS m/e: 152.15

Nicotinamide:[64]

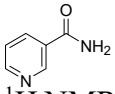

^{1}H NMR (600.17 MHz, DMSO-d6): δ 9.02 (s, 1H), 8.69 (s, 1H), 8.19 (d, *J* =7.98 Hz, 1H), 8.16 (s, 1H), 7.61 (s, 1H), 7.49 (t, *J* =6.30 Hz, 1H), 7.52 (t, *J* =8.04 Hz, 1H); ^{13}C NMR (150.92 MHz, DMSO-d6) δ 166.48, 151.93, 148.71, 135.18, 129.68, 123.45; GC-MS m/e: 122.10.

Naphthalen-1-carboxylic acid amide:[68]

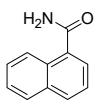

^{1}H NMR (600.17 MHz, DMSO-d6): δ 8.32 (d, *J* =7.98 Hz, 1H), 8.02 (s, 1H), 7.99 (d, *J* =7.98 Hz, 1H), 7.96 (d, *J* =9.18 Hz, 1H), 7.65 (d, *J* =6.92 Hz, 1H), 7.62 (s, 1H), 7.58 -7.52(m, 3H); ^{13}C NMR (150.92 MHz, DMSO-d6) δ 170.63, 134.67, 133.21, 129.80, 129.73, 128.19, 126.63, 126.15, 125.60, 125.16, 124.95; GC-MS m/e: 171.20.

Thiophene-2-carboxylic acid amide:[68]

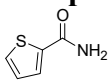

^{1}H NMR (600.17 MHz, DMSO-d6): δ 7.97 (br s, 1H), 7.75-7.72 (m, 2H), 7.39 (br s, 1H), 7.12 (t, *J* =7.98 Hz, 1H); ^{13}C NMR (150.92 MHz, DMSO-d6) δ 162.93, 140.34, 131.01, 128.69, 127.93; GC-MS m/e: 127.15.

Furan-2-carboxylic acid amide:[68]

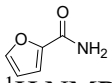

^{1}H NMR (600.17 MHz, DMSO-d6): δ 7.79 (s, 1H), 7.76 (s, 1H), 7.36 (s, 1H), 7.08 (d, *J* =3.48 Hz, 1H), 6.58 (d, *J* =3.42 Hz, 1H); ^{13}C NMR (150.92 MHz, DMSO-d6) δ 159.42, 140.06, 145.03, 113.62, 111.80; GC-MS m/e: 111.10.

Terephthalamide:[64]

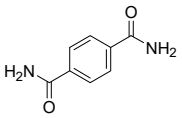

^{1}H NMR (600.17 MHz, DMSO-d6): δ 8.06 (s, 2H), 7.92 (s, 4H), 7.49 (s, 2H),; ^{13}C NMR (150.92 MHz, DMSO-d6) δ 166.26 (C×2), 136.57(C×2), 127.37 (C×4); GC-MS m/e: 164.15.

Malonamide:[63]

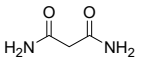

^{1}H NMR (600.17 MHz, DMSO-d6): δ 7.44 (s, 2H), 7.03 (s, 2H), 2.94 (s, 2H); ^{13}C NMR (150.92 MHz, DMSO-d6) δ 169.20 (C×2), 43.14; GC-MS m/e102.10.

Conclusions

We have developed an efficient, simple, mild and versatile heterogenous Nb_2O_5 catalytic system for two challenging reactions: 1) hydrolysis of amides to carboxylic acids and 2) amidation of carboxylic acids to amides with ammonia. Here, it is obtained that the quantity and strength of Lewis acid (LA) sites of Nb_2O_5 catalysts are dependent on their structure and morphology, where the surface area and no. of LA sites as well as their interaction with carbonyl group are decreased with the increase of catalyst calcination temperature. However, low temperature calcined TT and T-phased Nb_2O_5 are found more reactive towards hydrolysis-amidation reactions than that of high temperature calcined (M and H-phased) one. Further, based on comparative kinetic study, it suggests that even though T-phase of Nb_2O_5 catalyzes hydrolysis reaction effectively but amidation is found as solely phase independent reaction. The catalytic performance is attributed to the facile activation of carbonyl bond (soft

base) by surface Nb^{5+} LA sites even in presence of hard bases like as H_2O and NH_3.

References

[1] H. T. Kreissl, M. M. J. Li, Y. K. Peng, K. Nakagawa, T. J. N. Hooper, J. V. Hanna, A. Shepherd, T. S. Wu, Y. L. Soo, S. C. E. Tsang, *J. Am. Chem. Soc.* **2017**, *139*, 12670–12680.

[2] C. Nico, T. Monteiro, M. P. F. Graça, *Prog. Mater. Sci.* **2016**, *80*, 1–37.

[3] F. S. H. Schafer, R. Gruehn, *Angew. Chemie - Int. Ed.* **1966**, *5*, 40–52.

[4] S. Li, Q. Xu, E. Uchaker, X. Cao, G. Cao, *CrystEngComm* **2016**, *18*, 2532–2540.

[5] K. Shimizu, S. M. A. H. Siddiki, M. N. Rashed, M. A. Ali, T. Toyao, P. Hirunsit, M. Ehara, *ChemCatChem* **2018**, 1–15.

[6] T. Murayama, J. Chen, J. Hirata, K. Matsumoto, W. Ueda, *Catal. Sci. Technol.* **2014**, *4*, 4250–4257.

[7] I. Nowak, M. Ziolek, *Chem. Rev.* **1999**, *99*, 3603–3624.

[8] X. Fang, L. Hu, K. Huo, B. Gao, L. Zhao, M. Liao, P. K. Chu, Y. Bando, D. Golberg, *Adv. Funct. Mater.* **2011**, *21*, 3907–3915.

[9] K. Nakagawa, T. Jia, W. Zheng, S. M. Fairclough, M. Katoh, S. Sugiyama, S. C. Edman Tsang, *Chem. Commun.* **2014**, *50*, 13702–13705.

[10] K. Tanabe, *Catal. Today* **2003**, *78*, 65–77.

[11] R. A. Rani, A. S. Zoolfakar, A. P. O'Mullane, M. W. Austin, K. Kalantar-Zadeh, *J. Mater. Chem. A* **2014**, *2*, 15683–15703.

[12] J.-M. Jehng, I. E. Wachs, *Chem. Mater.* **1991**, *3*, 100–107.

[13] M. B. Pinto, A. L. Soares, A. Mella Orellana, H. A. Duarte, H. A. De Abreu, *J. Phys. Chem. A* **2017**, *121*, 2399–2409.

[14] Y. Zhao, X. Zhou, L. Ye, S. Chi Edman Tsang, *Nano Rev.* **2012**, *3*, 17631.

[15] J. G. Weissman, E. I. Ko, P. Wynblatt, J. M. Howe, *Chem. Mater.* **1989**, *1*, 187–193.

[16] A. Le Viet, M. V. Reddy, R. Jose, B. V. R. Chowdari, S. Ramakrishna, *J. Phys. Chem. C* **2010**, *114*, 664–671.

[17] L. A. Reznichenko, V. V. Akhnazarova, L. A. Shilkina, O. N. Razumovskaya, S. I. Dudkina, *Crystallogr. Reports* **2009**, *54*, 483–491.

[18] A. M. Raba, J. Barba-Ortega, M. R. Joya, *Appl. Phys. A Mater. Sci. Process.* **2015**, *119*, 923–928.

[19] J. M. Jehng, I. E. Wachs, *J. Phys. Chem.* **1991**, *95*, 7373–7379.

[20] T. McQueen, Q. Xu, E. N. Andersen, H. W. Zandbergen, R. J. Cava, *J. Solid State Chem.* **2007**, *180*, 2864–2870.

[21] G. E. Fernandez, *J. Phys. Chem Solids* **1998**, *59*, 867–870.

[22] K. Kato, S. Tamura, *Acta Crystallogr. Sect. B* **1975**, *31*, 673–677.

[23] Y. Kobayashi, H. Hata, M. Salama, T. E. Mallouk, *Nano Lett.* **2007**, *7*, 2142–2145.

[24] R. G. W. mertin, S. Andersson, *J. solid state Chem.* **1970**, 419–424.

[25] S. M. A. H. Siddiki, M. N. Rashed, M. A. Ali, T. Toyao, P. Hirunsit, M. Ehara, K. Shimizu, *ChemCatChem* **2019**, *11*, 383–396.

[26] P. Hirunsit, T. Toyao, S. M. A. H. Siddiki, K. Shimizu, M. Ehara, *ChemPhysChem* **2018**, *19*, 2848–2857.

[27] T. Okuhara, *Chem. Rev.* **2002**, *102*, 3641–3666.

[28] A. Ali, S. K. Moromi, A. S. Touchy, K. Shimizu, *ChemCatChem* **2016**, *8*, 891–894.

[29] K. Nakajima, Y. Baba, R. Noma, M. Kitano, J. N. Kondo, S. Hayashi, M. Hara, *J. Am. Chem. Soc.* **2011**, *133*, 4224–4227.

[30] M. N. Rashed, S. M. A. H. Siddiki, M. A. Ali, S. K. Moromi, A. S. Touchy, K. Kon, T. Toyao, K. Shimizu, *Green Chem.* **2017**, *19*, 3238–3242.

[31] G. S. Nair, E. Adrijanto, A. Alsalme, I. V. Kozhevnikov, D. J. Cooke, D. R. Brown, N. R. Shiju, *Catal. Sci. Technol.* **2012**, *2*, 1173–1179.

[32] Q. Sun, Y. Fu, H. Yang, A. Auroux, J. Shen, *J. Mol. Catal. A Chem.* **2007**, *275*, 183–193.

[33] K. Nakajima, T. Fukui, H. Kato, M. Kitano, J. N. Kondo, S. Hayashi, M. Hara, *Chem. Mater.* **2010**, *22*, 3332–3339.

[34] H. T. Kreissl, K. Nakagawa, Y. K. Peng, Y. Koito, J. Zheng, S. C. E. Tsang, *J. Catal.* **2016**, *338*, 329–339.

[35] S. Okazaki, H. Harada, *Chem. Lett.* **1988**, *17*, 1313–1316.

[36] A. J. M. Van Dijk, R. Duchateau, E. J. M. Hensen, J. Meuldijk, C. E. Koning, *Chem. - A Eur. J.* **2007**, *13*, 7673–7681.

[37] G. S. Foo, D. Wei, D. S. Sholl, C. Sievers, *ACS Catal.* **2014**, *4*, 3180–3192.

[38] S. Furukawa, Y. Ohno, T. Shishido, K. Teramura, T. Tanaka, *ACS Catal.* **2011**, *1*, 1150–1153.

[39] S. Furukawa, T. Shishido, K. Teramura, T. Tanaka, *ChemPhysChem* **2014**, *15*, 2665–2667.

[40] S. Kobayashi, *European J. Org. Chem.* **1999**, *1999*, 15–27.

[41] K. Yamashita, M. Hirano, K. Okumura, M. Niwa, *Catal. Today* **2006**, *118*, 385–391.

[42] A. Takagaki, D. Lu, J. N. Kondo, M. Hara, S. Hayashi, K. Domen, *Chem. Mater.* **2005**,

17, 2487–2489.

[43] M. A. Ali, S. M. A. H. Siddiki, W. Onodera, K. Kon, K. Shimizu, *ChemCatChem* **2015**, *7*, 3555–3561.

[44] K. Nakajima, J. Hirata, M. Kim, N. K. Gupta, T. Murayama, A. Yoshida, N. Hiyoshi, A. Fukuoka, W. Ueda, *ACS Catal.* **2018**, *8*, 283–290.

[45] S. Kobayashi, K. Manabe, *Acc. Chem. Res.* **2002**, *35*, 209–217.

[46] Y. Koito, K. Nakajima, R. Hasegawa, H. Kobayashi, M. Kitano, M. Hara, *Catal. Today* **2014**, *226*, 198–203.

[47] Y. Koito, K. Nakajima, H. Kobayashi, R. Hasegawa, M. Kitano, M. Hara, *Chem. - A Eur. J.* **2014**, *20*, 8068–8075.

[48] L. Hie, N. F. Fine Nathel, T. K. Shah, E. L. Baker, X. Hong, Y.-F. Yang, P. Liu, K. N. Houk, N. K. Garg, *Nature* **2015**, *524*, 79–83.

[49] H. Nagae, T. Hirai, D. Kato, S. Soma, S. Akebi, K. Mashima, *Chem. Sci.* **2019**, DOI 10.1039/C8SC05819A.

[50] G. Li, P. Lei, M. Szostak, *Org. Lett.* **2018**, *20*, 5622–5625.

[51] T. Toyao, M. Nurnobi Rashed, Y. Morita, T. Kamachi, S. M. A. Hakim Siddiki, M. A. Ali, A. S. Touchy, K. Kon, Z. Maeno, K. Yoshizawa, et al., *ChemCatChem* **2019**, *11*, 449–456.

[52] L. Hie, E. L. Baker, S. M. Anthony, J.-N. Desrosiers, C. Senanayake, N. K. Garg, *Angew. Chemie Int. Ed.* **2016**, *55*, 15129–15132.

[53] Y. Kita, Y. Nishii, T. Higuchi, K. Mashima, *Angew. Chemie Int. Ed.* **2012**, *51*, 5723–5726.

[54] A. M. Barrios, S. J. Lippard, *J. Am. Chem. Soc.* **1999**, *121*, 11751–11757.

[55] J. I. Mujika, J. M. Mercero, X. Lopez, *J. Am. Chem. Soc.* **2005**, *127*, 4445–4453.

[56] V. Gotor, V. Gotor-Fernández, E. Busto, *Compr. Chirality* **2012**, *7*, 101–121.

[57] M. Heravi, D. Zargarani, R. Hekmat Shoar, S. Khaleghi, *J. Chem. Res.* **2005**.

[58] X. Zhang, K. Luo, W. Chen, L. Wang, *Chinese J. Chem.* **2011**, *29*, 2209–2212.

[59] M. Tamura, K. Shimizu, A. Satsuma, *"Applied Catal. A, Gen.* **2012**, *433–434*, 135–145.

[60] E. I. Ko, J. G. Weissman, *Catal. Today* **1990**, *8*, 27–36.

[61] R. Kodama, Y. Terada, I. Nakai, S. Komaba, N. Kumagai, *J. Electrochem. Soc.* **2006**, *153*, A583.

[62] Y. Bourne-Branchu, C. Gosmini, G. Danoun, *Chem. - A Eur. J.* **2017**, *23*, 10043–10047.

[63] Y. Inamoto, Y. Kaga, Y. Nishimoto, M. Yasuda, A. Baba, *Org. Lett.* **2013**, *15*, 3452–3455.

[64] J. Chen, Y. Peng, M. Liu, J. Ding, W. Su, H. Wu, *Adv. Synth. Catal.* **2012**, *354*, 2117–

2122.

[65] J. S. Ruso, N. Rajendiran, R. S. Kumaran, *Tetrahedron Lett.* **2014**, *55*, 2345–2347.

[66] H. N. Roy, A. H. Al Mamun, *Synth. Commun.* **2006**, *36*, 2975–2981.

[67] S. Chun, Y. K. Chung, *Org. Lett.* **2017**, *19*, 3787–3790.

[68] J. X. Xu, X. F. Wu, *Org. Lett.* **2018**, *20*, 5938–5941.

Chapter 4

Esterification of Tertiary Amides by Alcohols Through C–N Bond Cleavage over CeO_2

4.1 Introduction

Amides are important structural moieties in the preparation of a wide variety of pharmaceutical compounds and natural products.[1,2] Moreover, amides are thermodynamically stable compounds owing to delocalization of the nitrogen lone pair into the carbonyl moiety. Whereas C–N bonds of amides are readily cleaved under mild conditions by enzymes such as proteases,[3,4] similar non-enzymatic processes usually require strongly acidic or basic conditions.[5,6] Although much effort has been devoted to developing C–N bond cleavage reactions,[7–12] synthetic applications of amide chemistry are still limited by this reactivity issue. Among amide transformations, alcoholysis has received much attention because the resulting esters are more reactive and, as a result, undergo many useful transformations.[13] Although various non-catalytic methods have been reported for amide alcoholysis,[14–17] they generally suffer from the required use of excess amounts of promoters such as HCl and $NaNO_2$, the generation of inorganic or organic wastes, and limited substrate scope. It is noteworthy that twisted amides undergo alcoholysis under relatively mild neutral conditions.[18,19] However, synthetic application of these substances are very limited.

From the viewpoint of sustainable chemistry, amide alcoholysis ideally should be carried out using catalytic processes. In this context, Mashima and co-workers developed a catalytic amide alcoholysis protocol that uses $Zn(OTf)_2$, $Sc(OTf)_3$ or $Mn(acac)_2$ together with additives as promotors.[20–22] Later, Atkinson and co-workers demonstrated that $Sc(OTf)_3$ is an effective catalyst for this reaction.[23] Subsequently, our group described an amide alcoholysis reaction, which uses CeO_2 as a heterogeneous catalyst and does not require additives.[24] The CeO_2 catalyzed ester forming reaction occurs with 1-3 orders of magnitude higher rates than those promoted by other metal oxides. Moreover, the CeO_2 catalyzed reaction has a wide amide substrate scope and CeO_2 can be recycled. Furthermore, the results of density functional theory (DFT) calculations suggest that promotion of alcoholysis of primary amides by CeO_2 is a consequence of synergistic action of Lewis acid and base sites of the surface of the metal oxide.[25]

The reports describing both homogeneous and heterogeneous catalytic amide esterification processes represent important contributions to the field of synthetic chemistry. However, the fact that these catalytic reactions only apply to primary and secondary amides limits their preparative versatility. In general, C–N bond cleavage reactions of tertiary amides are more difficult owing to the higher degree of steric blocking of the carbonyl group and thermodynamic limitations associated with reverse reactions between ester and secondary amine products, which are more facile than those of NH_3 and primary amines produced from

primary and secondary amides.[26,27] In order to overcome this limitation, Garg and co-workers recently developed a method for conversion of various amides, including tertiary amides, to the corresponding esters that utilizes a Ni-based N-heterocyclic carbene (NHC) complex as a catalyst.[27] In addition, this strategy was extended to develop a C–C bond forming reaction that produces ketones from tertiary amides.[28,29] Several subsequent reports have described the use of similar catalysts (e.g., Pd-based NHC complexes) for C–N bond cleavage reactions of tertiary amides.[30,31] Although enhancing the synthetic importance of C–N bond cleavage reactions, the processes require additives and/or the use of elaborate ligand such as NHC, and difficulties are encountered with catalyst recycling. In order to be environmentally benign and adaptable to large-scales, catalyst employed for amide C–N bond cleavage reactions need to be readily available, heterogeneous and recyclable. To the best of our knowledge, such recyclable and additive-free heterogeneous systems have not yet been reported.

In the studies described below, we have described a heterogeneous catalytic system for esterification of tertiary amides by alcohols, which utilizes CeO_2 as the catalyst. The developed catalytic process is facile and it has a wide amide and alcohol substrate scope. The combined results arising from theoretical and experimental studies indicate that the reaction proceeds through the same mechanistic pathway followed in the alcoholysis reaction of primary amides. Importantly, cooperative effects of acid-base functions of CeO_2 would be a key for efficient promotion of the reaction. The results of this investigation have not only demonstrated the utility of a new C–N bond cleavage reaction of amides, they have also led to a better understanding of the behavior of CeO_2, a catalyst that has attracted much attention recently.[32–36]

4.2 Experimental Section

4.2.1 Materials and Catalyst Preparation

Organic and inorganic compounds were purchased from common commercial suppliers (Tokyo Chemical Industry, Kanto Chemical, Wako Pure Chemical Industries, Nacalai Tesque, and SigmaAldrich) and used without further purification. CeO_2 was prepared by calcination (T = 600 °C, t = 3 h, in air) of CeO_2 supplied from Daiichi Kigenso Kagaku Kogyo Co., Ltd (Type A). TiO_2 (JRC-TIO-8), MgO (JRC-MGO-3), SiO_2-Al_2O_3 (JRC-SAL-2, Al_2O_3 = 13.75 wt%) and H-Beta zeolite (SiO_2/Al_2O_3 = 25±5, JRC-Z-HB25) were supplied by the Catalysis Society of Japan. γ-Al_2O_3 was prepared by calcination of γ-AlOOH (Catapal B Alumina, Sasol) at 900 °C for 3 h. SiO_2 (Q-10) was supplied by Fuji Silysia Chemical Ltd. SiO_2 (Q-10) was supplied by Fuji Silysia Chemical Ltd., while Nb_2O_5 was prepared by calcination (T = 500 °C,

t = 3 h) of niobic acid (CBMM). ZnO was prepared by calcination (T = 500 °C, t = 3 h) of a hydroxide of Zn (Kishida Chemical). ZrO_2 was prepared by calcining Zr hydroxide at 773 K for 3 h that was made via hydrolysis of $ZrO(NO_3)_2 \cdot 2H_2O$ with an aqueous NH_4OH solution. SnO_2 was prepared by calcination (T = 500 °C, t = 3 h) of H_2SnO_3 (Kojundo Chemical Laboratory Co., Ltd.). CaO was prepared by calcination (T = 500 °C, t = 3 h) of $Ca(OH)_2$ (Kanto Chemical)). H-ZSM-5 (SiO_2/AI_2O_3 = 22) and HY (SiO_2/AI_2O_3 = 5.5) zeolites were obtained from TOSO Co., Ltd. Sulfated ZrO_2 was kindly provided by Wako Pure Chemical Industries. Sulfonic resins (Amberlyst-15 and Nafion-SiO_2 composite) were purchased from Sigma-Aldrich.

4.2.2 Catalyst Characterization

In situ FT-IR spectra were recorded at 120 °C by using a JASCO FT/IR-4200 with an MCT (Mercury-Cadmium-Telluride) detector. A sample (40 mg) was pressed to obtain a self-supporting pellet (ϕ = 2 cm). The obtained pellet was placed in the quartz IR cell with CaF_2 windows connected to a conventional gas flow system. Prior to the measurement, the sample pellet was heated under He flow (20 cm^3 min^{-1}) at 500 °C for 0.5 h. After cooling to 120 °C under the He flow, 1 μL of *N,N*-dimethylacetamide was injected to the sample through a line which was preheated at ca. 200 °C to vaporize *N,N*-dimethylacetamide. Spectra were measured accumulating 15 scans at a resolution of 4 cm^{-1}. A reference spectrum taken at 120 °C under He flow was subtracted from each spectrum.

X-ray diffraction (XRD; Rigaku Miniflex) measurements were conducted using CuKα radiation. BET (Brunauer-Emmett-Teller) specific surface area of CeO_2 was determined to be 81 m^2 g^{-1} from N_2 adsorption data measured by using BELCAT (MicrotracBEL). Transmission electron microscopy (TEM) was measured using a JEOL JEM-2100F TEM operated at 200 kV. Inductively coupled plasma-atomic emission spectroscopy (ICP-AES) analysis was carried out by using a SHIMADZU ICPE-9000 instrument.

CO_2- and NH_3-TPD measurements were carried out using BELCAT. Prior to each experiment, a catalyst (50 mg) was heated in a flow of He (20 mL min^{-1}) at 500 °C for 10 min, followed by cooling to ca. 40 °C under He flow. The catalyst was then exposed to a flow of CO_2 or NH_3 (20 mL min^{-1}) for 10 min. After purged in He for 30 min, the catalyst was heated linearly at 10 °C min^{-1} until 600 °C in a flow of He, and outlet gas (CO_2, m/e = 44) were analyzed by the mass spectrometer (BEL Mass, BEL Japan, Inc.).

4.2.3 Catalytic Reactions

Typically, tertiary amide (1 mmol), alcohol (2 mmol) and CeO_2 (80 mg) were added to a Pyrex reaction vessel (16 mL). HY zeolite (5.5) (0.1 g) wrapped by a filter paper was also placed at the upper side of the reaction vessel for removal of formed amine as a by-product, as given in **Figure 1**. After sealing, the mixture was degassed and purged with N_2. This was repeated for 5 times. The reaction vessel was placed on a heater equipped with a reflux condenser and a magnetic stirrer. The reaction mixture was heated at 175 °C and stirred at 400 rpm for 36 h under N_2 atmosphere. After completion of the reaction, 2-propanol (6 mL) was added to the mixture and the products were analyzed by GC (Shimadzu GC-14B with Ultra ALLOY capillary column UA^+-1 of Frontier Laboratories Ltd., N_2) and GCMS (SHIMADZU GCMS-QP2010 with Ultra ALLOY capillary column UA^+-1 of Frontier Laboratories Ltd., N_2). Product isolation was carried out by using column chromatography on silica gel 60 (spherical, 50-100 □m, Kanto Chemical Co. Ltd.) with hexane/ethylacetate (9/1) as the eluting solvent. The isolated products were then analyzed by using GC, and ^1H and ^{13}C NMR. ^1H and ^{13}C NMR spectra were recorded at ambient temperature on a JEOL-ECX 600 spectrometer (^1H: 600.17 MHz, ^{13}C: 150.92 MHz), using tetramethylsilane as the internal standard. Isolated yields were determined relative to the starting amides.

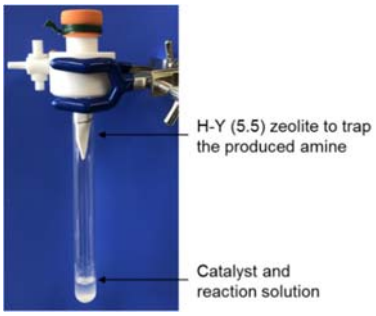

Figure 1. Picture of the typical reaction apparatus for the esterification reaction of a tertiary amide by an alcohol.

For reusing the catalyst, after completion of the reaction, 2-propanol (6 ml) was added to the reaction mixture and the catalyst was separated by centrifugation. The recovered catalyst was washed with 2-propanol for 3 times (3 mL for each time). After separating the catalyst by centrifugation, the recovered catalyst was dried at 100 °C in air for 12 h, and subsequently employed for the next run. A leaching test was performed in the same manner for the recycling test. After 6 h period of the reaction, the catalyst was separated by centrifugation. Subsequently, the separated solution was transferred to the reactor, followed by heating at 175 °C with magnetically stirring for another 29 h.

4.2.4 Computational Methods

Periodic DFT calculations were performed with the DMol3 program[37,38] in Material Studio of Accelrys Inc. Perdew–Burke–Ernzerhof (PBE) generalized gradient functional was employed for the exchange-correlation energy. The wave functions were expanded in terms of numerical basis sets. We employed the DND basis set (double numerical basis set with the d-type polarization functions) for geometry optimization. Single-point energy calculations were performed with the larger DNP basis set (double numerical basis set with the d-type polarization functions for heavy atoms and the p-type polarization functions for hydrogen atoms). Brillouin zone integrations are performed on a Monkhorst–Pack[39] k-point grid with a k-point spacing of 0.05 $Å^{-1}$ unless otherwise noted. The transition state was determined by using the linear and quadratic synchronous transit (LST/QST) complete search method.[40]

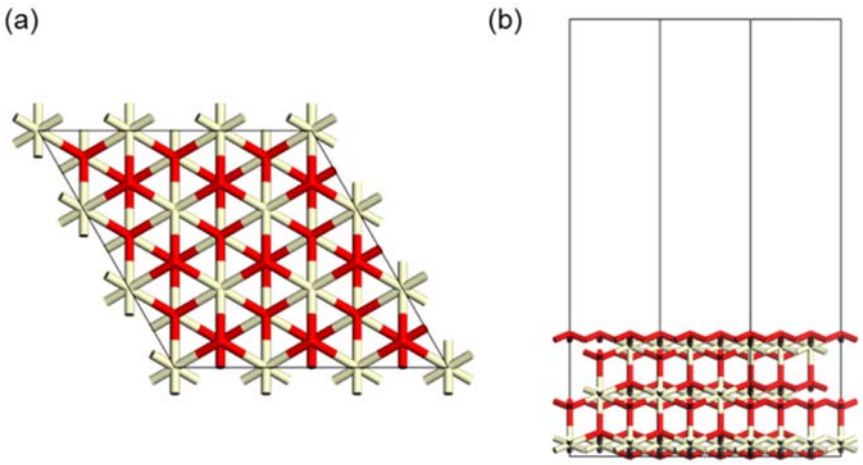

Figure 2. Structure model of CeO_2(111) used in this study. (a) Top view and (b) side view. Color code: beige: Ce; red: O.

As shown in Figure 2, the CeO_2 catalyst was modeled by a supercell slab that consists of a 3×3 surface unit cell with nine atomic (111) surface layers (lattice constants $a = b = 11.5$ Å, 81 atoms) unless otherwise noted. The slab was separated by a vacuum space with a height of 20 Å. All atoms except the oxygen atoms in the bottom layer were fully relaxed.

4.3 Results and Discussion

4.3.1 Catalysts design and screening

The initial phase of this effort was designed to screen catalysts for the reaction between *N,N*-dimethylbenzamide and 1-octanol that forms octyl benzoate. Reactions were performed using the following conditions: amide (1 mmol), alcohol (4 mmol), CeO_2 (80 mg) and dodecane (0.2 mmol) as an internal standard in a Pyrex reaction tube (18 mL) under a N_2 atmosphere at 175 °C

for 36 h. The results are showed in **Table 1.**

Table 1. Catalyst screening for ester formation from *N,N*-dimethylbenzamide and 1-octanol.[a]

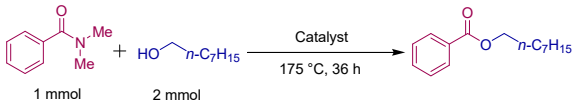

Entry	Catalyst	Yield [%][b]
1	CeO_2	97
2[c]	CeO_2	94
3	Nb_2O_5	43
4	CaO	38
5	ZrO_2	28
6	MgO	24
7	TiO_2	7
8	Al_2O_3	6
9	Y_2O_3	4
10	SiO_2	6
11	ZnO	3
12	Fe-mont	20
13	Mont. K10	8
14	H-ZM-5 (22)	7
15	H-Beta (75)	5
16	HY 5.5	5
17	Amberlyst-15	38
18	Nafion-SiO_2	12
19	Sulfated ZrO_2	5
20[d]	$Sc(OTf)_3$	43
21[d]	$Ce(NO_3)_4$	35
22[d]	$Ce_3(PO_4)_4$	29
23[d]	*p*-Toluenesulfonic acid (PTSA)	22
24[d]	H_2SO_4	23

[a] Reaction conditions: 80 mg catalyst, 175 °C, 36 h, N_2 atmosphere, N,N-dimethylbenzamide (1 mmol), 1-octanol (2 mmol), HY zeolite (0.1 g) as a trapping agent, *n*-dodecane (0.2 mmol) as an internal standard; [b] Yields were determined by using GC; [c] Without HY zeolite; [d] The same molar amount employed for CeO_2 was used.

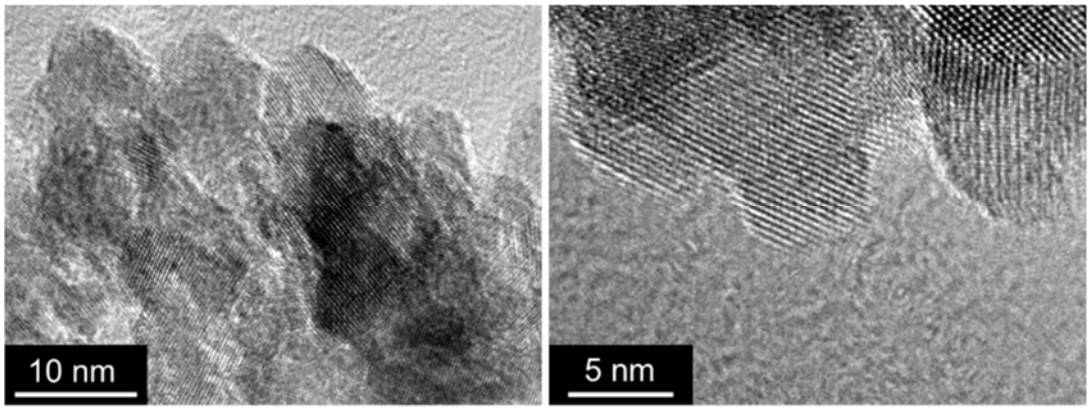

Figure 3. TEM images of the CeO_2 catalyst.

Among the metal oxides, solid acid and homogeneous catalysts tested, CeO_2 (Daiichi Kigenso Kagaku Kogyo Co., Ltd. (Type A), calcined at 600 °C for 3 h. see **Figure 3** for TEM images) promoted the most efficient process giving the target ester in 97% GC yield. In reactions designed to remove the formed *N,N*-dimethylamine, HY zeolite (SiO_2/Al_2O_3 = 5.5) (0.1 g) enclosed in a filter paper was placed at the upper portion of the reaction vessel.

In addition, it was found that the CeO_2 catalyzed reaction performed without utilizing HY zeolite generates the target ester in 94% yield. We checked the effect of the use of HY zeolite for the reaction several times and found that the reaction with the zeolite always gives better yield. In addition, the formed secondary amine (*N,N*-diethylamine) trapped by the HY zeolite was experimentally detected after the reaction between *N,N*-diethylbenzamide and 1-octanol that forms octyl benzoate. Note that *N,N*-diethylbenzamide was used as a substrate for this purpose for ease of handling thanks to its higher boiling point than that of *N,N*-dimethylamine. The use of the HY zeolite could overcome the thermodynamic limitations associated with reverse reactions between the formed ester and secondary amine that is an well-known difficulty for the ester forming alcoholysis reactions of tertiary amides.[26,27,41] The use of soluble Ce salts such as $Ce(NO_3)_4$ and $Ce_3(PO_4)_4$ as catalysts leads to lower yielding raections, Notably, the typical homogeneous Brønsted acids, *p*-toluenesulfonic acid (PTSA) and H_2SO_4, catalyze reactions that occur in only 22% and 23% respective yields.

4.3.2 Optimization of reaction conditions

Results from studies exploring the effect of alcohol concentration see at **Table 2** which showed that, even though a slight excess of 1-octanol was necessary to bring about complete reaction, 86% yield of *N,N*-dimethylbenzamide was obtained when 1.0 eq of the alcohol was employed.

Table 2. Effect of reaction temperature and amount of 1-octanol on the ester formation reaction over CeO_2 from *N,N*-dimethylbenzamide and 1-octanol.[a]

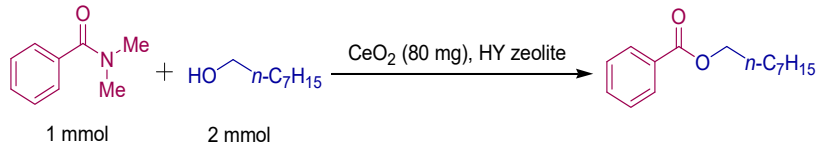

Amount of 1-octanol [mmol]	*t* [h]	*T* [°C]	Yield [%][b]
1.0	24	155	15
1.0	24	165	67
1.0	24	175	67
1.0	30	175	72
1.0	36	175	86
1.5	36	175	92
2.0	36	175	97
3.0	36	175	97

[a]Reaction conditions: 80 mg CeO_2 catalyst, N_2 atmosphere, *N,N*-dimethylbenzamide (1 mmol), 1-octanol, HY zeolite (0.1 g) as a trapping agent, *n*-dodecane (0.2 mmol) as an internal standard. [b]Yields were determined by GC.

In addition, a gram-scale, CeO_2 promoted reaction of *N,N*-dimethylbenzamide using 2 eq. of 1-octanol (**Scheme 1**) proceeds efficiently to produce octyl benzoate in a yield reaching 86% after 72 h.

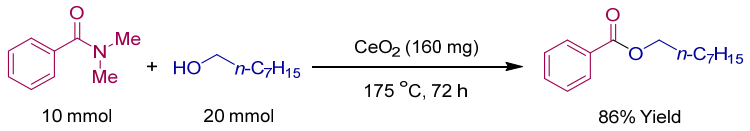

Scheme 1. Gram-scale reaction of *N,N*-dimethylbenzamide and 1-octanol. Conditions: 160 mg CeO_2, 175 °C, 72 h, N_2 atmosphere, *N,N*-dimethylbenzamide (10 mmol), 1-octanol (20 mmol).

4.3.3 Recycling and leaching study of CeO_2 catalyst

To examine the re-usability of the CeO_2 catalyst, a recycling test was performed (**Figure 4**).

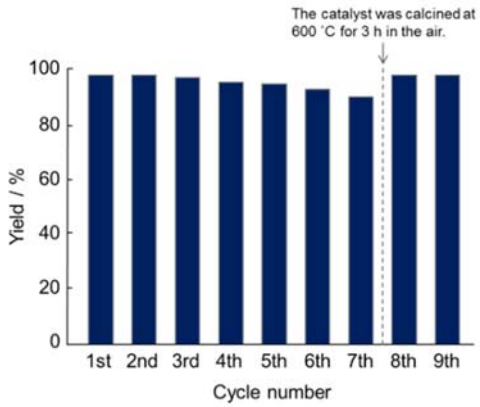

Figure 4. Recycling study for octyl benzoate formation process from *N,N*-dimethylbenzamide and 1-octanol over CeO_2.

Following reaction of *N,N*-dimethylbenzamide and 1-octanol, CeO_2 was separated, washed with isopropanol, dried in air and used for an ensuing reaction. CeO_2 was found to be recyclable but the yield gradually decreased. It was also found that the catalytic performance can be recovered if the catalyst was subject to calcination at 600 °C for 3 h in the air.

The results of a leaching test to demonstrate the heterogeneous nature of CeO_2 revealed that removal of the solid catalyst after a 6 h caused the alcoholysis reaction to cease (**Figure 5**). Inductively coupled plasma atomic emission spectroscopy (ICP-AES) was also utilized to confirm the heterogeneous nature of CeO_2. Specifically, the mixture after the reaction was subjected to filtration. Examination of the filtrate by using ICP-AES showed that less than 10 ppm of CeO_2 was present.

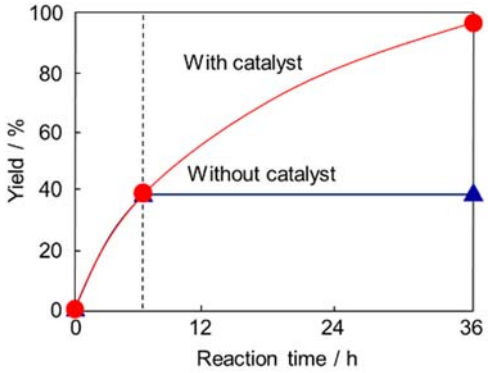

Figure 5. Leaching test for octyl benzoate formation process from *N,N*-dimethylbenzamide and 1-octanol over CeO_2. Reaction conditions: 80 mg catalyst, 175 °C, N_2 atmosphere, *N,N*-dimethylbenzamide (1 mmol), 1-octanol (2 mmol), HY zeolite (0.1 g) as a trapping agent, *n*-dodecane (0.2 mmol) as an internal standard.

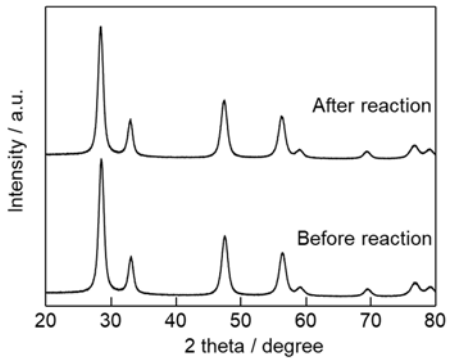

Figure 6. XRD patterns of CeO_2 before and after the reactions

In addition, x-ray diffraction (XRD) analysis showed that recovered CeO_2 is essentially the same as the original catalyst (**Figure 6**).

4.3.4 Mchanistic study of Alcoholysis reaction

4.3.4.1 In situ FT-IR studies

The sample was employed to gain information about interactions occuring between the amide and CeO_2 surface. For this purpose, 1 μL of *N,N*-dimethylacetamide preheated to 200 °C was injected into a self-supporting pellet of CeO_2 at 120 ºC and surface species were analyzed (Figure 7(a)). After introduction of *N,N*-dimethylacetamide, the spectrum of CeO_2 contains bands assigned to C=O stretching of adsorbed acetamide (1606 cm^{-1}) together with bands associated with a acetate ester (1554, 1430 cm^{-1}).[25,42] The C=O stretching band of the acetamide adsorbed on CeO_2 (1606 cm^{-1}) appears at a lower wavenumber than that adsorbed on SiO_2 (1623 cm^{-1}) used for a reference (**Figure 7(a))** , This finding indicates that a strong interaction exists between the CeO_2 surface and the carbonyl oxygen of the amide. Moreover, the intensity of the IR band due to adsorbed acetamide decreases with time, while the intensity of bands arising from an adsorbed acetate species increase with time.

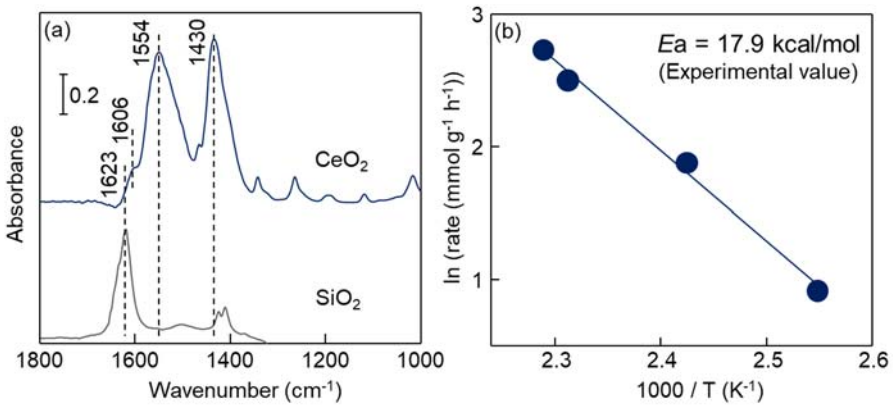

Figure 7. (a) FT-IR spectra of adsorbed *N,N*-dimethylacetamide species on CeO_2 and SiO_2 at 120 °C (*t* = 200 s). At *t* = 0 s, 1 μL of acetamide was introduced on preheated catalysts at 200 °C to the FT-IR cell. (b) Arrhenius-type plot for the rates of ester formation reaction in the reaction of *N,N*-dimethylbenzamide and benzylalcohol. Temperature range = 135-180 °C.

4.3.4.2 Periodic DFT calculation

Periodic DFT calculations were used to explore the mechanistic pathway proposed for the reaction of *N,N*-dimethylacetamide and benzylalcohol on the CeO_2(111) surface on the basis of the above findings by using *in situ* FT-IR. It was confirmed that CeO_2 gave the best performance for the reaction of *N,N*-dimethylacetamide and benzylalcohol (**Table 3**) among the catalysts tested in this study as well as the reaction of *N,N*-dimethlbenzamide and 1-octanol (**Table 1**).

Table 3. Catalyst screening for ester formation from *N,N*-dimethylacetamide and benzylalcohol.[a]

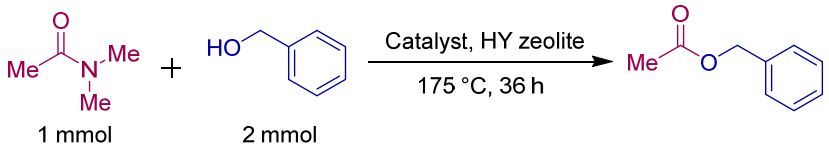

Entry	Catalyst	Yield [%][b]
1	CeO_2	93
2	Nb_2O_5	44
3	CaO	31
4	ZrO_2	26
5	MgO	22
6	TiO_2	10
7	Al_2O_3	7
8	SiO_2	7
9	Fe-mont	17
10	Mont. K10	13
11	H-Beta (75)	11
12	Amberlyst-15	37
13	Nafion-SiO_2	20
14	Sulfated ZrO_2	8
15[c]	$Sc(OTf)_3$	33
16[c]	$Ce(NO_3)_4$	25
17[c]	$Ce_3(PO_4)_4$	27
18[c]	*p*-Toluenesulfonic acid (PTSA)	30
19[c]	H_2SO_4	31

[a]Reaction conditions: 80 mg catalyst, 155 °C, 36 h, N_2 atmosphere, *N,N*-dimethylacetamide (1 mmol), benzylalcohol (2 mmol), HY zeolite (0.1 g) as a trapping agent, *n*-dodecane (0.2 mmol) as an internal standard. [b]Yields were determined by using GC. [c]The same molar amount employed for CeO_2 was used.

On the basis of the experimental findings, we explored a possible reaction pathway for the ester formation from *N,N*-dimethylacetamide and benzylalcohol on CeO_2(111) surface using periodic DFT calculations. The CeO_2(111) surface was selected since this is the most stable surface among the CeO_2 surfaces commonly investigated.[43,44] The proposed mechanistic pathway **(Scheme 2 and Scheme 3**) consists of (1) the deprotonation of benzylalcohol (**Figure 8**), (2) nucleophilic addition of the lattice oxygen of CeO_2 to the carbonyl carbon atom of acetamide (**Figure 9**), (3) deamination (**Figure 11**) and (4) ester formation (**Figure 12**). The

overall catalytic cycle is given in **Scheme 2** in the manuscript along with the computed activation energy for each step. A key step in the overall process is the nucleophilic addition of the lattice oxygen to the carbonyl carbon atom of acetamide, in which the stable *N,N*-dimethylacetamide is activated on the CeO_2(111) surface as in the case with our previous study dealing with alcoholysis of primary amides.[45] Because the processes participating in C–N bond cleavage are considered to be the rate-determining step of the reaction, we have considered two possible pathways for activation of the amide C-N bond on the CeO_2(111) surface, one given in **Scheme 2** in which nucleophilic addition of a CeO_2 lattice oxygen to the amide and the other where hydroxide adds to carbonyl carbon atom (see **Figures 8 and 10**). In the former pathway, strongly basic lattice oxygen is responsible for amide activation.[46] Nucleophilic attack of a lattice oxygen atom to the carbonyl carbon of *N,N*-dimethylacetamide occurs via TS(3 → 4) to form a tetrahedral intermediate 4.In the transition state, the planar amide group is tilted toward the CeO_2(111) surface, while the carbonyl group remains bonded to the Ce atom in the course of the C–O bond formation. Nucleophilic addition is accompanied by the formation of a bond between the amide carbonyl oxygen and a Lewis acidic Ce site. The N atom in the $–N(CH_3)_2$ group has more sp^3 character in TS(3 → 4) and 4 than the one in the initial state (3) as a result of Ce–O bond formation. The Ce···O distance is shortened from 2.580 Å in 3 to 2.273 Å in 4, which indicates that the oxygen atom in 4 interacts with Lewis acidic Ce site. The computed activation barrier for this step of 17.0 kcal/mol is in good agreement with the apparent barrier of 17.9 kcal/mol for the overall reaction. Although this step (3 → 4 shown in **Figure 8**) is endothermic by 10.6 kcal/mol, subsequent deamination would make the cerate ester forming process more thermodynamically facile, (see **Figure 11**).

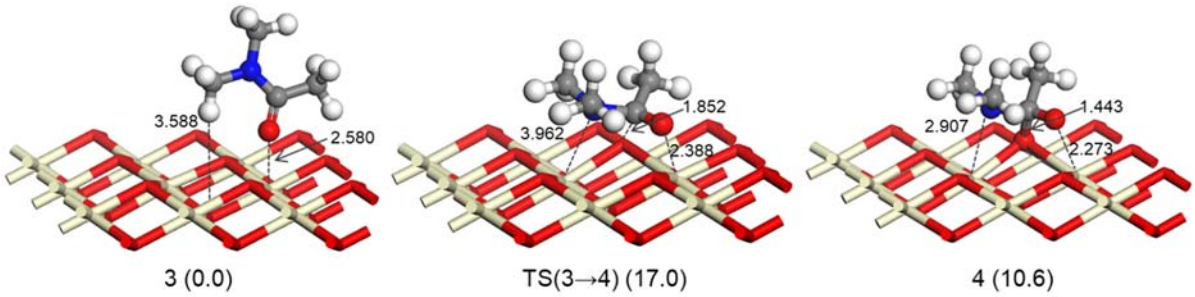

Figure 8. Optimized structures and relative energies for the deprotonation of benzylalcohol on the CeO_2 surface. Only important part is displayed for clarity. Units in Å and kcal/mol. Color code: beige: Ce; red: O; grey: C; white; H.

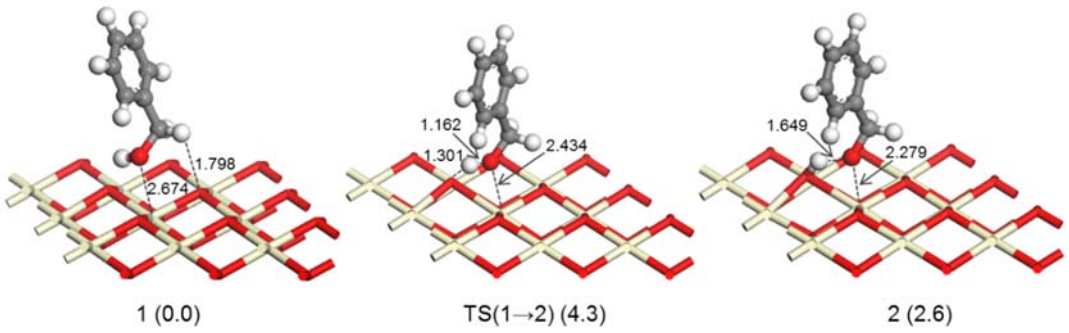

Figure 9. Optimized structures and relative energies for the nucleophilic attack of the lattice oxygen atom to the carbonyl carbon atom of *N,N*-dimethylacetamide on the CeO_2 surface. Only important part is displayed for clarity. Units in Å and kcal/mol. Color code: beige: Ce; red: O; grey: C; blue: N; white; H.

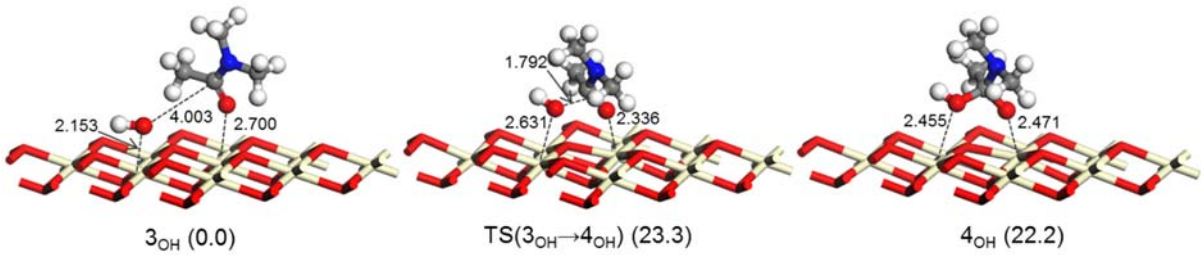

Figure 10. Optimized structures and relative energies for the nucleophilic attack of the OH group to the carbonyl carbon atom of *N,N*-dimethylacetamide on the CeO_2 surface. Only important part is displayed for clarity. Units in Å and kcal/mol. Color code: beige: Ce; red: O; grey: C; blue: N; white; H.

In the alternative pathway shown in **Figure 10**, nucleophilic addition of an OH group (derived from co-adsorbed water molecules)[45,47–49] to the carbonyl carbon atom of acetamide occurs via TS(3_{OH} → 4_{OH}) to form a C–O bond. This reaction is highly endothermic with an activation barrier of 23.3 kcal/mol, which indicates that the OH group is not sufficiently nucleophilic for the amide activation. In addition, a Ce–O bond is not formed in 4_{OH}. After the nucleophilic addition of a lattice oxygen atom to the carbonyl carbon atom of *N,N*-dimethylacetamide, subsequent deamination occurs to form a cerate ester. This ester then reacts with benzyl alcoholate (formed through deprotonation of benzyl alcohol) via TS(5 → 6) to form the tetrahedral intermediate 6 in an endothermic manner (8.7 kcal/mol) with an activation energy of 11.2 kcal/mol (**Figure 12**).[45] This barrier is lower than that for the nucleophilic addition of lattice oxygen to carbonyl carbon atom of acetamide. Finally benzyl acetate is produced by the cleavage of a C–O bond via TS(6→7) with the regeneration of CeO_2 (**Figure 12**). These computational results show that the stable amide bond is effectively activated by

the strongly basic lattice oxygen with the aid of the Lewis acidic Ce site on the CeO_2(111) surface.

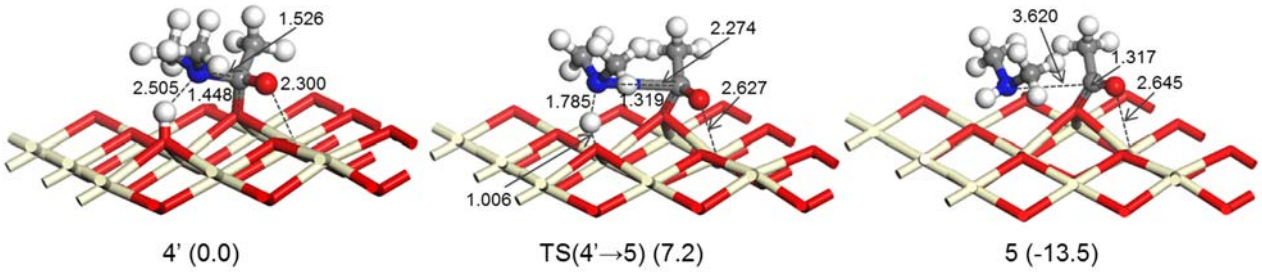

Figure 11. Optimized structures and relative energies for the deamination of 4' promoted by a Brønsted acid site on the CeO_2 surface. Only important part is displayed for clarity. Units in Å and kcal/mol. Color code: beige: Ce; red: O; grey: C; blue: N; white; H.

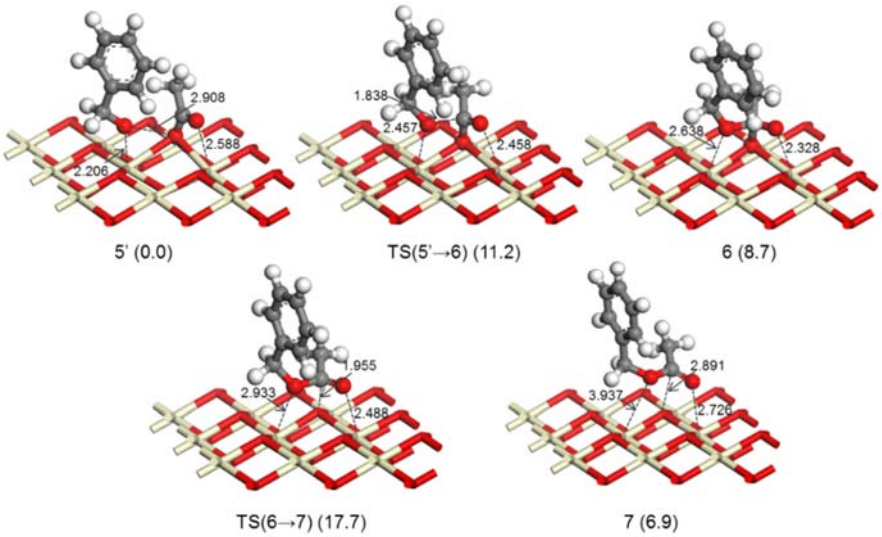

Figure 12. Optimized structures and relative energies for the ester formation on the CeO_2 surface. Only important part is displayed for clarity. Units in Å and kcal/mol. Color code: beige: Ce; red: O; grey: C; white; H.

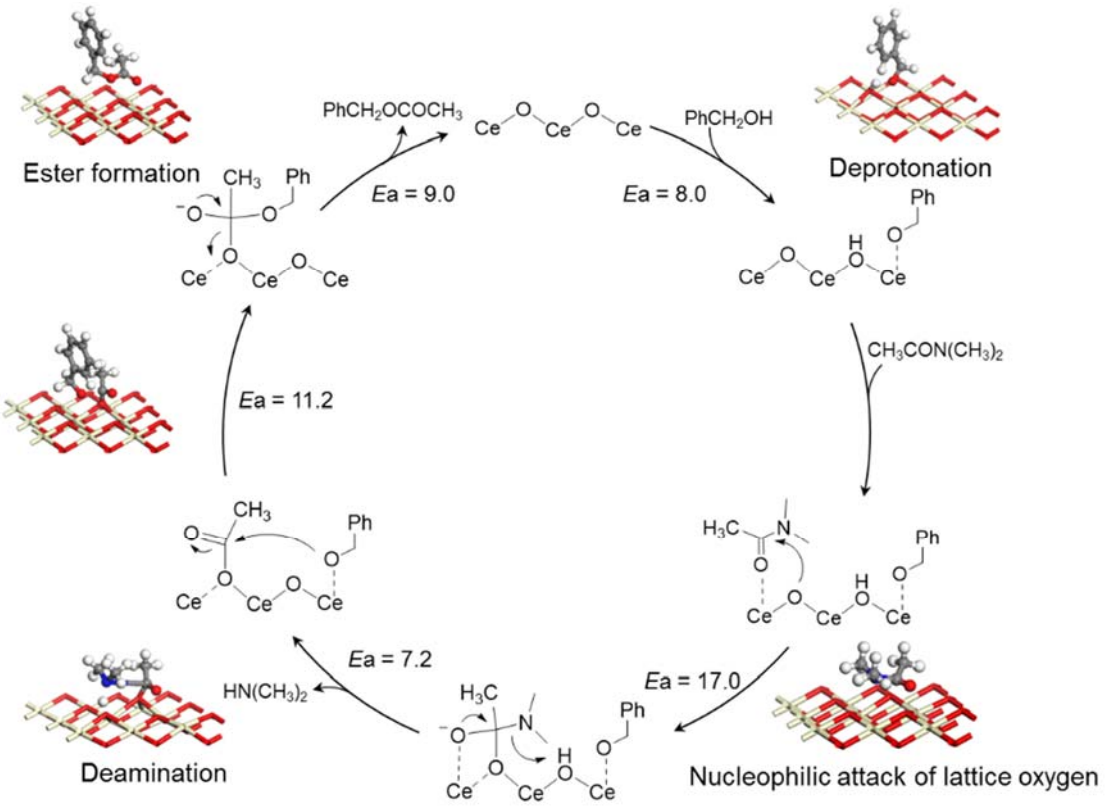

Scheme 2. Proposed mechanism for alcoholysis of amides on the CeO_2 surface. Computed activation energies (*E*a) are given in kcal/ mol. Color code: beige: Ce; red: O; grey: C; blue: N; white; H.

In the summary results of DFT calculations, which show that an alternative route involving OH addition to the carbonyl carbon of acetamide is less favorable (see **Figure 10**). The computional results also show that the rate determining step for the alcoholysis reaction involves addition of a lattice oxygen of CeO_2 to the carbonyl carbon atom of the amide. It should be noted that the calculated energy barrier for this rate determining step of 17.0 kcal/mol matches the experimentally determined value of 17.9 kcal/mol obtained from analysis of the Arrhenius plot displayed in **Figure 7b**.

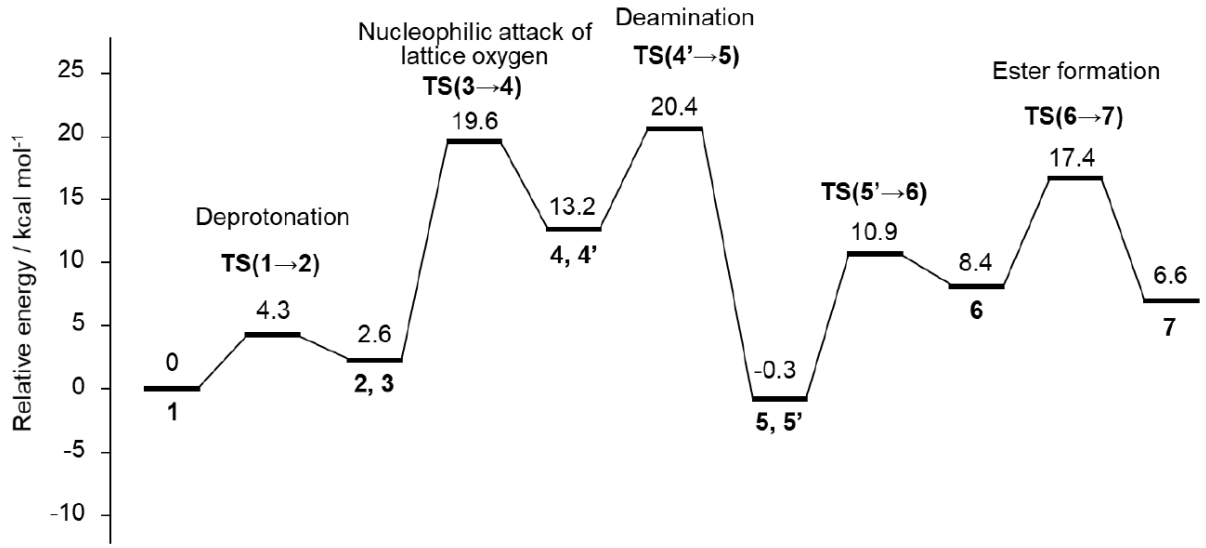

Scheme 3. DFT-computed reaction energy diagram for alcoholysis of amides on CeO_2 surface.

Rationalizing the properties of catalysts and establishing theories for heterogeneous catalysis are challenging but inevitable tasks in order to understand the underlying phenomena and ultimately develop improved catalysts. As discussed above, the nucleophilic attack of the lattice oxygen atom to the carbonyl carbon atom of the tertially amide is a key step for this catalytic process. This fact suggests that strong basicity of lattice oxygen in metal oxides can lead to high reactivity and the basicity could be used as a descriptor to explain the catalytic activity of the metal oxide catalysts for the alcoholysis of amides. It is known that O_{1s} binding energy of metal oxides determined by XPS analysis decreases with an increase in basicity of the metal oxides surface.[50,51] Note that the XPS measurements were performed without any pretreatments.[51]

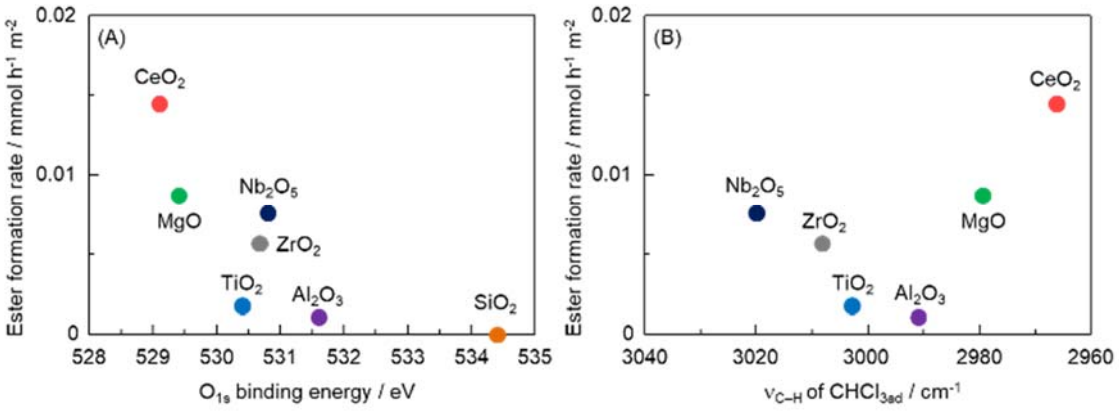

Figure 13. Correlation between initial reaction rates of ester formation from *N,N*-dimethylbenzamide and 1-octanol and (A) XPS O_{1s} binding energies,[51] and (B) FT-IR band positions of C–H stretching mode of $CHCl_3$ adsorbed onto the supports.[52]

Ester formation rate for the model reaction employing *N,N*-dimethylbenzamide and 1-octanol was plotted as a function of O_{1s} binding energy of metal oxide catalysts, as shown in **Figure 13(A)**. Note that the ester formation rates were obtained for reactions with yields below 30%. **Figure 13(A)** indicates that there is a correlation between the catalytic performance and basicity of the metal oxides. This is most likely because that the activation energy for the nucleophilic attack (the rate-determining step) decreases with a decrease of the O_{1s} binding energy. In addition, the peak positions of the C–H stretching bands (ν_{CH}) in the FT-IR spectra for adsorbed $CHCl_3$ on various metal oxides were also employed to rationalize the catalytic activities (**Figure 13(B)**).

It is known that the red shift of the bands indicate the presence of basic sites and the degree of the band shift is used as an indicator for basic strength.[52] It should be noted that the spectrum of SiO_2 showed no peak, indicating that SiO_2 has no basic sites. It is clear that CeO_2 showed the highest bascity and initial reaction rate among the oxide catalysts explored.

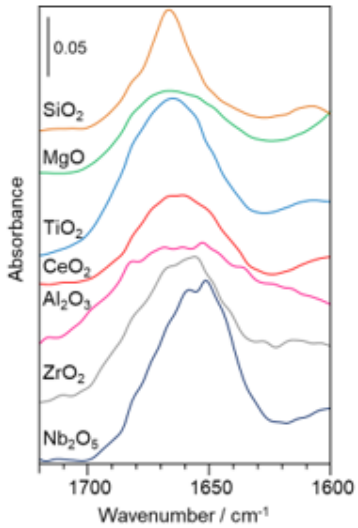

Figure 14. FT-IR spectra of *N,N*-dimethylacetamide adsorbed on the supports measured at 40 °C.

It was also observed that Nb_2O_5 and ZrO_2 showed relatively high initial reaction rate toward the reaction whereas they are not strongly basic from the results of FT-IR studies using $CHCl_3$. This fact suggests that Lewis acidic properties play role to promote the C–N bond cleavage reaction of amides as indicated by the DFT calculations. In order to examine the role of Lewis acidic nature of the catalysts more quantitatively, *in situ* FT-IR study was conducted by adsorbing *N,N*-dimethylacetamide on various metal oxide catalysts at 40 °C as given in **Figure 14**. At this low temperature, *N,N*-dimethylacetamide is not converted to acetate ester species even on the CeO_2 surface

The position of the C=O stretching bands (ν_{CO}) of *N,N*-dimethylacetamide on Nb_2O_5 resonates at lower wavenumber (1651 cm^{-1}, **Figure 15)** than on other oxides (1656-1667 cm^{-1}), indicating that the Lewis-acidic sites on Nb_2O_5 interact more strongly with the carbonyl oxygen of *N,N*-dimethylacetamide than those on the other oxides.[21]

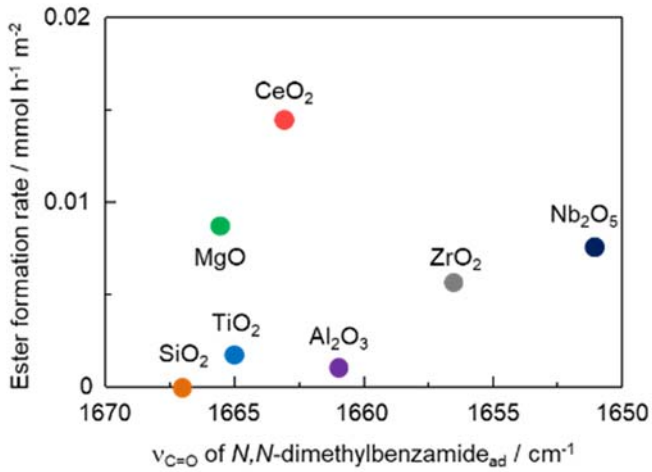

Figure 15. Correlation between initial reaction rates of ester formation from *N,N*-dimethylbenzamide and 1-octanol and FT-IR band positions of C=O stretching mode of *N,N*-dimethylacetamide adsorbed onto the supports measured at 40 °C.

The position of the ν_{CO} on CeO_2 is seen at 1663 cm^{-1}, showing stronger Lewis acidic activation of C=O bond of *N,N*-dimethylacetamide than SiO_2, MgO and TiO_2. These results indicate that CeO_2 has both acid and base sites to activate *N,N*-dimethylacetamide, and therefore, CeO_2 serves as the best catalysts for the alcoholysis of amides. This fact is furthermore supported by temperature programmed desorption (TPD) measurements with CO_2 and NH_3 as probe molecules (**Figure 16**). These resullts demonstrate that both acidic and basic properties are important for the efficient progression of the alcoholysis reaction as indicated by DFT studies, and as a result, CeO_2 showed the best performance.

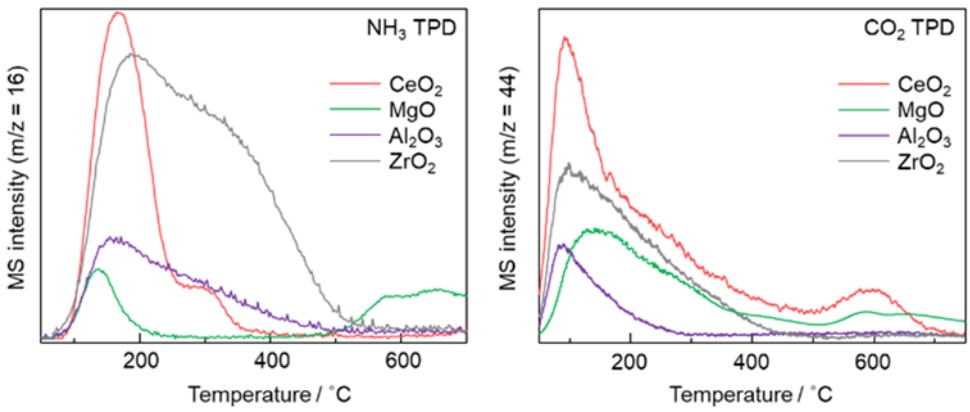

Figure 16. NH_3- and CO_2-TPD profiles for various oxide

4.3.5 Scopes of the catalytic system

The substrate scope of CeO_2-catalyzed amide alcoholysis process under optimal reaction conditions was explored.

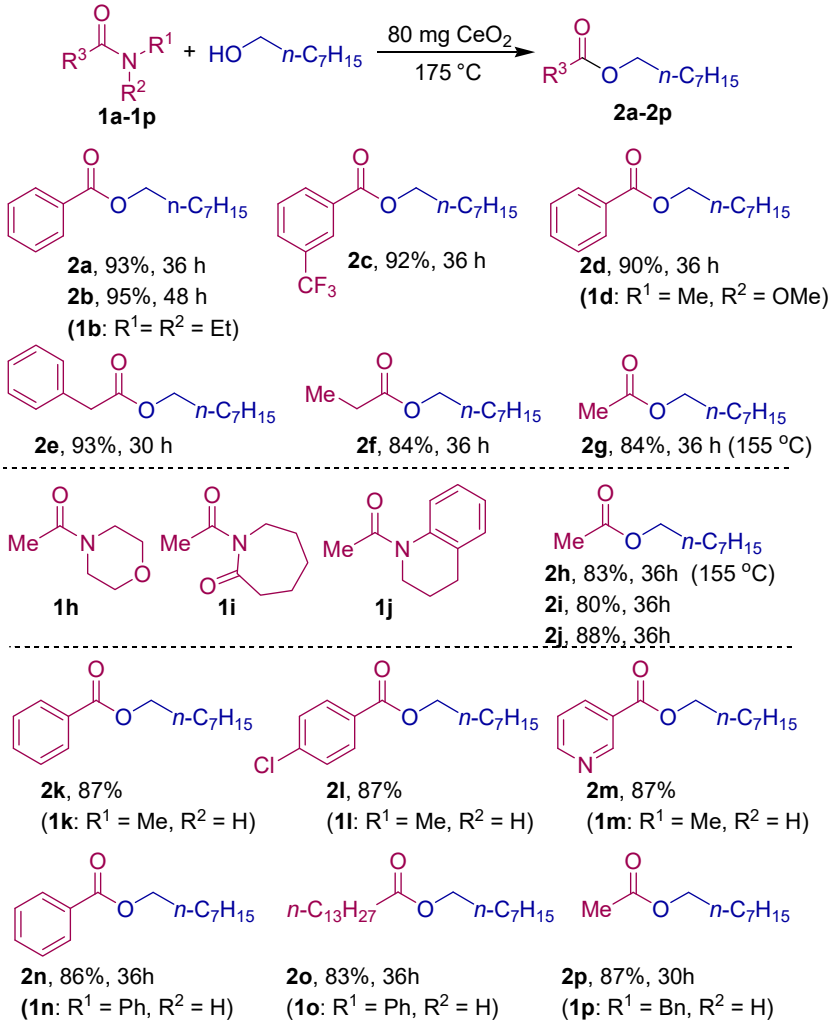

Scheme 4. CeO_2-catalyzed ester formation from various amides and 1-octanol. Reaction conditions: 80 mg catalyst, 175 °C, 30-36 h, N_2 atmosphere, amide (1 mmol), 1-octanol (2 mmol), HY zeolite (0.1 g) as a trapping agent, Isolated yields are shown.

The results displayed in **Schemes 4** shows that the reaction is applicable to a wide range of amides and alcohols. In addition to the *N,N*-dimethylbenzamide (**1a**) used for the model reaction, benzamides containing *N,N*-diethyl (**1b**), *N*-methoxy-*N*-methyl (**1d**) were successfully transformed to the corresponding ester, octylbenzoate. *N,N*-Dimethyl amides of *m*-trifluoromethyl phenyl (**1c**), benzyl (**1e**) also gave the desired esters in excellent yields. Notably, alkyl amides (**1f**), (**1g**) of *N,N*-dimethyl and *N*-heterocyclic moieties (**1h-1j**) undergo esterification in high isolated yields. Secondary amides containing phenyl (**1k** and **1n**), 4-chloro-phenyl (**1l**), pyridyl (**1m**) and alkyl (**1o** and **1p**) were also tolerated in alcoholysis reactions to give target esters.

The alcohol scope of this CeO_2 catalyzed esterification reaction with *N,N*-dimethylbenzamide (**1a**) is given in **Scheme 5**

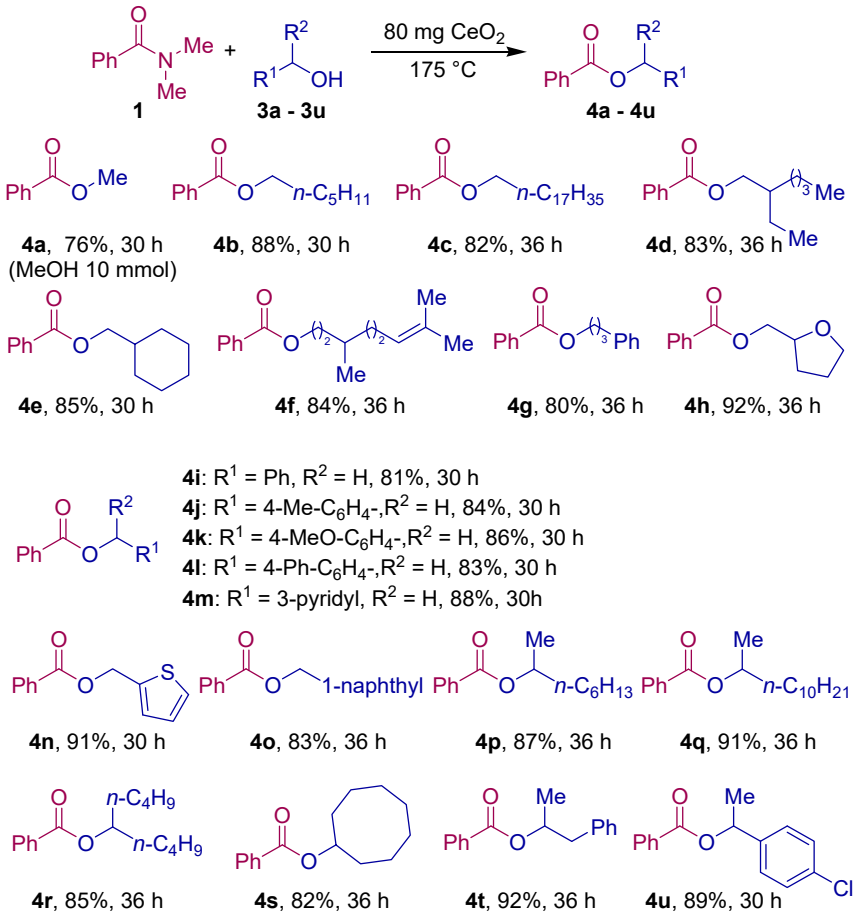

Scheme 5. CeO_2-catalyzed ester formation from *N,N*-dimethyl benzamide and various alsohols. Reaction conditions: 80 mg catalyst, 175 °C, 30-36 h, N_2 atmosphere, *N,N*-dimethyl benzamide (1 mmol), alcohol (2 mmol), HY zeolite (0.1 g) as a trapping agent, Isolated yields are shown.

Various alcohols including aliphatic (**3a-3e**, **3g**), olefinic (**3f**), methyl-tetrahydrofuryl (**3h**), benzylic alcohols (**3i-3l**) with electron-donating and electron-withdrawing substituents, heteroaromatic pyridyl (**3m**), methyl-thiophenyl (**3n**) and naphthyl (**3o**) were successfully undergo alcoholysis reactions of **1a** in high isolated yilds. In addition to the primary alcohols various secondary alcohols including aliphatic linear, branched, cyclic and aromatic (**3p-3u**) were also well tollerated in alcoholysis of *N,N*-dimethylbenzamide (**1a**) and gave corresponding esters.

It was also demonstrated that *N,N*-dimethylacetamide (**1g**) efficiently reacted with various alcohols at 155 °C to afford the corresponding esters (**Scheme 6**). At present, this CeO_2-catalyzed process requires high temperature (155-175 °C) for completing the reaction. However, the wide substrate scope obtained in this study is compatible with homogeneous catalytic systems.[26,27,30,31,53] This wide substrate scope suggests that the present system can potentially be utilized for synthetic applicationos.

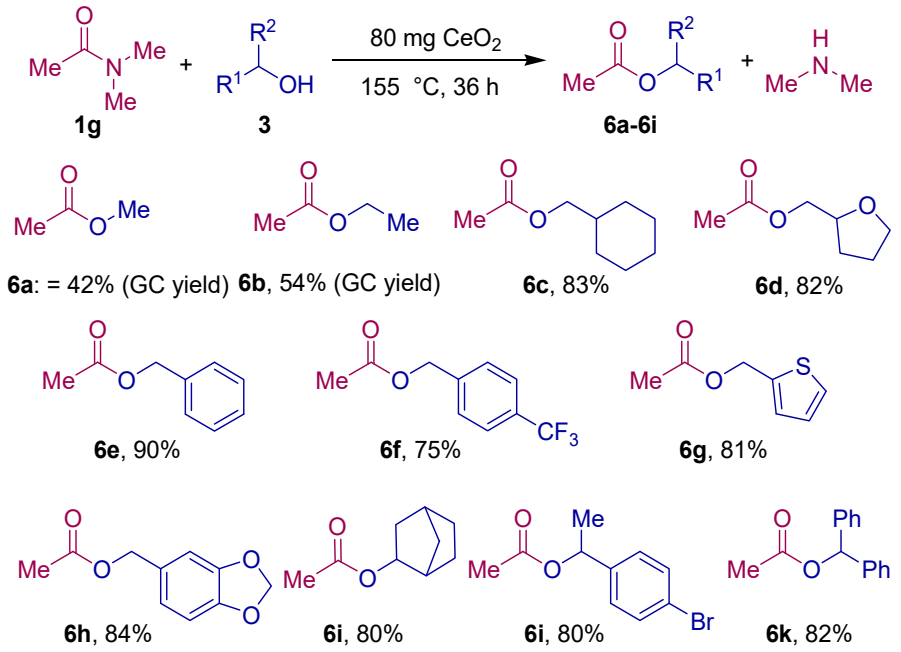

Scheme 6. CeO_2-catalyzed ester formation from *N,N*-dimethylacetamide and various alsohols. Reaction conditions: 80 mg catalyst, 155 °C, 36 h, N_2 atmosphere, *N,N*-dimethylacetamide (1 mmol), alcohol (2 mmol, for **6a** and **6b**;10 mmol of MeOH and EtOH were used), HY zeolite (0.1 g) as a trapping agent, Isolated yields are shown.

4.3.6 GC-MS and NMR data of products

^{1}H and ^{13}C NMR spectra for alcohols of scheme 3, 4 and 5 were assigned and reproduced to the corresponding literature. ^{1}H and ^{13}C NMR spectra were recorded using at ambient temperature on JEOL-ECX 600 operating at 600.17 and 150.92 MHz or JEOL-ECX 400 operating at 399.78 and 100.52 MHz, respectively with tetramethylsilane as an internal standard. Abbreviations used in the NMR experiments: s, singlet; d, doublet; dd, doublet of doublet; t, triplet; q, quartet; m, multiplet. GC-MS spectra were taken by SHIMADZU QP2010.

SI-2a,2c,2j,2m: Octyl benzoate[54]

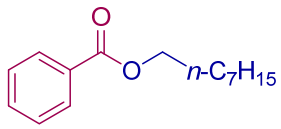

^{1}H NMR (600.17 MHz, $CDCl_3$, TMS): δ 8.04 (d, *J* =8.22 Hz, 2H), 7.53 (t, *J* =7.56 Hz, 1H), 7.42 (t, *J* =7.92 Hz , 2H), 4.31 (t, *J* =6.51 Hz, 2H), 1.79-1.73 (m, 2H), 1.46-1.41 (m, 2H) , 1.32-1.25 (m, 8H), 0.88 (t, *J* =6.87 Hz, 3H); ^{13}C NMR (150.92 MHz, $CDCl_3$, TMS) δ 166.60, 132.69, 130.51, 129.48 (C×2), 128.23 (C×2), 65.07, 31.75, 29.20, 29.15, 28.69, 26.00, 22.59, 14.03; GC-MS m/e: 234.15.

SI-2b: Octyl 3-(trifluoromethyl) benzoate

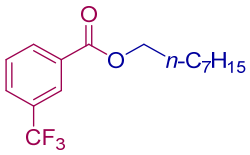

^{1}H NMR (600.17 MHz, $CDCl_3$, TMS): δ 8.30 (s, 1H), 8.23 (d, *J* =7.72 Hz, 1H), 7.81 (d, *J* =8.15 Hz, 1H), 7.59 (t, *J* =8.61 Hz, 1H), 4.35 (t, *J* =8.16 Hz, 2H), 1.83-1.75 (m, 2H), 1.48-1.41 (m, 2H), 1.38-1.28 (m, 8H), 0.88 (t, *J* =6.79 Hz, 3H); ^{13}C NMR (99.54 MHz, $CDCl_3$, TMS) δ 165.34, 132.74, 131.35, 130.99 (q, *J* =34.19 Hz, CX1), 129.31 (q, *J* =2.88 Hz, CX1), 128.98, 126.43 (q, *J* =2.88 Hz, CX1), 123.59 (q, *J* =271.66 Hz, CX1), 65.74, 31.75, 29.21, 29.15, 28.62, 25.96, 22.62, 14.06; GC-MS m/e: 302.15

SI-2c: Same as 2a

SI-2d: Octyl 2-phenylacetate[55]

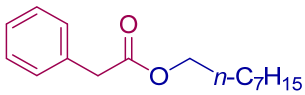

^{1}H NMR (600.17 MHz, $CDCl_3$, TMS): δ 7.33-7.26 (m, 5H), 4.08 (t, *J* =5.82 Hz, 2H), 3.61 (s, 2H), 1.60 (t, *J* =6.18 Hz, 2H), 1.33-1.27 (m, 10H) , 0.88 (t, *J* =8.25 Hz, 3H); ^{13}C NMR (150.92 MHz, $CDCl_3$, TMS) δ 171.69, 134.29, 129.32 (C×2), 128.60 (C×2), 127.10, 65.14, 41.68, 31.92, 29.28 (C×2), 28.57, 25.91, 22.73, 14.18; GC-MS m/e: 248.35

SI-2e: Octylpropanoate[56]

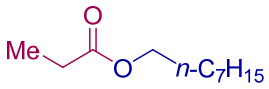

^{1}H NMR (600.17 MHz, $CDCl_3$, TMS): δ 4.06 (t, *J* =6.87 Hz, 2H), 2.34-2.30 (m, 2H), 1.63-1.59 (m, 2H), 1.36-1.24 (m, 10H), 1.14 (t, *J* =7.56 Hz, 3H), 0.88 (t, *J* =7.20 Hz, 3H); ^{13}C NMR (150.92 MHz, $CDCl_3$, TMS) δ 174.62, 64.48, 31.76, 29.19, 29.15, 28.61, 27.60, 25.89, 22.62, 14.07, 9.14; GC-MS m/e: 186.15

SI-2f-2i,2o: Octylacetate[57]

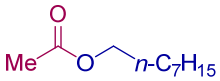

^{1}H NMR (600.17 MHz, $CDCl_3$, TMS): δ 4.07-4.03 (m, 2H), 2.05 (s, 3H), 1.65-1.59 (m, 2H), 1.37-1.23 (m, 10H), 0.88 (t, *J* =6.87 Hz, 3H); ^{13}C NMR (150.92 MHz, $CDCl_3$, TMS) δ 171.23, 64.64, 31.75, 29.18, 29.15, 28.56, 25.88, 22.61, 20.99, 14.05; GC-MS m/e: 172.15

SI-2g: Same as 2f

SI-2h: Same as 2f

SI-2i: Same as 2f

SI-2j: Same as 2a

SI-2k: Octyl-4-chlorobenzoate[58]

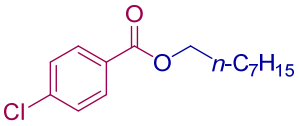

^{1}H NMR (600.17 MHz, $CDCl_3$, TMS): δ 7.97 (d, *J* =8.94 Hz, 2H), 7.40 (d, *J* =7.56 Hz , 2H), 4.31 (t, *J* =6.87 Hz, 2H), 1.79-1.73 (m, 2H), 1.45-1.39 (m, 2H) , 1.36-1.27 (m, 8H), 0.88 (t, *J* =6.87 Hz, 3H); ^{13}C NMR (150.92 MHz, $CDCl_3$, TMS) δ 165.73, 139.18, 130.88(C×2), 128.95, 128.61 (C×2), 65.35, 31.75, 29.19, 29.15, 28.65, 25.99, 22.59, 14.04; GC-MS m/e: 268.10

SI-2l: Octyl nicotinate[59]

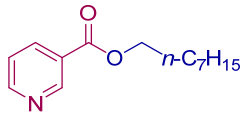

^{1}H NMR (600.17 MHz, $CDCl_3$, TMS): δ 9.23 (s, 1H), 8.77 (d, *J* =7.56 Hz, 1H), 8.29 (d, *J* =8.22 Hz, 1H), 7.41-7.36 (m, 1H), 4.35 (t, *J* =6.87 Hz, 2H), 1.79-1.75 (m, 2H), 1.47-1.41 (m, 2H) , 1.36-1.28 (m, 8H), 0.88 (t, *J* =6.87 Hz, 3H); ^{13}C NMR (150.92 MHz, $CDCl_3$, TMS) δ 165.32, 153.30, 150.89, 136.96, 126.34, 123.21, 65.57, 31.74, 29.18, 29.14, 28.61, 25.96, 22.60, 14.04; GC-MS m/e: 235.15**SI-2m: Same as 2a**

SI-2n: octyltetradecanoate[60]

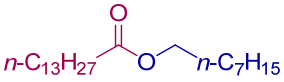

^{1}H NMR (600.17 MHz, $CDCl_3$, TMS): δ 4.08-4.03 (m, 2H), 2.31-2.26 (m, 2H), 1.63-1.60 (m, 4H), 1.36-1.20 (m, 30H), 0.87 (t, *J* =9.27 Hz, 6H); ^{13}C NMR (150.92 MHz, $CDCl_3$, TMS) δ 174.05, 65.39, 29.67, 29.64 (Cx4), 29.59, 29.47, 29.27, 29.21 (Cx2), 29.18 (Cx2), 29.15, 28.64, 25.96, 25.04, 22.68, 22.63, 14.11, 14.08; GC-MS m/e: 340.35

SI-2o: Same as 2f

SI-4a: Methyl Benzoate[54]

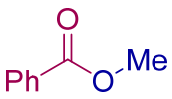

^{1}H NMR (399.78 MHz, $CDCl_3$, TMS): δ 8.04 (d, *J*=5.15 Hz, 2H), 7.54 (t, *J*=5.87 Hz, 1H), 7.42 (t, *J*=5.87 Hz, 2H), 3.90 (s, 3H); ^{13}C NMR (150.92 MHz, $CDCl_3$, TMS) δ 167.00, 132.82, 130.05, 129.47, 128.26, 52.00; GC-MS m/e: 136.15

SI-4b: Hexyl benzoate[61]

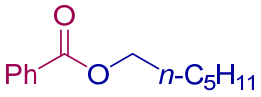

^{1}H NMR (600.17 MHz, $CDCl_3$, TMS): δ 8.05 (d, *J* =8.22 Hz, 2H), 7.54-7.51 (m, 1H), 7.45-7.40 (m, 2H), 4.31 (t, *J* =3.11 Hz, 2H), 1.78-1.73 (m, 2H), 1.47-1.42 (m, 2H), 1.36-1.31 (m, 4H), 0.90 (t, *J* =5.46 Hz, 3H); ^{13}C NMR (150.92 MHz, $CDCl_3$, TMS) δ 166.59, 132.69, 130.48, 129.46 (C×2), 128.23 (C×2), 65.05, 31.41, , 28.63, 25.65, 22.49, 13.94 GC-MS m/e: 206.15

SI-4c: Octadecyl benzoate[62]

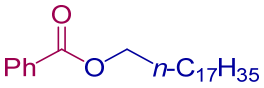

^{1}H NMR (600.17 MHz, $CDCl_3$, TMS): δ 8.05 (d, *J* =6.18 Hz, 2H), 7.55 (t, *J* =8.24 Hz, 1H), 7.43 (t, *J* =7.89 Hz, 2H), 4.31 (t, *J* =7.20 Hz, 2H), 1.79-1.74 (m, 2H), 1.46-1.41 (m, 2H) , 1.37-1.21 (m, 28H), 0.87 (t, *J* =6.51 Hz, 3H); ^{13}C NMR (150.92 MHz, $CDCl_3$, TMS) δ 166.69, 132.76, 130.53, 129.572 (C×2), 128.30 (C×2), 65.15, 31.92, 29.69 (Cx4), 29.58 (Cx4), 29.52, 29.36, 29.29, 28.71, 26.04, 22.69, 14.12; GC-MS m/e: 374.30

SI-4d: 2-ethylhexylbenzoate[54]

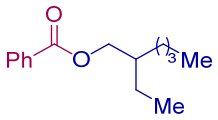

^{1}H NMR (600.17 MHz, $CDCl_3$, TMS): δ 8.04 (d, *J* =8.28 Hz, 2H), 7.54 (t, *J* =4.80 Hz, 1H), 7.43 (t, *J* =7.89 Hz, 2H), 4.28-4.21 (m, 2H), 1.74-1.69 (m, 1H), 1.47-1.41 (m, 2H) , 1.40-1.37 (m, 2H), 1.34-1.31 (m, 4H), 0.94 (t, *J* =8.25 Hz, 3H), 0.90 (t, *J* =6.51 Hz, 3H); ^{13}C NMR (150.92 MHz, $CDCl_3$, TMS) δ 166.67, 132.72, 130.55, 129.47 (C×2), 128.28 (C×2), 67.25, 38.91, 30.56, 28.96, 23.96, 22.94, 14.00, 11.05; GC-MS m/e: 234.15

SI-4e: Cyclohexylmethyl benzoate[54]

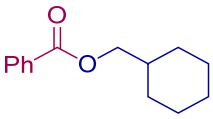

^{1}H NMR (600.17 MHz, $CDCl_3$, TMS): δ 8.04 (d, *J* =8.24 Hz, 2H), 7.54 (t, *J* =7.56 Hz, 1H), 7.43 (t, *J* =6.87 Hz, 2H), 4.13 (d, *J* =6.18 Hz, 2H), 1.84-1.68 (m, 6H), 1.30-1.18 (m, 3H) , 1.10-1.05 (m, 2H); ^{13}C NMR (100.53 MHz, $CDCl_3$, TMS) δ 166.61, 132.72, 130.49, 129.48 (C×2), 128.26 (C×2), 70.00, 37.23, 29.72 (Cx2), 26.33, 25.68 (Cx2); GC-MS m/e: 218.15

SI-4f: 3,7-dimethyloct-6-en-1-ylbenzoate[63]

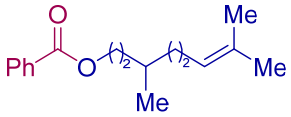

^{1}H NMR (600.17 MHz, $CDCl_3$, TMS): δ 8.04 (d, *J* =8.22 Hz, 2H), 7.54 (t, *J* =7.56 Hz, 1H), 7.43 (t, *J* =7.89 Hz, 2H), 5.09 (t, *J* =7.20 Hz, 1H), 4.38-4.32 (m, 2H), 2.06-1.95 (m, 2H), 1.85-1.79 (m, 1H), 1.67 (s, 3H), 1.65-1.63 (m, 1H), 1.60 (s, 3H), 1,58-1.54 (m, 1H), 1.42-1.37 (m, 1H) , 1.26-1.21 (m, 1H), 0.97 (d, *J* =6.84 Hz, 3H); ^{13}C NMR (150.92 MHz, $CDCl_3$, TMS) δ 166.61, 132.73, 130.50, 130.49, 129.48 (C×2), 128.26 (C×2), 124.53, 63.44, 36.95, 35.47, 29.51, 25.66, 25.35, 19.47, 17.62; GC-MS m/e: 260.20

SI-4g: 3-phenylpropyl benzoate[64]

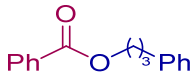

^{1}H NMR (600.17 MHz, $CDCl_3$, TMS): δ 8.04 (d, *J* =8.28 Hz, 2H), 7.55 (t, *J* =7.56 Hz, 1H), 7.43 (t, *J* =7.92 Hz, 2H), 7.29 (t, *J* =7.56 Hz, 2H), 7.23-7.17 (m, 3H), 4.34 (t, *J* =6.54 Hz, 2H), 2.79 (t, *J* =7.56 Hz, 2H), 2.13-2.08 (m, 2H); ^{13}C NMR (150.92 MHz, $CDCl_3$, TMS) δ 166.56, 141.15, 132.85, 130.33, 129.52 (C×2), 128.44 (C×2), 128.41 (C×2), 128.31 (C×2), 125.99, 64.23, 32.27, 30.27; GC-MS m/e: 240.10

SI-4h: (tetrahydrofuran-2-yl)methyl benzoate[65]

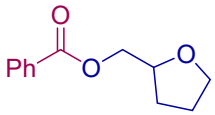

^{1}H NMR (600.17 MHz, $CDCl_3$, TMS): δ 8.05 (d, *J* =8.22 Hz, 2H), 7.56 (t, *J* =6.87 Hz, 1H), 7.44 (t, *J* = 7.23 Hz, 2H), 4.41-4.38 (m, 1H), 4.28 (d, *J* =7.14 Hz, 2H), 3.96-3.92 (m, 1H), 3.86-3.82 (m, 1H), 2.12-2.06 (m, 1H), 1.98-1.91 (m, 2H), 1.76-1.72 (m, 1H); ^{13}C NMR (150.92 MHz, $CDCl_3$, TMS) δ 166.57, 132.98, 130.06, 129.69 (C×2), 128.33 (C×2), 76.59, 68.56, 66.94, 28.10, 25.78; GC-MS m/e: 260.10

SI-4i: Benzyl benzoate[54]

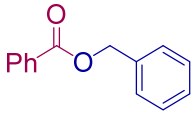

^{1}H NMR (600.17 MHz, $CDCl_3$, TMS): δ 8.06 (d, *J* =7.56 Hz, 2H), 7.50 (t, *J* =6.84 Hz, 1H), 7.43-7.34 (m, 6H), 7.30 (t, *J* =7.56 Hz, 1H), 5.34 (s, 2H); ^{13}C NMR (150.92 MHz, $CDCl_3$, TMS) δ 166.75, 135.96, 132.89, 130.05, 129.58 (C×2), 128.47 (C×2), 128.24 (Cx2), 128.11, 128.03 (Cx2), 65.53; GC-MS m/e: 212.10

SI-4j: 4-methylbenzyl benzoate[54]

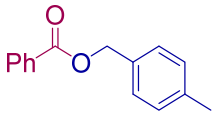

^{1}H NMR (600.17 MHz, $CDCl_3$, TMS): δ 8.06 (d, *J* =8.22 Hz, 2H), 7.55 (t, *J* =6.18 Hz, 1H), 7.42 (t, 7.56 Hz, 2H), 7.34 (t, *J* =7.56 Hz, 2H), 7.19 (d, *J* =7.56 Hz, 2H), 5.32 (s, 2H), 2.36 (s, 2H); ^{13}C NMR (150.92 MHz, $CDCl_3$, TMS) δ 166.89, 138.09, 133.01, 132.96 (Cx2),130.20, 129.68 (C×2), 129.25 (Cx2), 128.33 (Cx3), 66.59, 21.21; GC-MS m/e: 226.10

SI-4k: 4-methoxybenzyl benzoate[54]

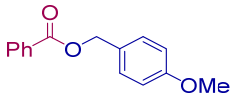

^{1}H NMR (600.17 MHz, $CDCl_3$, TMS): δ 8.06 (d, *J* =8.22 Hz, 2H), 7.54 (t, *J* =6.87 Hz, 1H), 7.43-7.38 (m, 4H), 6.91 (d, *J* =8.22 Hz,, 2H), 5.29 (s, 2H), 3.81 (s, 3H); ^{13}C NMR (150.92 MHz, $CDCl_3$, TMS) δ 166.49, 159.68, 132.89 (Cx2), 130.25, 130.05 (C×2), 129.65 (Cx2), 128.31 (C×2), 128.17, 113.96, 66.53, 55.18; GC-MS m/e: 242.10

SI-4l: [1,1´-biphenyl]-4-ylmethyl benzoate[66]

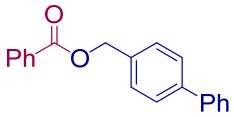

^{1}H NMR (600.17 MHz, $CDCl_3$, TMS): δ 8.10 (d, *J* =8.22 Hz 2H), 7.63-7.59 (m, 4H), 7.57-7.56 (m, 1H), 7.53 (d, *J*=8.28, 2H), 7.45 (t, *J* =7.56 Hz, 4H), 7.36 (t, *J* =6.21 Hz, 1H), 5.45 (s, 2H); ^{13}C NMR (150.92 MHz, $CDCl_3$, TMS) δ 166.48, 141.23, 140.68, 135.03, 133.06, 130.10, 129.72 (C×2), 128.79 (C×2), 128.67 (C×2), 128.38 (C×2), 127.43, 127.36 (C×2), 127.13 (C×2), 66.44; GC-MS m/e: 288.15

SI-4m: (pyridin-3-yl)methyl benzoate[67]

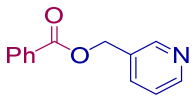

^{1}H NMR (600.17 MHz, $CDCl_3$, TMS): δ 8.73 (s, 1H), 8.60 (d, *J* =6.56 Hz, 1H), 8.06 (d, *J* =8.22 Hz, 2H), 7.78 (t, *J* = 7.23 Hz, 2H), 7.58-7.55 (m, 1H), 7.46-7.43 (m, 2H), 7.33-7.31 (m, 1H), 5.38 (s, 2H); ^{13}C NMR (150.92 MHz, $CDCl_3$, TMS) δ 166.35, 149.77 (C×2), 136.10, 133.37 (C×2), 131.76 (C×2), 129.79 (C×2), 128.56 (C×2), 123.60, 66.24; GC-MS m/e: 213.10

SI-4n: (thiophen-2-yl)methyl benzoate[68,69]

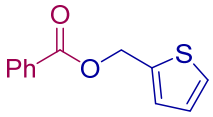

^{1}H NMR (600.17 MHz, $CDCl_3$, TMS): δ 8.05 (d, *J* =7.56 Hz, 2H), 7.55 (t, *J* =7.56 Hz, 1H), 7.42 (t, *J* = 8.22 Hz, 2H), 7.32 (d, *J* = 5.52 Hz, 1H), 7.17 (d, *J* = 3.42 Hz, 1H), 7.02-7.00 (m, 1H), 5.51 (s, 2H); ^{13}C NMR (150.92 MHz, $CDCl_3$, TMS) δ 166.23, 138.09, 133.21, 129.84 (C×2), 128.46 (C×2), 128.30, 126.96, 126.93, 61.14; GC-MS m/e: 218.05

SI-4o: (naphthalen-1-yl)methyl benzoate[70]

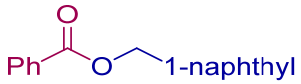

^{1}H NMR (600.17 MHz, $CDCl_3$, TMS): δ 8.10 (d, *J* =6.84 Hz, 2H), 7.91 (s, 1H), 7.86 (t, *J* =7.23 Hz, 3H), 7.57 (t, *J* =8.25 Hz, 2H), 7.50 (d, *J* =8.22 Hz, 2H), 7.44 (t, *J* =7.89 Hz, 2H) 5.54 (m, 2H); ^{13}C NMR (150.92 MHz, $CDCl_3$, TMS) δ 166.48, 133.54, 133.30, 133.22, 133.15, 130.20, 129.82 (C×2), 128.51, 128.48 (C×2), 128.09, 127.81, 127.42, 126.41, 126.36, 125.98, 66.86; GC-MS m/e: 262.10

SI-4p: Octane-2-yl-benzoate[71]

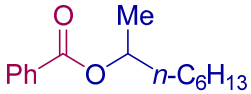

^{1}H NMR (600.17 MHz, $CDCl_3$, TMS): δ 8.04 (d, *J* =7.536 Hz, 2H), 7.53 (t, *J* =6.87 Hz, 1H), 7.43 (t, *J* =7.79 Hz, 2H), 5.16-5.13 (m, 1H), 1.79-1.69 (m,1H), 1.65-1.57 (m, 1H) , 1.43-1.1.37 (m, 2H), 1.34 (d, *J* =6.18 Hz, 3H), 1.31-1.25 (m, 6H), 0.87 (t, *J* =6.79 Hz, 3H); ^{13}C NMR (99.54 MHz, $CDCl_3$, TMS) δ 166.21, 132.64, 130.93, 129.48 (C×2), 128.25 (C×2), 71.72, 36.05, 31.72, 29.16, 25.39, 22.57, 20.06, 14.05; GC-MS m/e: 234.15

SI-4q: Undecan-2-ylbenzoate

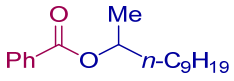

^{1}H NMR (600.17 MHz, $CDCl_3$, TMS): δ 8.04 (d, *J* =7.56 Hz, 2H), 7.54 (t, *J* =8.25 Hz, 1H), 7.43 (t, *J* =7.56 Hz, 2H), 5.17-5.13 (m, 1H), 1.77-1.70 (m, 1H), 1.62-1.57 (m, 1H), 1.42-1.36 (m, 2H) , 1.34 (d, *J* =6.18 Hz, 3H), 1.29-1.20 (m, 12H), 0.87 (t, *J* =6.87 Hz, 3H); ^{13}C NMR (150.92 MHz, $CDCl_3$, TMS) δ 166.21, 132.64, 130.94, 129.49 (C×2), 128.24 (C×2), 71.73, 36.05, 31.86, 29.51 (Cx2), 29.47, 29.28, 25.42, 22.65, 20.07, 14.08; GC-MS m/e: 276.20

SI-4r: Nonan-5-ylbenzoate[72]

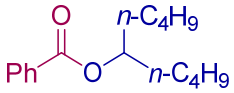

^{1}H NMR (600.17 MHz, $CDCl_3$, TMS): δ 8.04 (d, *J* =7.56 Hz, 2H), 7.53 (t, *J* =6.87 Hz, 1H), 7.42 (t, *J* =7.56 Hz, 2H), 5.16-5.09 (m, 1H), 1.71-1.61 (m, 4H), 1.38-1.31 (m, 8H) , 0.88 (t, *J* =6.81 Hz, 6H); ^{13}C NMR (99.54 MHz, $CDCl_3$, TMS) δ 166.34, 132.63, 130.86, 129.51 (C×2), 128.26 (C×2), 76.67, 33.91 (C×2), 27.49 (C×2), 22.62 (C×2), 13.98 (C×2); GC-MS m/e: 248.15

SI-4s: Cyclooctyl benzoate[73]

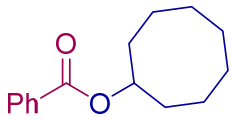

^{1}H NMR (600.17 MHz, $CDCl_3$, TMS): δ 8.04 (d, *J* =7.56 Hz, 2H), 7.53 (t, *J* =7.56 Hz, 1H), 7.42 (t, *J* =7.56 Hz, 2H), 5.21-5.18 (m, 1H), 1.94-1.91 (m, 2H), 1.89-1.85 (m, 2H) , 1.79-1.75 (m, 2H), 1.66-1.54 (m, 8H),; ^{13}C NMR (150.92 MHz, $CDCl_3$, TMS) δ 166.89, 132.59, 131.06, 129.46 (C×2), 128.22 (C×2), 76.79, 31.45 (Cx2), 27.13 (Cx2), 25.33, 22.88 (Cx2); GC-MS m/e: 235.15

SI-4t: 1-phenylpropan-2-yl benzoate[74]

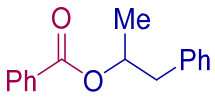

^{1}H NMR (600.17 MHz, $CDCl_3$, TMS): δ 8.01 (d, *J* =7.56 Hz, 2H), 7.53 (t, *J* =7.48 Hz, 1H), 7.41(t, *J* =7.56 Hz, 2H), 7.29-7.24 (m, 4H), 7.20 (t, *J* =7.56 Hz, 1H), 5.39-5.34 (m, 1H), 3.09-3.06 (m, 1H), 2.91-2.87 (m, 1H), 1.34 (d, *J* =6.18 Hz, 3H); ^{13}C NMR (150.92 MHz, $CDCl_3$, TMS) δ 166.98, 137.48, 132.73 (Cx2), 130.65, 129.47 (C×2), 128.32 (C×2), 128.24 (Cx2), 126.45 (Cx2), 72.09, 42.27, 19.45; GC-MS m/e: 240.10

SI-4u: 1-(-4-chlorophenyl)propan-2-yl benzoate

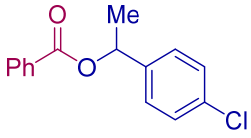

^{1}H NMR (600.17 MHz, $CDCl_3$, TMS): δ 8.07 (d, *J* =8.22 Hz, 2H), 7.56 (t, *J* =8.25 Hz, 1H), 7.44 (t, *J* =7.63 Hz, 2H), 7.38 (d, *J* =8.94 Hz, 2H), 7.34 (d, *J* =7.56 Hz, 2H), 6.11-6.07 (m, 1H), 1.65 (d, *J* =6.84 Hz, 3H); ^{13}C NMR (150.92 MHz, $CDCl_3$, TMS) δ 165.71, 140.29, 133.64, 132.92, 130.25, 129.61 (C×2), 128.73 (C×2), 128.38 (Cx2), 127.47 (Cx2), 72.18, 22.31; GC-MS m/e: 274.10

SI-6a: Methyl acetate

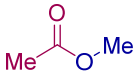

GC-MS m/e: 74.10

SI-6b: Ethyl acetate

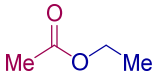

GC-MS m/e: 88.15

SI-6c: Cyclohexylmethyl acetate[75]

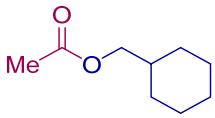

^{1}H NMR (600.17 MHz, $CDCl_3$, TMS): δ3.87 (d, J =8.22 Hz, 2H), 2.05 (s, 3H), 1.73 (d, J =7.98 Hz, 4H),1.68-1.61 (m, 2H), 1.25-1.15 (m, 10H), 0.99-0.93 (m, 2H); ^{13}C NMR (150.92 MHz, $CDCl_3$, TMS) δ 171.28, 69.66, 37.00, 29.62 (C×2), 26.33, 25.63 (C×2), 20.93; GC-MS m/e: 156.10

SI-6d: (tetrahydrofuran-2-yl)methyl acetate[76]

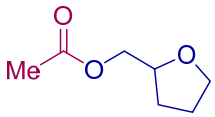

^{1}H NMR (600.17 MHz, $CDCl_3$, TMS): δ 4.13-4.10 (m, 1H), 4.09-4.04 (m, 1H), 3.07-3.92 (m, 1H), 3.88-3.83 (m, 1H), 3.79-3.74 (m, 1H), 2.05 (s, 3H), 1.98-1.94 (m, 1H), 1.88-1.85 (m, 2H), 1.59-1.52 (m, 1H); ^{13}C NMR (150.92 MHz, $CDCl_3$, TMS) δ 171.14, 76.53, 68.49, 66.65, 28.01, 25.69, 20.99; GC-MS m/e: 144.10

SI-6e: Benzyl acetate[75]

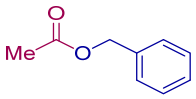

^{1}H NMR (600.17 MHz, $CDCl_3$, TMS): δ7.37 (s, 5H), 5.12 (s, 2H), 2.10 (s, 3H); ^{13}C NMR (150.92 MHz, $CDCl_3$, TMS) δ 170.73, 135.82, 128.44 (C×2), 128.33, 128.14, 128.12, 66.17, 20.87; GC-MS m/e: 150.10

SI-6f: 4-(trifluoromethyl)benzyl acetate[77]

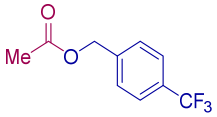

^{1}H NMR (600.17 MHz, $CDCl_3$, TMS): δ 7.62 (d, *J* =8.22 Hz, 2H), 7.47 (d, *J* =8.22 Hz, 2H), 5.16 (s, 1H), 2.12 (s, 3H); ^{13}C NMR (150.92 MHz, $CDCl_3$, TMS) δ 170.64, 139.90, 130.32 (q, *J* =31.78 Hz, CX1), 128.12 (C×2), 123.97 (q, *J* =271.64 Hz, CX1), 125.49, 125.46, 65.26, 20.82; GC-MS m/e: 218.05

SI-6g: (thiophen-2-yl)methyl acetate[76]

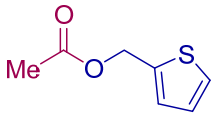

^{1}H NMR (600.17 MHz, $CDCl_3$, TMS): δ 7.31 (d, *J*=4.80 Hz, 1H), 7.09 (d, *J*=3.42 Hz, 1H), 6.98 (t, *J*=4.47 Hz, 1H), 5.25 (s, 2H), 2.08 (s, 3H); ^{13}C NMR (150.91 MHz, $CDCl_3$, TMS) δ 170.67, 137.85, 128.18, 126.82, 126.79, 60.43, 20.93; GC-MS m/e: 156.05

SI-6h: Benzo[d][1,3]dioxol-4-ylmethyl acetate[78]

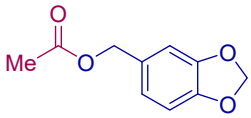

^{1}H NMR (600.17 MHz, $CDCl_3$, TMS): δ 6.83-6.80 (m, 2H), 6.76 (d, *J*=8.28 Hz, 1H), 5.92 (s, 2H), 4.97 (s, 2H), 2.06 (s, 3H); ^{13}C NMR (150.92 MHz, $CDCl_3$, TMS) δ 170.57, 147.57, 147.40, 129.48, 122.04, 108.81, 107.96, 100.94, 65.99, 20.73; GC-MS m/e: 194.05

SI-6i: bicyclo[2.2.1]heptan-2-yl acetate[79]

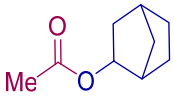

^{1}H NMR (600.17 MHz, $CDCl_3$, TMS): δ 4.58 (d, *J* =6.18 Hz, 1H), 2.28 (t, *J* =8.22 Hz, 2H), 2.08 (s, 3H), 1.74-1.69 (m, 1H), 1.54-1.49 (m, 2H), 1.46-1.40 (m, 2H), 1.17-1.07 (m, 3H); ^{13}C NMR (150.92 MHz, $CDCl_3$, TMS) δ 170.81, 77.57, 41.36, 39.57, 35.34, 35.21, 28.10, 24.29, 21.38; GC-MS m/e: 154.10

S-6j: 1-(4-bromophenyl)ethyl acetate[80]

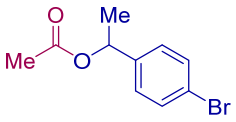

^{1}H NMR (600.17 MHz, $CDCl_3$, TMS): δ 7.46 (d, *J* =8.22 Hz, 2H), 7.22 (d, *J* =8.22 Hz, 2H), 5.81 (d, *J* = 6.90 Hz, 1H), 2.06 (m, 3H), 1.50 (s, 3H); ^{13}C NMR (150.92 MHz, $CDCl_3$, TMS) δ 170.29, 140.81, 131.72 (C×2), 127.93 (C×2), 121.82, 71.71, 22.21, 21.38; GC-MS m/e: 241.10

SI-6k: Benzhydryl acetate[81]

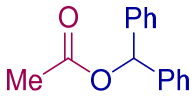

^{1}H NMR (600.17 MHz, $CDCl_3$, TMS): δ 7.34-7.32 (m, 8H), 7.30-7.26 (m, 2H), 6.88 (s, 1H), 2.16 (s, 3H); ^{13}C NMR (150.92 MHz, $CDCl_3$, TMS) δ 170.01, 140.17 (Cx2), 128.48 (Cx4), 127.88 (Cx2), 127.06 (Cx4), 76.83, 21.28; GC-MS m/e: 226.10

4.4 Conclusions

In summary, we developed a heterogeneous catalytic system that promotes alcoholysis reactions of tertiary amides with alcohols. Unlike typical reactions utilizing homogeneous catalytic systems and requiring NHC complexes, the new process is operationally convenient and does not require additives. In addition, the catalyst is recyclable, and the process has a wide substrate scope. A plausible mechanism, involving rate limiting nucleophilic addition of a CeO_2 lattice oxygen to the amide carbonyl, is proposed for the process based on the results from density functional theory (DFT) and *in situ* FT-IR studies. The presented catalysis of CeO_2 was tried to be ratinalized with its acid and base properties by employing various methods such as XPS, FT-IR, and TPD. These results show that the catalysis required for promoting the C–N bond cleavage reaction is not simply understood by utilizing independent probe techniques. This is in agreement with the findings by DFT studies that acid-base cooperation is necessary for efficient progression of the reaction. As a result, CeO_2, which has both acid and base properties, exhibits the best performance.

References

[1] A. Radzicka, R. Wolfenden, *J. Am. Chem. Soc.* **1996**, *118*, 6105–6109.

[2] R. M. Smith, D. E. Hansen, *J. Am. Chem. Soc.* **1998**, *120*, 8910–8913.

[3] B. W. Matthews, *Acc. Chem. Res.* **1988**, *21*, 333–340.

[4] D. W. Christianson, W. N. Lipscomb, *Acc. Chem. Res.* **1989**, *22*, 62–69.

[5] J. M. BOBBITT, D. A. SCOLA, *J. Org. Chem.* **1960**, *25*, 560–564.

[6] M. J. P. D. J. HAMILTON, **1969**, *1969*.

[7] Tohru Takarada, Morio Yashiro, Makoto Komiyama, *Chem. - A Eur. J.* **2000**, *6*, 3906–3913.

[8] M. Yashiro, Y. Sonobe, A. Yamamura, T. Takarada, M. Komiyama, Y. Fujii, *Org. Biomol.*

Chem. **2003**, *1*, 629–632.

[9] J. Hong, Y. Jiao, W. He, Z. Guo, Z. Yu, J. Zhang, L. Zhu, *Inorg. Chem.* **2010**, *49*, 8148–8154.

[10] A. M. Protas, A. Bonna, E. Kopera, W. Bal, *J. Inorg. Biochem.* **2011**, *105*, 10–16.

[11] K. Stroobants, E. Moelants, H. G. T. Ly, P. Proost, K. Bartik, T. N. Parac-Vogt, *Chem. - A Eur. J.* **2013**, *19*, 2848–2858.

[12] Y. Seki, K. Tanabe, D. Sasaki, Y. Sohma, K. Oisaki, M. Kanai, *Angew. Chemie - Int. Ed.* **2014**, *53*, 6501–6505.

[13] T. Deguchi, H. L. Xin, H. Morimoto, T. Ohshima, *ACS Catal.* **2017**, *7*, 3157–3161.

[14] E. H. White, *J. Am. Chem. Soc.* **1954**, *76*, 4497–4498.

[15] D. T. Glatzhofer, R. R. Roy, K. N. Cossey, *Org. Lett.* **2002**, *4*, 2349–2352.

[16] D. M. Shendage, R. Fröhlich, G. Haufe, *Org. Lett.* **2004**, *6*, 3675–3678.

[17] P. L. Anelli, M. Brocchetta, D. Palano, M. Visigalli, *Tetrahedron Lett.* **1997**, *38*, 2367–2368.

[18] S. Yamada, *Angew. Chemie Int. Ed. English* **1993**, *32*, 1083–1085.

[19] M. Hutchby, C. E. Houlden, M. F. Haddow, S. N. G. Tyler, G. C. Lloyd-Jones, K. I. Booker-Milburn, *Angew. Chemie Int. Ed.* **2012**, *51*, 548–551.

[20] Y. Kita, Y. Nishii, T. Higuchi, K. Mashima, *Angew. Chemie Int. Ed.* **2012**, *51*, 5723–5726.

[21] Y. Kita, Y. Nishii, A. Onoue, K. Mashima, *Adv. Synth. Catal.* **2013**, *355*, 3391–3395.

[22] Y. Nishii, S. Akiyama, Y. Kita, K. Mashima, *Synlett* **2015**, *26*, 1831–1834.

[23] B. N. Atkinson, J. M. J. Williams, *Tetrahedron Lett.* **2014**, *55*, 6935–6938.

[24] S. M. A. H. Siddiki, A. S. Touchy, M. Tamura, K. Shimizu, *RSC Adv.* **2014**, *4*, 35803–35807.

[25] T. Kamachi, S. M. A. H. Siddiki, Y. Morita, M. N. Rashed, K. Kon, T. Toyao, K. Shimizu, K. Yoshizawa, *Catal. Today* **2018**, *303*, 256–262.

[26] L. Hie, N. F. Fine Nathel, T. K. Shah, E. L. Baker, X. Hong, Y.-F. Yang, P. Liu, K. N. Houk, N. K. Garg, *Nature* **2015**, *524*, 79–83.

[27] J. E. Dander, N. K. Garg, *ACS Catal.* **2017**, *7*, 1413–1423.

[28] B. J. Simmons, N. A. Weires, J. E. Dander, N. K. Garg, *ACS Catal.* **2016**, *6*, 3176–3179.

[29] N. A. Weires, E. L. Baker, N. K. Garg, *Nat. Chem.* **2016**, *8*, 75–79.

[30] P. Lei, G. Meng, M. Szostak, *ACS Catal.* **2017**, *7*, 1960–1965.

[31] G. Meng, P. Lei, M. Szostak, *Org. Lett.* **2017**, *19*, 2158–2161.

[32] M. Tamura, K. Shimizu, A. Satsuma, *Chem. Lett.* **2012**, *41*, 1397–1405.

[33] L. Vivier, D. Duprez, *ChemSusChem* **2010**, *3*, 654–678.

[34] M. Tamura, A. Satsuma, K. I. Shimizu, *Catal. Sci. Technol.* **2013**, *3*, 1386–1393.

[35] T. Montini, M. Melchionna, M. Monai, P. Fornasiero, *Chem. Rev.* **2016**, *116*, 5987–6041.

[36] M. Tamura, R. Kishi, Y. Nakagawa, K. Tomishige, *Nat. Commun.* **2015**, *6*, 1–9.

[37] B. Delley, *J. Chem. Phys.* **1990**, *92*, 508–517.

[38] B. Delley, *J. Chem. Phys.* **2000**, *113*, 7756–7764.

[39] Hendrik J. Monkhorst, *Phys. Rev. B* **1976**, *13*, 5188–5192.

[40] N. Govind, M. Petersen, G. Fitzgerald, D. King-Smith, J. Andzelm, *Comput. Mater. Sci.* **2003**, *28*, 250–258.

[41] Y.-C. L. J. P. GUTHRIE, D. C. PIKE, *Can. J. Chem.* **1992**, *70*, 1671–1683.

[42] A. Aboulayt, C. Binet, J. C. Lavalley, *J. Chem. Soc. Faraday Trans.* **1995**, *91*, 2913–2920.

[43] S. Agarwal, X. Zhu, E. J. M. Hensen, B. L. Mojet, L. Lefferts, *J. Phys. Chem. C* **2015**, *119*, 12423–12433.

[44] A. Trovarelli, J. Llorca, *ACS Catal.* **2017**, *7*, 4716–4735.

[45] T. Kamachi, S. M. A. H. Siddiki, Y. Morita, M. N. Rashed, K. Kon, T. Toyao, K. Shimizu, K. Yoshizawa, *Catal. Today* **2018**, *303*, 256–262.

[46] M. Tamura, K. Shimizu, A. Satsuma, *Chem. Lett.* **2012**, *41*, 1397–1405.

[47] M. Fronzi, S. Piccinin, B. Delley, E. Traversa, C. Stampfl, *Phys. Chem. Chem. Phys.* **2009**, *11*, 9188–9199.

[48] M. Molinari, S. C. Parker, D. C. Sayle, M. S. Islam, *J. Phys. Chem. C* **2012**, *116*, 7073–7082.

[49] J. Paier, C. Penschke, J. Sauer, *Chem. Rev.* **2013**, *113*, 3949–3985.

[50] Y. Nagai, T. Hirabayashi, K. Dohmae, N. Takagi, T. Minami, H. Shinjoh, S. Matsumoto, *J. Catal.* **2006**, *242*, 103–109.

[51] C. Chaudhari, S. M. A. Hakim Siddiki, M. Tamura, K. I. Shimizu, *RSC Adv.* **2014**, *4*, 53374–53379.

[52] M. Tamura, K. I. Shimizu, A. Satsuma, *Appl. Catal. A Gen.* **2012**, *433–434*, 135–145.

[53] T. Deguchi, H.-L. Xin, H. Morimoto, T. Ohshima, *ACS Catal.* **2017**, *7*, 3157–3161.

[54] S. M. a. H. Siddiki, A. S. Touchy, M. Tamura, K. Shimizu, *RSC Adv.* **2014**, *4*, 35803.

[55] S. K. Aavula, A. Chikkulapalli, N. Hanumanthappa, I. Jyothi, C. H. Vinod Kumar, S. G. Manjunatha, *Tetrahedron Lett.* **2013**, *54*, 5690–5694.

[56] H. Shimakoshi, Z. Luo, K. Tomita, Y. Hisaeda, *J. Organomet. Chem.* **2017**, *839*, 71–77.

[57] J. E. Taylor, J. M. J. Williams, S. D. Bull, *Tetrahedron Lett.* **2012**, *53*, 4074–4076.

[58] M. Hosseini-Sarvari, E. Sodagar, *Comptes Rendus Chim.* **2013**, *16*, 229–238.

[59] M. Tamura, T. Tonomura, K. Shimizu, A. Satsuma, *Green Chem.* **2012**, *14*, 984.

[60] B. Narasimhan, V. Mourya, A. Dhake, *Bioorg. Med. Chem. Lett.* **2006**, *16*, 3023–3029.

[61] Z. Tang, Q. Jiang, L. Peng, X. Xu, J. Li, R. Qiu, C.-T. Au, *Green Chem.* **2017**, DOI 10.1039/C7GC02174G.

[62] S. S. Weng, C. S. Ke, F. K. Chen, Y. F. Lyu, G. Y. Lin, *Tetrahedron* **2011**, *67*, 1640–1648.

[63] A. Kapat, A. König, F. Montermini, P. Renaud, *J. Am. Chem. Soc.* **2011**, *133*, 13890–13893.

[64] V. K. Yadav, K. G. Babu, *J. Org. Chem.* **2004**, *69*, 577–580.

[65] V. D. V. Bodduri, K. M. Choi, R. R. Vaidya, K. Patil, S. Chirumarry, K. Jang, Y. J. Yoon,

J. R. Falck, D. S. Shin, *Tetrahedron Lett.* **2015**, *56*, 7089–7093.

[66] S. Burugupalli, S. Shah, P. L. van der Peet, S. Arora, J. M. White, S. J. Williams, *Org. Biomol. Chem.* **2016**, *14*, 97–104.

[67] S. Ko, C. Lee, M. G. Choi, Y. Na, S. Chang, *J. Org. Chem.* **2003**, *68*, 1607–1610.

[68] A. V. Iosub, S. S. Stahl, *J. Am. Chem. Soc.* **2015**, *137*, 3454–3457.

[69] J. Horiuti, T. Nakamura, *Adv. Catal.* **1967**, *17*, 1–74.

[70] B. Lu, F. Zhu, H. M. Sun, Q. Shen, *Org. Lett.* **2017**, *19*, 1132–1135.

[71] M. Tamura, S. M. A. Hakim Siddiki, K. Shimizu, *Green Chem.* **2013**, *15*, 1641.

[72] M. Hatano, Y. Furuya, T. Shimmura, K. Moriyama, S. Kamiya, T. Maki, K. Ishihara, *Org. Lett.* **2011**, *13*, 426–429.

[73] O. Chantarasriwong, D. O. Jang, W. Chavasiri, *Synth. Commun.* **2008**, *38*, 2845–2856.

[74] P. Kleman, P. J. González-Liste, S. E. García-Garrido, V. Cadierno, A. Pizzano, *ACS Catal.* **2014**, *4*, 4398–4408.

[75] Y. Kon, T. Chishiro, D. Imao, T. Nakashima, T. Nagamine, H. Hachiya, K. Sato, *Tetrahedron Lett.* **2011**, *52*, 6739–6742.

[76] R. Singha, J. K. Ray, *Tetrahedron Lett.* **2016**, *57*, 5395–5398.

[77] W. H. Fields, J. J. Chruma, *Org. Lett.* **2010**, *12*, 316–319.

[78] A. Khazaei, A. Rostami, F. Mantashlo, *Chinese Chem. Lett.* **2010**, *21*, 1430–1434.

[79] M. Jereb, D. Vražič, M. Zupan, *Tetrahedron Lett.* **2009**, *50*, 2347–2352.

[80] B. Wang, X. Tang, J. Liu, H. Yu, *Tetrahedron Lett.* **2010**, *51*, 6360–6364.

[81] R. A. Squitieri, G. P. Shearn-Nance, J. E. Hein, J. T. Shaw, *J. Org. Chem.* **2016**, *81*, 5278–5284.

Chapter 5

Direct Phenolysis Reactions of Unactivated Amides into Phenolic Esters Promoted by a Heterogeneous CeO_2 Catalyst

5.1 Introduction

Amides represent one of the most abundant functional moieties in natural and synthetic compounds.[1,2] They are an indispensable structural motif in proteins, peptides, resins, fibers, polymers, enzymes, drugs, and define most of the biological functionalities in plants.[3] The direct functionalization of amides is thus a highly attractive strategy in organic syntheses, where the major challenge lies in the cleavage of the amide C–N bond, which is due to the functional group interconversion arising from amidic resonance (**Figure 1A**)[4] that renders amides poor electrophiles and unreactive toward nucleophiles.

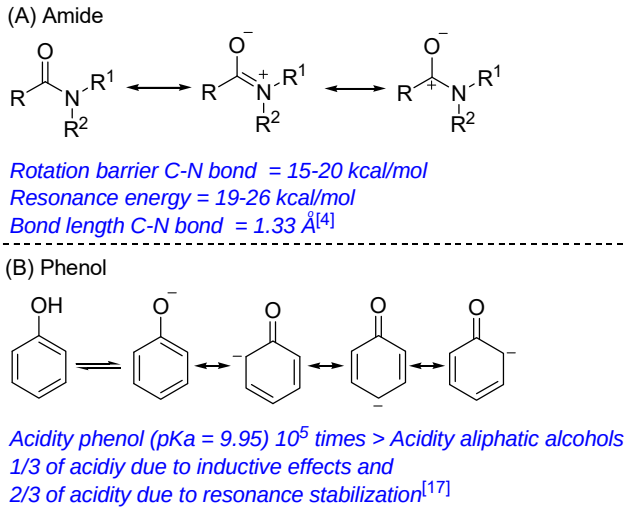

Figure 1. Comparative stability of amides (A) and phenols (B).

Conventionally, enzyme- or strong-acid/base-mediated C–N bond cleavage reactions of amides with alcohols generate huge amounts of undesired byproducts.[5–8] Recently, catalytic C–N bond cleavage reactions, specifically the alcoholysis of amides into the corresponding esters, have received much attention and several examples have been reported.[9–15] In general, the structural diversity of esters is relatively wide and they have found numerous applications in the chemical and pharmaceutical industry.[16] It should also be noted here that the transformation and derivatization of esters is easier than that of amides due to the higher reactivity of the former relative to the latter. The direct phenolysis of amides into the corresponding phenolic esters has not yet been studied extensively, mostly due to the stability of the amide group and the phenoxide ion, respectively (**Figure 1B**).[17] Phenolic esters are encountered in a wide range of biologically active compounds, agrochemicals, and natural products.[18] Additionally, the conversion of phenols into the corresponding esters is an environmentally beneficial process as phenol is considered a severe pollutant due to its harmful and toxic effects.[19] Generally, phenolic esters are synthesized via non-catalytic reactions between phenols and acyl halides, carboxylic acids, or

anhydrides in the presence of stoichiometric amounts of strong acids or bases.[20] A series of alternative catalytic methods for the esterification of phenols has been reported, including the Cu-catalyzed synthesis of phenolic esters of aryl boronic acids,[21] the Pd-catalyzed alkoxycarbonylation of aryl hydrazines with phenols,[22] the $Mo(CO)_6$-mediated alkoxycarbonylation of arylhalides,[23] and the Pd/C-catalyzed synthesis of aromatic esters from aryl halides.[16] However, the synthesis of phenolic esters from amides has rarely been studied.

Szostak and co-workers have reported a non-catalytic method for the synthesis of phenyl esters from *N*-Boc- or tosyl-activated amides using a large excess of K_3PO_4.[4] Xiuling and co-workers have reported the phenolysis of amides into esters mediated by sub-stoichiometric amounts of iron salts as well as mineral and carboxylic acids.[24] The first catalytic example for the phenolysis of *N*-Boc-activated aromatic amides using a homogeneous cobalt catalyst was reported by Danoun and co-workers.[25] This method requires several additives including a bipyridine ligand, a large excess of an activated Mn reductant, trimethylsilylchloride as a manganese-activating agent, and a hazardous dimethylformamide/pyridine mixture as the solvent. However, the method suffers from limited scope (only two examples) and a low yield of the esters (35-39%).

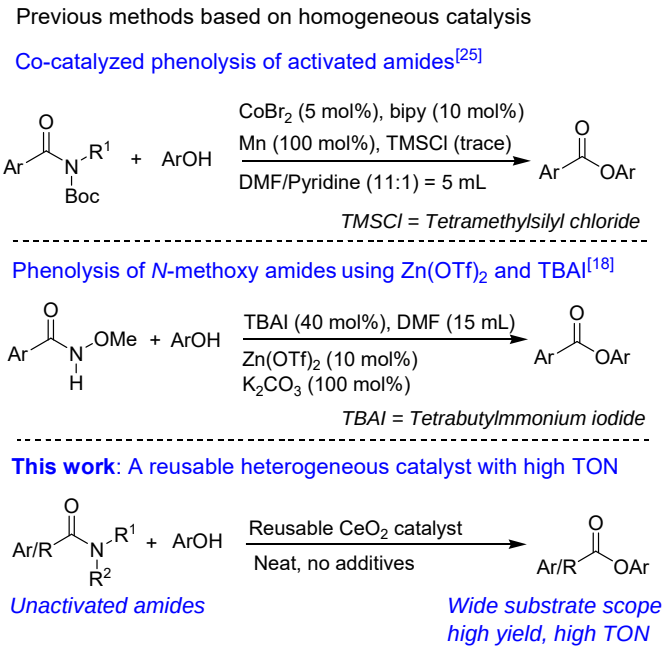

Scheme 1. Comparison of different phenolysis methods for activated amides (homogeneous systems) and the present study, which uses a CeO_2 catalyst for unactivated amides.

Recently, Bhanage and co-workers have reported a tandem electrochemical on-off catalytic method for the synthesis of phenolic esters of activated *N*-methoxyamides.[18] In this method, the electrocatalyst *t*-butylammonium iodide in a Pt-Cu electrode system forms dimers of the

N-alkoxyamide, followed by an acylation of this dimer with phenol catalyzed by $Zn(OTf)_2$ in the presence of a large excess of solvent and base. However, this system produces undesirable byproducts and its sensitivity toward unactivated, hindered, and/or heterocyclic substrates is relatively low.

Thus, the direct catalytic conversion of amides into phenolic esters, which would potentially be conducted under mild reaction conditions, represents a synthetic challenge. Furthermore, the aforementioned homogeneous methods suffer from the use of stochiometric amounts of catalysts as well as inorganic and organic additives (acids/bases), and from difficulties associated with catalyst/product separation. Hence, a direct reusable catalytic method for the phenolysis of unactivated amides into the corresponding esters represents a highly desirable research target.

Herein, we report a simple, additive-free and reusable heterogenous catalytic system based on CeO_2 for the direct phenolysis of unactivated amides into the corresponding phenolic esters. A systematic mechanistic study revealed that the unique combination of acid/base and redox properties of CeO_2[26–30] promotes this esterification reaction. This catalytic system not only offers a facile means to cleave the amide C–N bond, but also significantly promotes the use of amides and phenols as important building blocks for the synthesis of valuable esters. Moreover, the obtained results also provide a better understanding of the catalytic behavior of CeO_2, which has been of significant interest recently.[31–41]

5.2 Experimental section

5.2.1 General

We used commercially available organic and inorganic compounds that were purchased from Sigma Aldrich, Tokyo Chemical Industry, Wako Pure Chemical Industries, Kishida Chemical, or Mitsuwa Chemicals. The reagents were used as received. *N*-Boc-*N*-methyl acetamide and *N*-Boc-*N*-methyl benzamide were synthesized according to literature procedures.[25,42] Substrates and products were analyzed by GC (Shimadzu GC-2014) and GC-MS (Shimadzu GCMS-QP2010) with an Ultra ALLOY capillary column UA$^+$-1 (Frontier Laboratories Ltd.) using N_2 and He as the carrier gas. ^{1}H and ^{13}C NMR spectra were recorded at ambient temperature on JEOL-ECX 600 (^{1}H: 600.17 MHz; ^{13}C: 150.92 MHz) or JEOL-ECX (^{1}H: 400 395.88; ^{13}C: 99.54 MHz) spectrometer with tetramethylsilane as an internal standard.

5.2.2 Catalysts preparation

CeO_2 (Type A) was supplied from Daiichi Kigenso Kagaku Kogyo Co., Ltd. and calcined (600 °C, 3 h) prior to use. TiO_2 (JRC-TIO-8) was supplied by the Catalysis Society of Japan. γ-Al_2O_3 was prepared by calcination (900 °C, 3 h) of γ-AlOOH (Catapal B Alumina, Sasol). SiO_2 (Q-10) was supplied by Fuji Silysia Chemical Ltd., while Nb_2O_5 was prepared by calcination (500 °C, 3 h) of niobic acid (CBMM). ZnO was prepared by calcination (500 °C, 3 h) of a hydroxide of Zn (Kishida Chemical). Y_2O_3 and ZrO_2 were prepared by calcination (500 °C, 3 h) of the corresponding hydroxides, which were prepared via hydrolysis of $Y(NO_3)_3.6H_2O$ and $ZrO(NO_3)_2{\cdot}2H_2O$ with an aqueous NH_4OH solution. CaO was prepared by calcination (500 °C, 3 h) of $Ca(OH)_2$ (Kanto Chemical). La_2O_3 and $Ce(NO_3)_4$ were supplied by Wako Pure Chemical Industries, Japan. $Sc(OTf)_3$ (>98%) and $C_3CeF_9O_9S_3$ were obtained from TCI Co. Ltd., while $Ce_3(PO_4)_4$ (min. 99%) was supplied by Alfa Aesar, Ward Hill, China. Montmorillo-nite K10 clay (mont. K10) and Nafion-SiO_2 composite were purchased from Sigma-Aldrich.

5.2.3 Catalyst characterization

In situ FT-IR spectra were recorded at 120 °C by using a JASCO FT/IR-4200 with an MCT (Mercury-Cadmium-Telluride) detector. A sample (40 mg) was pressed to obtain a self-supporting pellet (ϕ = 2 cm). The obtained pellet was placed in the quartz IR cell with CaF_2 windows connected to a conventional gas flow system. Prior to the measurement, the sample pellet was heated under He flow (20 cm^3 min^{-1}) at 500 °C for 0.5 h. After cooling to 120 °C under the He flow, 1 μL of phenol was injected to the sample individually through a line which was preheated at ca. 200 °C to vaporize them. Spectra were measured accumulating 15 scans at a resolution of 4 cm^{-1}. A reference spectrum taken at 120 °C under He flow was subtracted from each spectrum. XRD measurements were conducted using a Rigaku Miniflex with a Cu-Kα radiation source. The ICP-AES analysis was performed using a SHIMADZU ICPE-9000. HAADF-STEM images were recorded on a JEM-ARM200F microscope (JEOL) at an acceleration voltage of 200 kV. The Cs-corrector CESCOR (CEOS) was used in the STEM mode.

5.2.4 Typical procedure for the phenolysis of amides

A Pyrex tube (20.0 mL) was charged with the amide (1.0 mmol), phenol (1.25 mmol), CeO_2 (80.0 mg), and dodecane (0.2 mmol) as an internal standard. The reaction mixture was heated

to 180 °C and stirred for 36 h under an N_2 atmosphere. After completion of the reaction, isopropanol (3 mL) was added and the products were analyzed by the GC and GC-MS. The isolation of the products was accomplished by column chromatography on silica gel 60 (spherical, 50-100 μm, Kanto Chemical Co. Ltd.) with hexane/ethylacetate (75/25) as the eluent. The isolated products were then analyzed by GC and GC-MS as well as ^{1}H and ^{13}C NMR spectroscopy. Isolated yields were determined relative to the starting amides.

5.3 Results and discussion

5.3.1 Optimization of the catalysts and the reaction conditions

To find the optimal catalyst and reaction conditions, we carried out an extensive survey of reaction parameters for the phenolysis of benzamide (**1a**) with phenol (**2a**) into the corresponding phenyl benzoate ester (**3a**). We screened a series of acidic or basic heterogeneous and homogeneous catalysts in the solvent-free model phenolysis reaction between **1a** (1 mmol) and **2a** (1.25 mmol) under an atmosphere of N_2 at 180 °C for 36 h. The conversion of **1a** and the yield of **3a** based on **1a** using different catalysts are summarized in **Table 1**. The phenolysis reaction in the absence of catalysts did not yield any **3a** (entry 1). Then, we tested a series of metal oxides (treated or untreated) in this benchmark reaction (entries 2-11). Among these, CeO_2 afforded the highest yield of **3a** (97%, entry 2). Acidic oxides such as Nb_2O_5, ZrO_2, TiO_2, and SiO_2 furnished **3a** in moderate to low yield (6-48%; entries 3-6). Amphoteric oxides such as Al_2O_3 and ZnO (entries 7 and 8) as well as basic oxides such as La_2O_3, Y_2O_3, and CaO (entries 9-11) provided **3a** in merely 2-27% yield. Commercially available solid acids, including montmorillonite K10 clay (entry 12) and Nafion/SiO_2 composite (entry 13), furnished lower yields of **3a** than CeO_2. The water-tolerant homogeneous Lewis acid $Sc(OTf)_3$ (entry 14) afforded **3a** in 50% yield. We also screened different Ce salts, including $Ce(NO_3)_4$, $Ce_3(PO_4)_4$, and $CeF_9O_9S_3$ (entries 15-17), which generated **3a** in 34%, 39%, and 52% yield respectively. Based on this screening study, it can be concluded that CeO_2 is the most effective catalyst for the phenolysis reaction between **1a** and **2a** to form **3a**.

Table 1. Catalyst screening for the phenolysis of benzamide (**1a**) with phenol (**2a**) to furnish phenyl benzoate (**3a**).

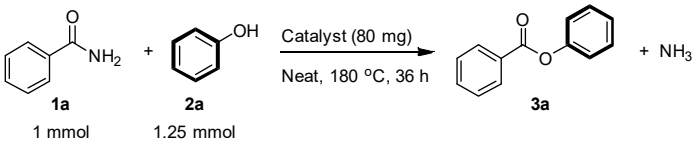

Entry	Catalyst	Conv. [%]	Yield [%][a]
1	none	0	0
2	CeO_2	100	97
3	Nb_2O_5	50	48
4	ZrO_2	47	44
5	TiO_2	40	36
6	SiO_2	8	6
7	Al_2O_3	27	25
8	ZnO	19	18
9	La_2O_3	32	27
10	Y_2O_3	9	7
11	CaO	5	2
12	Mont. K10	49	45
13	Nafion-SiO_2	41	38
14	$Sc(OTf)_3$	52	50
15	$Ce(NO_3)_4$	37	34
16	$Ce_3(PO_4)_4$	43	39
17	$CeF_9O_9S_3$	55	52

[a] GC yield.

Using CeO_2 as the most effective catalyst, we optimized the reaction conditions for the model phenolysis reaction as shown in **Figure 2**, which contains plots of the yield of **3a** and the conversion of **1a** as a function of (A) the amount of CeO_2 (20-100 mg), (B) the reaction temperature (150-190 °C), (C) the solvent, and (D) the reaction time (0-36 h).

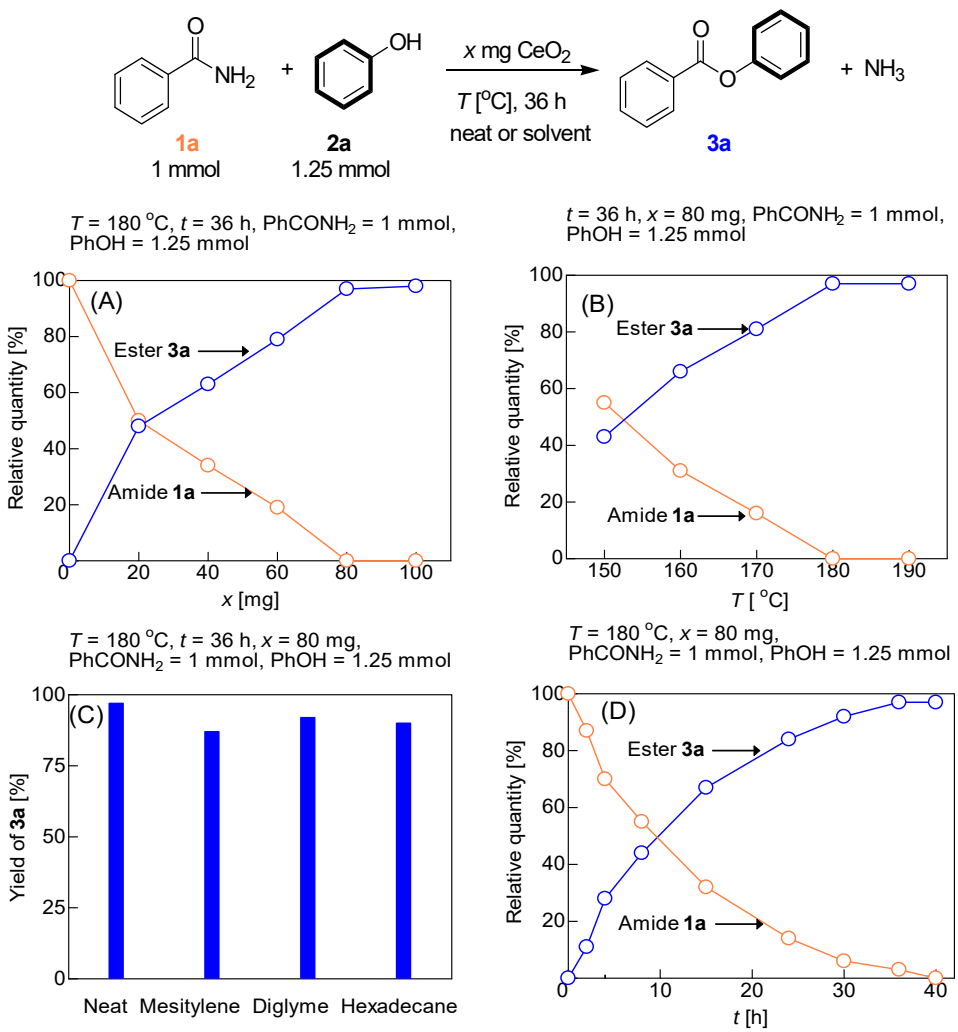

Figure 2. Optimization of the reaction conditions for the phenolysis of benzamide (**1a**) with phenol (**2a**) to produce phenyl benzoate (**3a**). The relative quantities of **1a** and **3a** are shown as a function of the (A) amount of CeO_2, (B) temperature, (C) solvent ($V_{solvent}$ = 0.5 mL), and (D) reaction time. The percentage yield of **3a** was analyzed by GC using *n*-dodecane as an internal standard.

The phenolysis yield of **3a** depends on the molar amount of **1a** and **2a** under otherwise optimized reaction conditions, i.e., 180 ºC, 36 h, 80 mg catalyst. The dependence of the yield of **3a** on the amount of catalyst (**Figure 2A**) under otherwise optimized conditions (180 °C, 36 h, 1 mmol **1a**, and 1.25 mmol **2a**) shows that 80 mg of CeO_2 affords the highest yield. **Figure 2B** shows the effect of the temperature on the yield of **3a** under otherwise optimized conditions (36 h, 80 mg CeO_2, 1 mmol **1a**, and 1.25 mmol **2a**), and allows identifying 180 °C as the optimal temperature for this phenolysis reaction.

A comparison of the reactions in **Figure 2C** shows the dependence of the reaction in the presence and absence of solvent(s) under otherwise optimized conditions (180 °C, 36 h, 80 mg CeO_2, 1 mmol **1a**, and 1.25 mmol **2a**). These reactions demonstrate that a solvent-free reaction system affords the maximum yield of **3a**. The time course of the reaction under the optimized

conditions (Figure 2D) shows the relative quantities of **1a** and **3a** as a function of time. The kinetic pattern revealed that a reaction time of 36 h was enough to obtain the maximum yield and selectivity of **3a** (97% yield).

5.3.2 CeO_2-catalyzed phenolysis of amides with phenols into esters

5.3.2.1 Heterogenous catalytic properties of CeO_2

We studied the heterogeneous catalytic properties of CeO_2 in the aforementioned phenolysis of amides under the previously established optimized reaction conditions. Moreover, we examined the reusability of this catalytic system in the model phenolysis reaction between **1a** and **2a** (**Figure 3A**). For that purpose, isopropanol (3 mL) was added to the reaction mixture after each reaction cycle, and CeO_2 was separated by centrifugation, followed by two consecutive washings with isopropanol (3 mL) and acetone (3 mL), and drying at 110 °C for 6 h. The thus recovered catalyst was then used for the next reaction cycle between **1a** and **2a**. The recovered catalyst was reusable for four cycles, albeit that a slight gradual decrease of the yield of **3a** (97-91%) was observed.

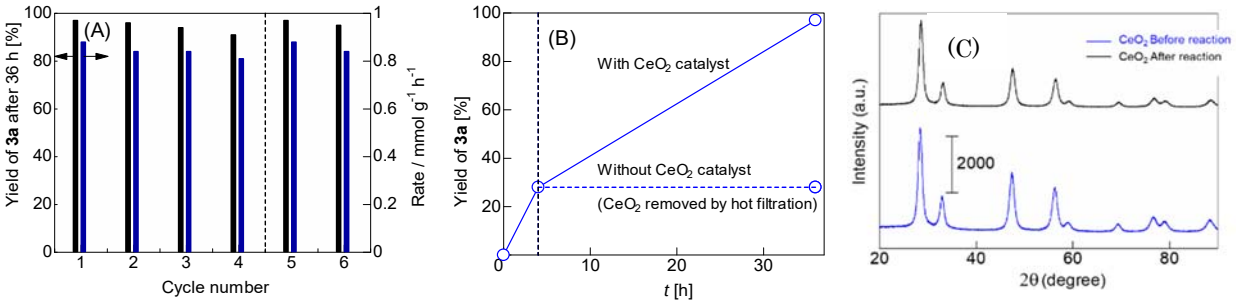

Figure 3. (A) Catalyst reusability for the CeO_2-catalyzed phenolysis of benzamide (**1a**) with phenol (**2a**) to afford phenyl benzoate (**3a**). Black bars: GC yield of **3a** after 36 h; blue bars: initial rate of the formation of **3a**, determined where the conversion of amide was below 30%. (B) Leaching study of the CeO_2 catalyst in the reaction affording phenyl benzoate. (C) X-ray diffraction (XRD) pattern of the CeO_2 catalyst before and after the catalytic reaction. Reaction conditions: catalyst (80 mg), benzamide (1 mmol), phenol (1.25 mmol), 180 °C, under N_2 atmosphere.

The catalytic performance of the recovered catalyst after the fourth cycle (dotted line in Figure 3A) could be increased to 96-97% by calcination (600 °C; 3 h; air). During this part of the recycling study, the initial rate of the formation of **3a**, where the conversion of the amide is below 30%, was also determined for each cycle (blue bars in **Figure 3A**); the results show that the initial rate gradually decreases with increasing number of catalytic and recycling cycles. We also confirmed that the powder X-ray diffraction (XRD) pattern of the CeO_2 catalyst after the catalytic reaction was almost identical to that of the original sample (**Figure 3C**), which indicates that the crystallinity of the catalyst remains almost unchanged during the catalysis.

To confirm the heterogeneous nature of the CeO_2 catalyst, leaching tests were carried out on the model reaction under standard conditions. For that purpose, the solid CeO_2 was separated by hot filtration after 4 h (28% yield of **3a**), which stopped the catalytic process (**Figure 3B**). Inductively coupled plasma atomic emission spectroscopy (ICP-AES) was used to confirm the heterogeneous nature of the CeO_2 catalyst. An ICP-AES analysis showed that the filtrate did hardly contain any leached Ce species ([Ce] below the detection limit of 10 ppb) in of the model reaction mixture under standard conditions after filtration. These results demonstrate that CeO_2 is a reusable heterogeneous catalyst for the phenolysis of amides into the corresponding esters.

5.3.2.2 Substrates Scopes

With the optimized reaction conditions in hand, we examined the substrate scope for the CeO_2-catalyzed phenolysis of amides. The results show that this system readily promotes the high-yield esterification of a wide range of amides with phenols (**Schemes 2 and 3).**

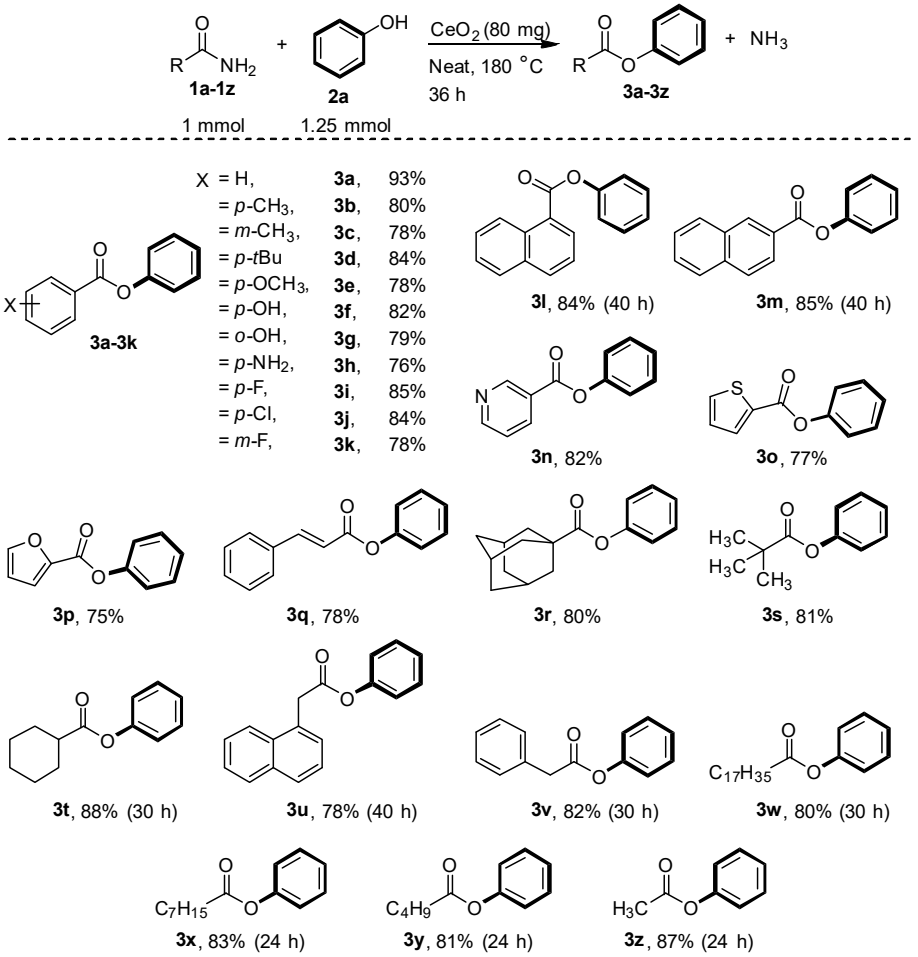

Scheme 2. Phenolysis of amides (**1a**-**1z**) with phenol (**2a**) into the corresponding esters (**3a**-**3z**); isolated yields are shown.

Initially we tested aromatic, heterocyclic, allylic, sterically hindered α-carbon-containing, benzylic, and aliphatic primary amides in the reaction with **2a** (**Scheme 2**). A series of benzamides, including electron-donating (methyl at the *para* and *meta* positions, *tert*-butyl, methoxy at the *para* position, hydroxyl at the *ortho* and *para* positions, and an amine at the *para* position; **1b**-**1h**) and electron-withdrawing groups (fluoride at the *para* and *meta* positions, as well as chloride at the *para* position; **1i**-**1k**) were successfully transformed into the corresponding phenyl esters in good to high isolated yield (76-93%). Regardless of the electronic nature, substrates with substituents at the *para* position afford higher yields than those containing substituents at the *ortho* and *meta* positions, as evident from the methyl- (**1b**,**1c**), hydroxyl- (**1f**, **1g**) and fluoride-substituted amides (**1i, 1k**). Naphthyl-substituted amides (1- and 2-naphthamide) are well tolerated in this phenolysis and afford phenyl 1-naphthoate (84%; **3l**) and phenyl 2-naphthoate (85%; **3m**) in high yield. It should be noted that all these phenolic esters are formed in higher yield compared to those obtained from the catalytic phenolysis of *N*-methoxy-activated aromatic amides.[18] Heteroaromatic amides (e.g. nicotinyl, thiophenyl, and furanyl groups) can also be successfully transformed into the corresponding phenyl esters in good to high isolated yield (75-82% yields; **3n**-**3p**).

In contrast, previously reported catalytic methods were only effective for the *N*-methoxy-activated furan-2-carboxamide. Allylic amides also underwent this phenolysis to give phenyl cinnamate ester **3q** in good yield. Aliphatic amides with sterically hindered quaternary (adamantyl- or pivaloyl-substituted) or tertiary (cyclohexyl-substituted) α-carbon atoms were also well tolerated in this reaction and the corresponding phenyl esters (**3r**-**3t**) were obtained in high isolated yield. It should also be noted that the quaternary-α-carbon-containing amides used in this reaction represent the first examples of such substrates in phenolysis reactions. Benzylic amides such as 2-(naphthalen-1-yl)-acetamide and 2-phenylacetamide were successfully transformed to the corresponding phenyl esters in good to high yield (**3u**: 78%; **3v**: 82%). Linear aliphatic amides of different chain length including C1, C4, C7, and C17 skeletons also underwent this phenolysis and furnished the corresponding phenyl alkanoate esters (**3w**-**3z**) in high yield (80-87%). It should also be noted that this is the first direct catalytic method for the phenolysis of unactivated primary amides to generate the corresponding phenyl esters.

Subsequently, we examined the reaction scope with respect to the phenol component for the phenolysis of **1a** into the corresponding esters (**Scheme 3**).

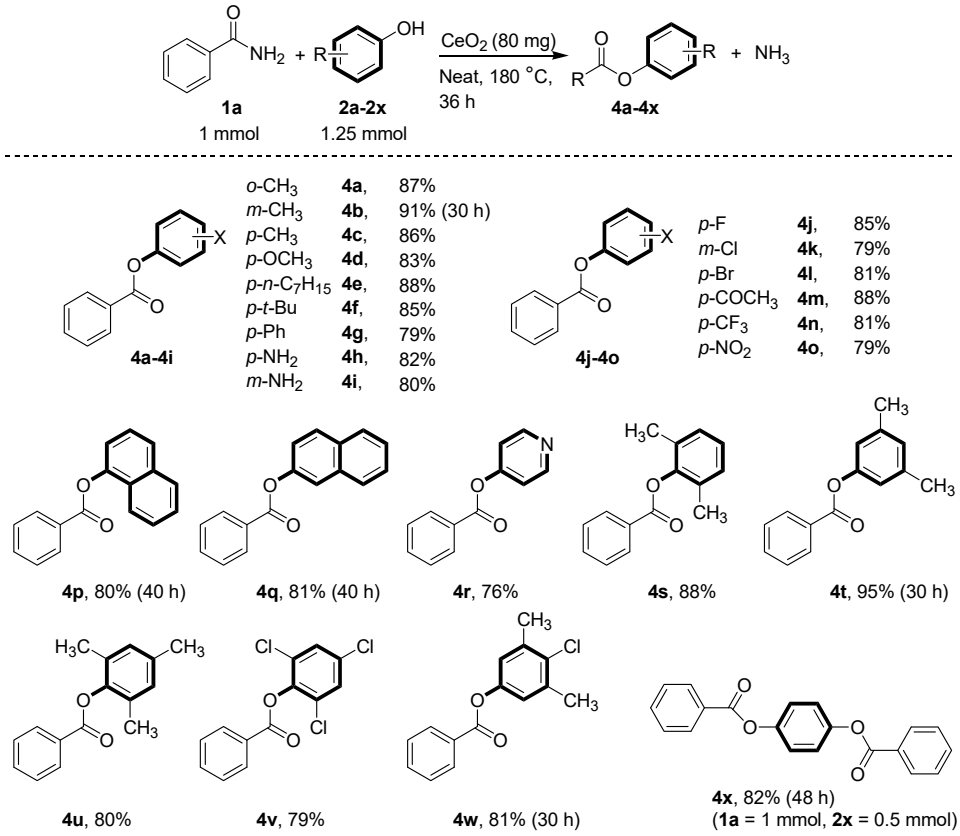

Scheme 3. Phenolysis of benzamide (**1a**) with various phenols (**2a**-**2x**) to afford the corresponding esters (**4a**-**4x**); isolated yields are shown.

A series of phenols with electron-donating and -withdrawing substituents afforded the corresponding esters in good to high isolated yield (77-92%). Regardless of the position of the methyl group (*ortho*, *meta*, or *para*) in toluol, excellent yields of tolyl benzoate (**4a**-**4c**; 87-90%) were obtained. Moreover, phenols with *para*-methoxy, *para*-*n*-hexyl, *para*-*t*-butyl, *para*-phenyl, and *para*- or *meta*-amine substituents furnished the corresponding esters (**4d**-**4i**) in high yield. The *meta*- and *para*-amino-substituted phenols represent unprecedented examples for the catalytic phenolysis of *p*-aminophenyl benzoate (**4h**) and *m*-aminophenyl benzoate (**4i**), respectively. Phenols containing electron-withdrawing substituents such as the weakly electron-withdrawing *p*-fluoride-, *m*-chloride-, and *p*-bromide groups, or the moderately electron-withdrawing acyl group, as well as strongly electron-withdrawing trifluoromethyl and nitro groups generated the corresponding esters (**4j**-**4o**) in good to high yield. This phenolysis method is also applicable to phenol homologues including 1-naphthanol and 2-naphthanol for the synthesis of corresponding benzoate esters (**4p**: 80%; **4q**: 81%). Pyridin-4-ol, a hetero-homologue of phenol, is the first example that engages in a phenolysis reaction with **1a** to form pyridin-4-yl benzoate ester (**4r**). Phenols that possess sterically hindered substituents including electron-donating and -withdrawing groups such as 3,5-dimethyl, 2,4,6-trimethyl, 2,4-6-

trichloride, and 4-chloro-3,5-dimethyl substituents engaged in phenolysis reactions with **1a** to form the corresponding esters (**4t-4w**) in good to excellent yield (77-95%). This catalytic method is also applicable to the challenging hydroquinone substrate, which affords 1,4-phenylene dibenzoate ester (**4x**) in high yield (82%). The thus obtained esters (**4s-4x**) are the first examples to be obtained via the esterification of amides.

5.3.2.3 Applicability of gram scale synthesis

We also examined this CeO_2-promoted phenolysis reaction (100 h) on the gram scale, using different amides (10 mmol) with phenols (12.5 mmol) and CeO_2 (80 mg); the observed results are summarized in **Scheme 4**. Acetamide (**1a**), and *o*-hydroxy benzamide in combination with **2a** as well as **1a** in combination with different *p*-substituted phenols and phenol homologues were transformed into the corresponding esters in 80-93% yield. The TON values of these reactions were ~ 95-110 based on the number of Ce cations on the surface of CeO_2 (1.067 mmol g^{-1}).[43] It should be noted that product **3g** acts as an antiseptic and analgesic, while **4q** acts as an antiseptic.[18] **Table 2** compares the catalytic activity of our method to that of the representative catalyst $Zn(OTf)_2$ in the phenolysis of amides. This homogeneous catalytic system is only effective for *N*-methoxy-activated amides, whereas our system is effective for unactivated and *N*-methoxy-activated amides. In the phenolysis of **1a** by *p*-nitrophenol, the TON of the CeO_2 catalyst (95) is by two orders of magnitude higher than that of $Zn(OTf)_2$ for the same *N*-methoxy-activated amide.

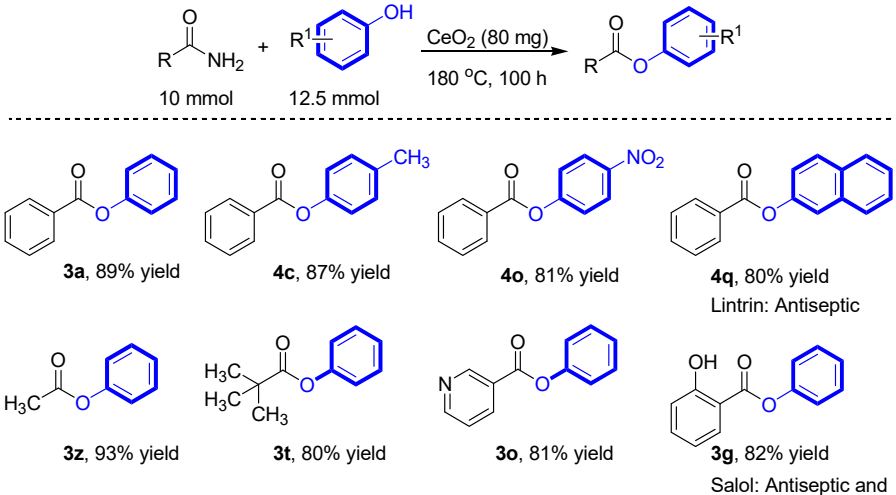

Scheme 4. Gram-scale phenolysis of amides to afford esters including the pharmaceutical agents Lintrin (**4q**) and Salol (**3g**)**;** GC yields are shown.

Table 2. Phenolysis of benzamide (**1a**) with *p*-nitrophenol

Catalyst	Additive	TON[a]	Catalyst reuse	Ref.
	0.4 equiv of TBAI			
$Zn(OTf)_2$	1.0 equiv of K_2CO_3	1.9	no	18
	15 mL of DMF			
CeO_2	none	95	4 runs	this work

[a] TON per Ce cation on the CeO_2 surface.

5.3.2.4 Applicability and comparative reactivity studies of phenolysis reactions

Scheme 5 shows the results of the applicability and a comparative reactivity study of the phenolysis of unactivated and activated primary, secondary, and tertiary aromatic (benzamides), as well as aliphatic (acetamides) amides with phenols under the previously established optimized reaction conditions.

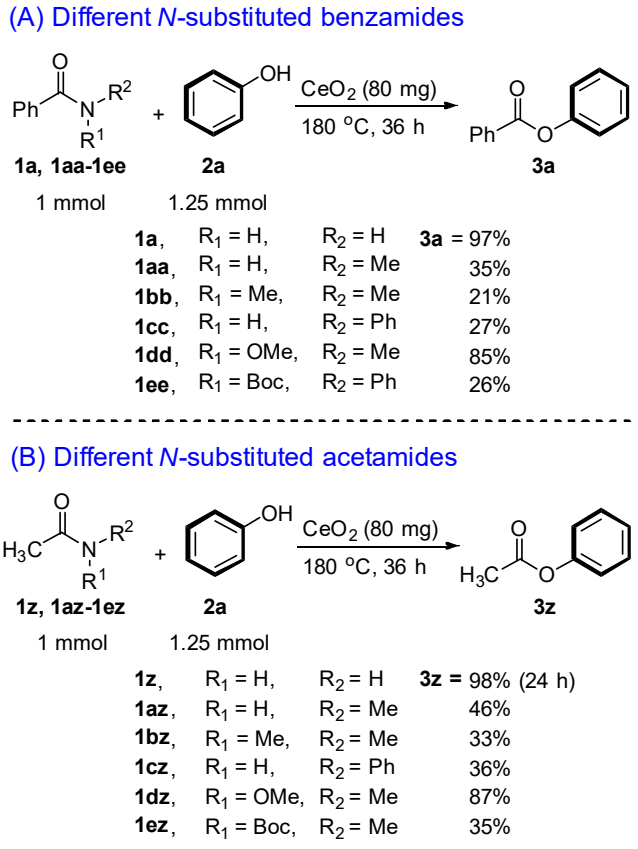

Scheme 5. Phenolysis of (A) activated and unactivated *N*-substituted benzamides (**1a**, **1aa-1ee**) into phenyl benzoate (**3a**), and (B) activated and unactivated acetamides (**1j**, **1jj-1nn**) into phenyl acetate (**3z**); reaction conditions: CeO_2 (80 mg), 180 ºC, 24-36 h, under N_2, amide (1 mmol), **2a** (1.25 mmol); GC yields are shown.

A series of unactivated benzamides (**1a**, *N*-methylbenzamide, *N,N*-dimethylbenzamide, and *N*-phenylbenzamide) were subjected to this phenolysis and the results regarding the formation of the corresponding phenyl benzoate esters reveal a significant reactivity trend, i.e., the reactivity decreases in the order: **1a**>**1aa**>**1cc**>**1bb** based on the yield of representative ester **3a** (97-27%). This trend was attributed to the steric hindrance generated by the methyl and phenyl substituents. A similar reactivity trend was observed for the reactions of unactivated acetamides (acetamides, *N*-methylacetamide, *N,N*-dimethylacetamide, *N*-phenylacetamide) with **2a** in the formation of the corresponding acetate ester **3z** (98-33%), i.e., the reactivity decreases in the order: **1z**>**1az**>**1cz**>**1bz**.

We also determined an experimental activation energy through an Arrhenius plot for the esterification of acetamide with different alcohols including *n*-octanol, benzyl alcohol, and phenol (**Figure 4**). The results show that a higher activation energy is required for the phenolysis of acetamide compared to that for the alcoholysis using *n*-octanol or benzyl alcohol.[14] This could potentially be rationalized in terms of the poor nucleophilicity and the generation of a weaker conjugate base of the phenoxide species relative to that of the alkoxide species, which retards the phenolysis toward the carboxylate species.

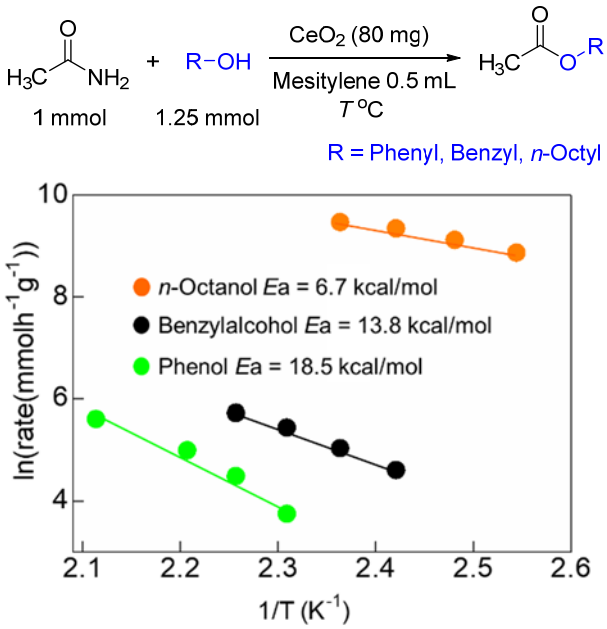

Figure 4. Arrhenius plots for the esterification of acetamide by *n*-octanol (120-150 ºC, 1 h), benzyl alcohol (135-175 ºC, 2 h), and **2a** (160-200 ºC, 4 h).

It is also important to consider the reactivity of the amides for this phenolysis by installation of amide-activating groups on the N atom under the concept of the amide-bond-destabilization platform.[4] In this context, we have examined activated benzamides (*N*-methoxy-*N*-

methylbenzamide **1dd** and *tert*-butyl benzoyl(phenyl)carbamate **1ee**) and acetamides (*N*-methoxy-*N*-methylacetamide **1dz** and *tert*-butyl acetyl(methyl) carbamate **1ez**). The results show that amides activated by a methoxy group engage in the phenolysis and generate the corresponding benzoate ester (**3a**: 85%) and acetate ester (**3z**: 87%) in high yield. *Tert*-butoxycarbonyl-(Boc)-activated benzamide **1ee** and acetamide **1dz** were also tested and furnished the corresponding esters in low yield. This was attributed to a scissoring of the Boc group, which would lead to the unactivated *N*-phenylbenzamide (**1cc**) and *N*-methylacetamide (**1az**).

5.3.2.4 Selectivity trend analysis of the reactions

To compare and ascertain the selectivity trends of this phenolysis reaction for different amides, we examined a series of competitive reactions (**Scheme 6**).

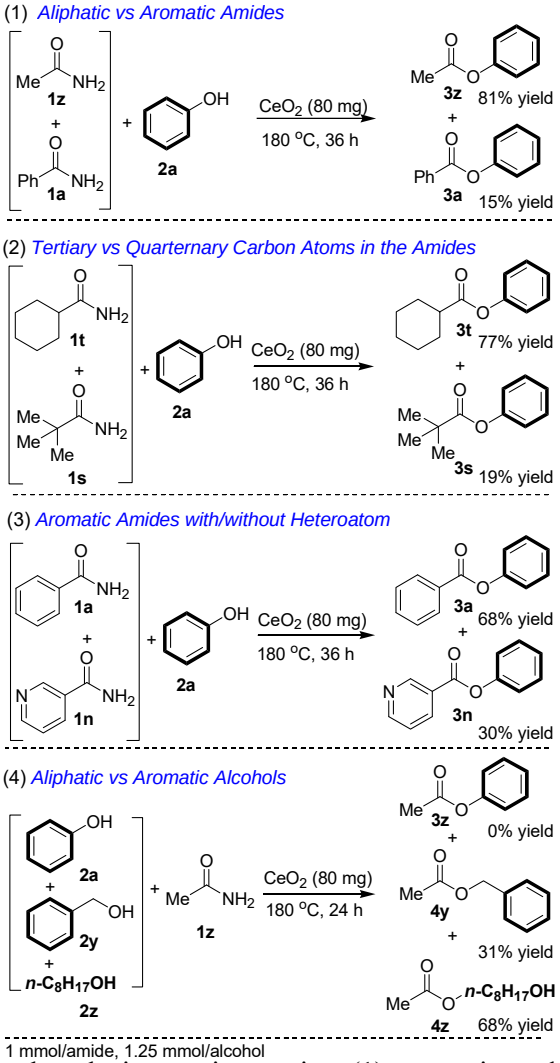

Scheme 6. Competitive phenolysis reactions using (1) aromatic and aliphatic amides, (2) amides containing tertiary or quaternary α carbon atoms, (3) aromatic and heteroaromatic amides, and (4) acetamide with a mixture of phenol, benzyl alcohol and *n*-octanol. GC yields are shown.

In this comparison, aliphatic and aromatic amides (Scheme 6(1)) were compared, i.e., the competitive reaction of **1a** and **1z** with **2a**. The results show that acetamide reacts predominantly with **2a** in the presence of **1a** to give ester **3z** (81% yield). Secondly, we compared the reactions of amides that contain tertiary (**1t**) or quaternary α-carbon atoms (**1s**) with **2a** (Scheme 6(2)) to get further insight into how the steric and electronic effects of the amide substrates affect the phenolysis. In the presence of the sterically more hindered amide (**1s**) **2a** preferentially reacts with **1t** to afford the corresponding ester (**3t**) in 77% yield. The competitive reaction of **1a** and nicotinamide **1n** with **2a** was also examined, which revealed that **2a** preferentially reacts with **1a** (Scheme 6(3)). Finally, we compared the competitive reactions of aliphatic and aromatic alcohols with **1z**. The results show that the aromatic alcohol **2a** is completely inert in the presence of benzyl alcohol **2y** and *n*-octanol **2z**, which generate the corresponding esters (**4y** and **4z**) in 31% and 68% yield respectively. These results could potentially be used as guidelines for the selective synthesis of esters from a mixture of amides or alcohols.

5.4 Mechanistic Study

5.4.1 Effect of calcination temperature of CeO_2 catalysis

The structure of the CeO_2 catalyst was characterized by XRD analysis (**Figure 5A**), N_2 adsorption measurements, and high-angle annular dark-field scanning transmission electron microscopy (HAADF-STEM) images (**Figure 5B**). The transmission electron microscopy (TEM) images of this sample have already been reported in our previous study.[14]

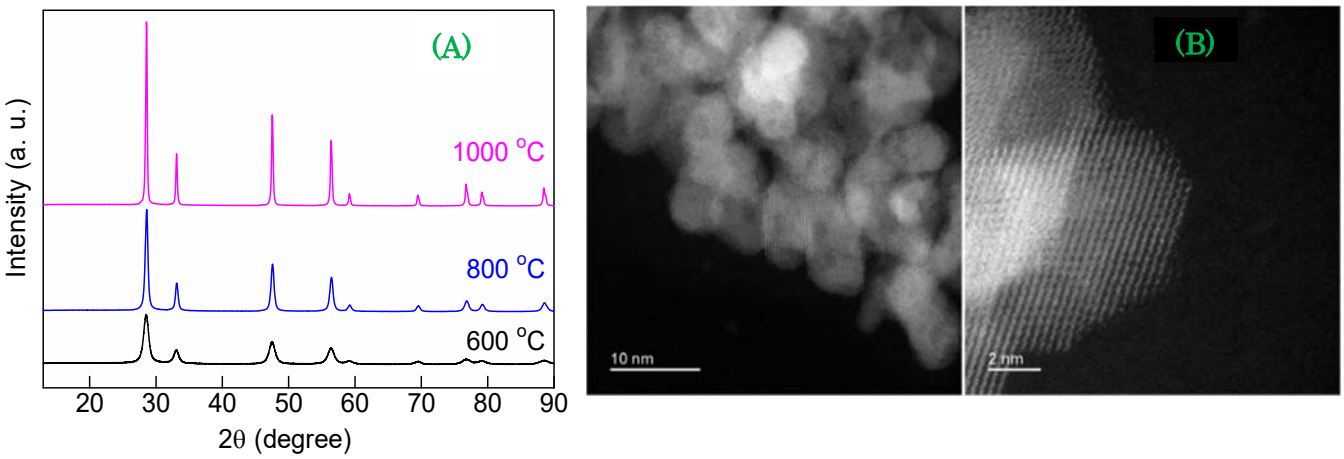

Figure 5: (A) XRD patterns of CeO_2 catalysts calcined at different temperature for 3 h and (B)high-angle annular dark-field scanning transmission electron microscopy (HAADF-STEM) images

Summarizing these results, our standard CeO_2 catalyst is composed of nanometer-sized CeO_2 particles with a fluorite-type structure and a BET specific surface area (S_{BET}) of 81 $m^2\ g^{-1}$. The

results of the temperature-programmed desorption (TPD) of NH_3 and CO_2 in our previous study[14] indicate the presence of acid and base sites on the standard CeO_2 catalyst. We calcined CeO_2 catalysts at three different temperatures (600 ºC, 800 ºC, and 1000 ºC). It should be noted that our standard CeO_2 catalyst was calcined at 600 ºC. The XRD results (**Figure 5A**) show that these catalysts share the same fluorite-type structure. Using these catalysts, we measured the rate of the formation of phenyl benzoate under conditions where conversions were < 30%. The rate per catalyst weight gradually decreased with increasing calcination temperature (**Figure 6**). The BET surface areas of the CeO_2 catalysts significantly decreased with increasing calcination temperature. The specific rate per surface areas of the CeO_2 catalysts increased with increasing calcination temperature. Taking into account a general trend that the number of surface oxygen vacancies and Ce^{3+} species on CeO_2 surfaces decreases upon calcination of CeO_2 at high temperatures, these results suggest that the formation of a highly crystalline CeO_2 surface with less Ce^{3+} and oxygen vacancies plays an important role in this catalytic system.

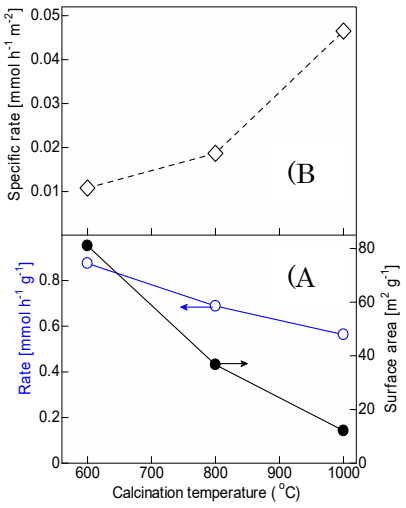

Figure 6. Effect of the calcination temperature of CeO_2 on the rates per catalyst weight (blue line) and surface areas (black line). (A) The initial reaction rate of the formation of phenyl benzoate per catalyst weight as a function of the calcination temperature. (B) The initial reaction rate normalized by the surface areas of the CeO_2 catalysts as a function of the calcination temperature. The reaction was carried out for 4 h under optimized conditions.

5.4.3 FT-IR and Kinetic studies

The FT-IR spectrum of adsorbed phenol species on the CeO_2 surface at 120 ºC is shown in **Figure 7**. The observed peaks were assigned to phenoxide species coordinated to a cationic site.[44] This result indicates that the Lewis-acid site (Ce cation) is close to a base site (proton-abstraction site).

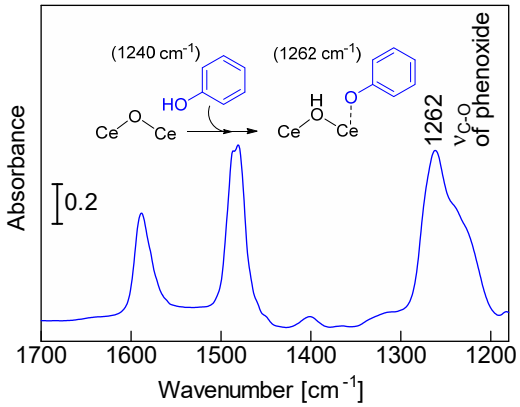

Figure 7. IR spectrum of phenoxide species on the CeO_2 surface at 120 °C (t = 700 s). Phenol (1 μL) was introduced to CeO_2, followed by purging with He (700 s).

To elucidate the reaction mechanism of the CeO_2-catalyzed phenolysis reaction, control reactions and kinetic studies were carried out. In our previous studies on the esterification of amides by alcohols via cleavage of the C–N bond over CeO_2,[14,45] we have demonstrated that the reaction proceeds via the transformation of the amide substrate into a lattice-oxygen-coordinated carboxylate initiated by the nucleophilic attack of the lattice-bound oxygen atom of CeO_2 onto the carbonyl carbon atom of the amide, followed by a reaction with the alkoxide (formed by the deprotonation of an alcohol) to give the ester. Both the experimental and computational investigations demonstrated that the cooperative effects of the acid-base functions of CeO_2 are important for an efficient progression of the alcoholysis of amides via the cleavage of the C–N bond, and consequently, CeO_2 exhibited the best catalytic performance.

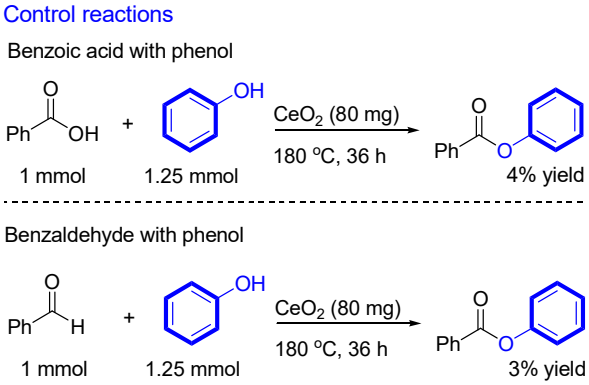

Scheme 7. Control reactions between phenol and benzoic acid or benzaldehyde under standard reaction conditions.

Based on this finding, we speculated that the CeO_2-coordinated carboxylate is the crucial intermediate, rather than a free acid and/or an aldehyde, which undergo reactions with the phenoxide to form phenolic esters under the present catalytic reaction conditions. Representative control reactions (**Scheme 7**) between phenol and benzoic acid and

benzaldehyde under standard reaction conditions were thus tested. The observed low yield of the phenyl benzoate (3-4%) supports our hypothesis and confirms that free acids or aldehydes do not act as reaction intermediates.

The influence of the concentration of acetamide and phenol on the initial rate of formation of phenyl acetate ester was also explored (**Figure 8**). We discovered a linear relationship on double logarithmic plots and the slopes of the lines correspond to the order (*n*) of the reaction. The ester formation rate increased with the concentration of phenol, which followed first-order reaction kinetics (n = +1.02, R^2 = 0.99) (**Figure 8A**). Conversely, a negative slope (n = -0.19) was observed upon increasing the concentration of acetamide (**Figure 8B**), which suggests that phenol is involved in the kinetically important steps.

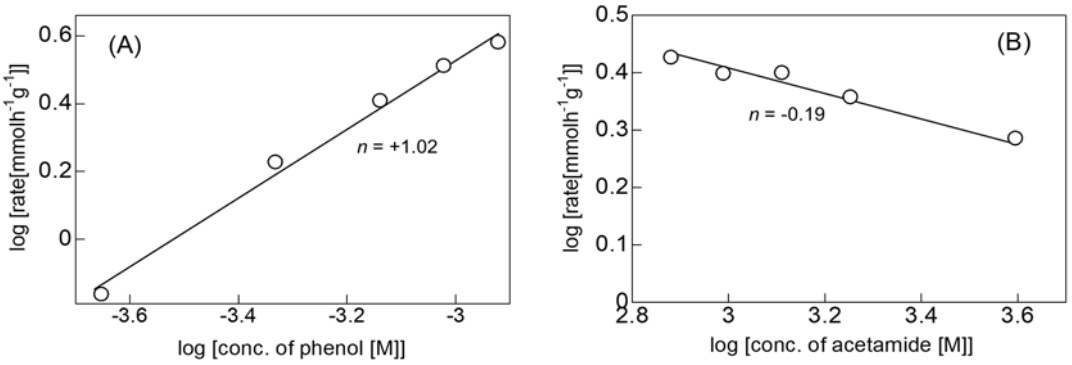

Figure 8. Formation rate of phenylacetate as a function of the concentration of (A) phenol (0.22 M to 1.19 M) and (B) acetamide (0.25 M to 1.32 M); reaction conditions: CeO_2 (80 mg), T = 180 ºC, t = 4 h.

The influence of different substituents (electron-donating and -withdrawing) on the phenol ring toward the reactivity divergence of the phenolysis reaction was examined using a Hammett study. During the phenolysis of benzamide (**Figure 9A**), the logarithm of the reaction rates was correlated directly to the substituent constant (σ), indicating that a linear free-energy relationship exists, wherein the slopes of the reaction rates are $0 < \rho < 1$. This in turn implies that the reaction is not very sensitive to the nature of the substituents on phenol and that a negative charge is generated (or a positive charge is lost) in the transition state of a kinetically important step.

The phenolysis of *para*-substituted benzamides with phenol revealed a good relationship between $\log(k_X/k_H)$ and the Brown-Okamoto parameter (σ^+).[27] Specifically, we observed good linearity with a positive slope (ρ = +0.26) (**Figure 9B**), which indicates that a transition state in the rate-limiting step of the phenolysis contains a negative charge at the α-carbon atom adjacent to the benzene ring. Accordingly, it can be concluded that the nucleophilic addition of the phenoxide species to the activated carbonyl carbon atom of the amide proceeds via a

negatively charged transition state, and that this could be the rate-limiting step of this reaction.[27]

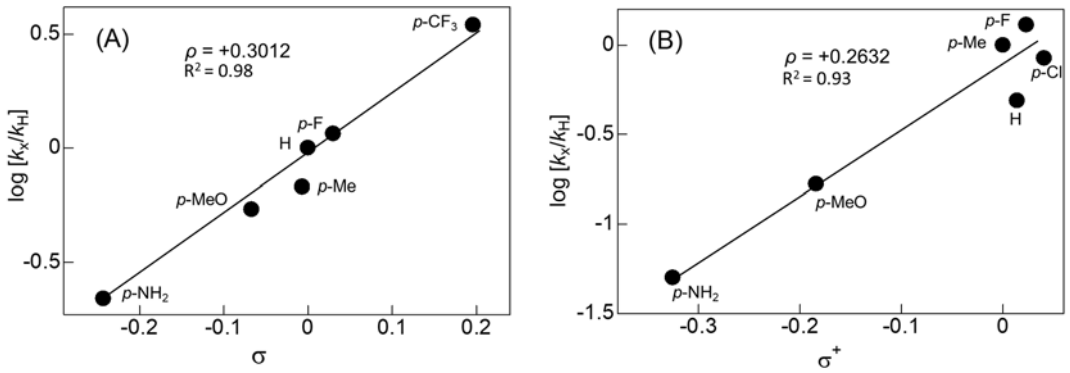

Figure 9. (A) Hammett study for sterically comparable *p*-substituted phenols with benzamide; (B) Brown-Okamoto plot for the phenolysis of *p*-substituted benzamide with phenol; reaction conditions: benzamide (1 mmol), phenol (1.25 mmol), CeO_2 (80 mg), T = 180 ºC, t = 4 h.

5.4.3 Plausive reaction mechanism

Thermodynamically, the reactions seem to proceed uphill, as amides are usually more stable than esters. A possible thermodynamic driving force that would explain the high yields of esters could be the release of NH_3 from the liquid phase, which would decrease the concentration of the product (NH_3) in the liquid phase, where the amide, phenol, ester, and catalyst are present. Based on aforementioned experimental results and our previous computational studies on esterification of amides by alcohols via C–N bond cleavage over CeO_2,[14,45] a plausible reaction mechanism for the CeO_2-catalyzed phenolysis of acetamide to form phenyl acetate ester is proposed in **Figure 10**.

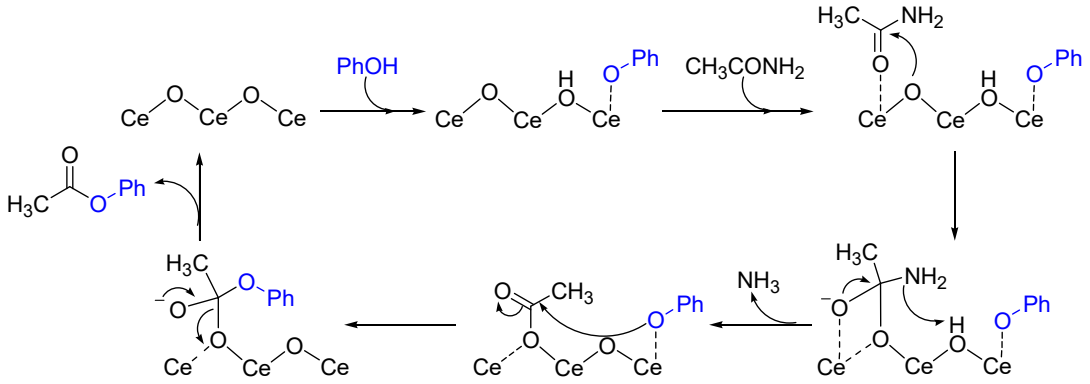

Figure 10. Plausible reaction mechanism for the CeO_2-catalyzed phenolysis of acetamide with phenol.

The catalytic cycle should start with the deprotonation of the phenol to phenolate on one of the acid-base pair sites of CeO_2. Then, the adsorbed acetamide is activated by a nucleophilic attack of a lattice-bound oxygen of CeO_2 to produce the acetate. After the deamination step, a

negatively charged transition state is produced via the addition of the phenolate to the acetate and this step would probably be rate-determining. Finally, the acetate ester would be desorbed to regenerate the free acid-base sites of the CeO_2 catalyst.

5.4.5 GC-MS and NMR analysis of reactants and products

^1H and ^{13}C NMR spectra of the products were assigned and reproduced to the corresponding literature. ^1H and ^{13}C NMR spectra were recorded using at ambient temperature on *J*EOL-ECX 600 operating at 600.17 MHz and 150.92 MHz and JEOL-ECX 400-2 operating at 399.78 MHz and 100.52 MHz respectively with tetramethylsilane as an internal standard. Abbreviations used in the NMR experiments: s, singlet; d, doublet; t, triplet; q, quartet; m, multiplet. GC-MS spectra were taken by SHIMADZU QP2010.

***tert*-Butyl benzoyl(phenyl)carbamate:**[25]

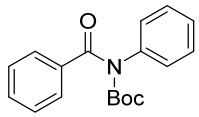

1ee

tert-Butyl benzoyl(phenyl)carbamate (**1ee**) was synthesized according to the experimental procedure presented in literature.[1] ^1H NMR (600.17 MHz, $CDCl_3$, TMS): δ 7.72 (d, *J* =10.26 Hz, 2H), 7.51 (t, *J* =11.34 Hz, 1H), 7.45-7.40 (m, 4H), 7.33 (t, *J* =10.93 Hz, 1H), 7.26 (d, *J* =11.70 Hz , 2H), 1.22 (s, 9H); ^{13}C NMR (150.92 MHz, $CDCl_3$, TMS) δ 172.73, 153.22, 139.0, 136.88, 131.64, 129.14 (C×2), 128.20 (C×2), 128.04 (C×2), 127.87 (C×2), 127.73, 83.42, 27.38 (C×3); GC-MS m/e: 297.15.

***N*-*tert*-Butoxycarbonyl-*N*-methylacetamide:**[42]

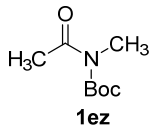

1ez

N-*tert*-Butoxycarbonyl-*N*-methylacetamide (**1ez**) was synthesized according to the experimental procedure provided in literature.[2] ^1H NMR (600.17 MHz, $CDCl_3$, TMS): δ 3.13 (s, 3H), 2.48 (s, 3H), 1.53 (s, 9H); ^{13}C NMR (150.92 MHz, $CDCl_3$, TMS) δ 172.99, 153.27, 82.95, 31.23, 28.01 (C×3), 26.76; GC-MS m/e: 173.05.

Phenyl benzoate:[4]

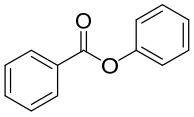

3a

^{1}H NMR (600.17 MHz, $CDCl_3$, TMS): δ 8.18 (d, *J* =6.84 Hz, 2H), 7.58 (t, *J* =7.56 Hz , 1H), 7.46 (t, *J* =7.92 Hz , 2H), 7.39 (t, *J* =6.87 Hz , 2H), 7.23 (t, *J* =7.56 Hz , 1H), 7.19 (d, *J* =7.56 Hz , 2H),; ^{13}C NMR (150.92 MHz, $CDCl_3$, TMS) δ 165.03, 150.84, 133.45, 130.02 (C×2), 129.36, 128.96 (C×2), 128.44 (C×2), 125.75, 121.59 (C×2); GC-MS m/e: 198.10.

Phenyl *p*-methylbenzoate:[4]

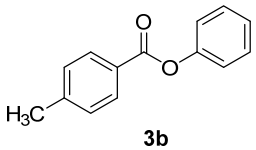

3b

^{1}H NMR (600.17 MHz, $CDCl_3$, TMS): δ 8.09 (d, *J* =8.22 Hz, 2H), 7.42 (t, *J* =8.22 Hz , 2H), 7.30 (d, *J* =7.56 Hz, 2H), 7.26 (t, *J* =7.20 Hz , 1H), 7.20 (d, *J* =7.56 Hz , 2H), 2.45 (s, 3H),; ^{13}C NMR (150.92 MHz, $CDCl_3$, TMS) δ 165.28, 151.04, 144.44, 130.19 (C×2), 129.44 (C×2), 129.26 (C×2), 126.81, 125.77, 121.75 (C×2), 21.75 ; GC-MS m/e: 212.10.

Phenyl *m*-methylbenzoate:[46]

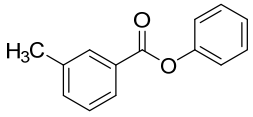

3c

^{1}H NMR (600.17 MHz, $CDCl_3$, TMS): δ 8.02 (s, 1H), 8.01 (d, *J* =8.01 Hz , 1H), 7.45-7.39 (m, 4H), 7.27 (t, *J* =7.92 Hz, 1H), 7.21 (d, *J* =8.01 Hz , 2H), 2.44 (s, 3H),; ^{13}C NMR (150.92 MHz, $CDCl_3$, TMS) δ 165.34, 150.96, 138.39, 134.34, 130.65, 129.46 (C×3), 128.44, 127.30, 125.83, 121.71 (C×2), 21.75 ; GC-MS m/e: 212.10.

Phenyl 4-(*tert*-butyl) benzoate:[47]

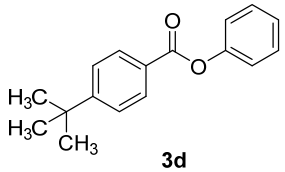

3d

^{1}H NMR (600.17 MHz, $CDCl_3$, TMS): δ 8.11 (d, *J* =13.02 Hz, 2H), 7.50 (d, *J* =13.02 Hz, 2H), 7.40 (t, *J* =12.0 Hz, 2H), 7.23 (t, *J* =5.85 Hz, 1H), 7.17 (d, *J* =10.32 Hz, 2H), 1.34 (s, 9H); ^{13}C NMR (150.92 MHz, $CDCl_3$, TMS) δ 165.24, 157.40, 150.96, 130.06 (C×2), 129.44 (C×2), 126.75, 125.77, 125.55 (C×2), 121.75 (C×2), 35.10, 31.11 (C×3); GC-MS m/e: 254.15.

Phenyl *p*-methoxybenzoate:[4]

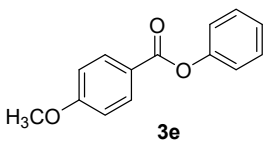

3e

^{1}H NMR (600.17 MHz, $CDCl_3$, TMS): δ 8.14 (t, *J* =8.94 Hz, 2H), 7.41 (t, *J* =7.89 Hz, 2H), 7.25

(t, *J* =7.56 Hz, 1H), 7.20 (t, *J* =8.94 Hz, 2H), 6.97 (d, *J* =8.94 Hz, 2H), 3.87 (s, 3H); ^{13}C NMR (150.92 MHz, $CDCl_3$, TMS) δ 165.24, 163.81, 151.00, 132.21 (C×2), 129.37 (C×2), 125.65, 121.79, 121.75 (C×2), 113.76 (C×2), 55.43; GC-MS m/e: 228.10.

Phenyl *p*-hydroxybenzoate:[48]

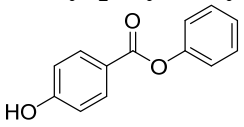

3f

^{1}H NMR (600.17 MHz, acetonitrile-d_3): δ 8.04 (d, *J* =10.32 Hz, 2H), 7.77 (s, 1H), 7.44 (t, *J* =8.25 Hz , 2H), 7.29 (t, *J* =7.56 Hz , 1H), 7.21 (d, *J* =8.28 Hz , 2H), 6.95 (d, *J* =8.94 Hz , 2H); ^{13}C NMR (150.91 MHz, acetonitrile-d_3) δ 165.84, 162.86, 152.25, 133.24 (C×2), 130.44 (C×2), 126.73, 122.98 (C×2), 122.01, 116.38 (C×2) ; GC-MS m/e: 214.05.

Phenyl *o*-hydroxybenzoate:[48]

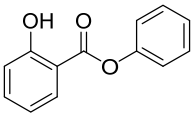

3g

^{1}H NMR (600.17 MHz, $CDCl_3$, TMS): δ 10.50 (s, 1H), 8.08 (d, *J* =11.64 Hz, 1H), 7.54 (t, *J* =11.67 Hz, 1H), 7.45 (t, *J* =11.01 Hz , 2H), 7.31 (t, *J* =10.98 Hz , 1H), 7.21 (d, *J* =11.70 Hz , 2H), 7.04 (d, *J* =13.08 Hz , 1H), 6.97 (t, *J* =11.67 Hz, 1H); ^{13}C NMR (150.91 MHz, acetonitrile-d_3) δ 168.78, 162.18, 149.57, 136.47, 130.34, 129.63 (C×2), 126.38, 121.63 (C×2), 119.46, 117.82, 111.83; GC-MS m/e: 214.05.

Phenyl *p*-aminobenzoate:[48]

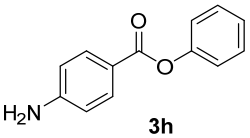

3h

^{1}H NMR (600.17 MHz, acetonitrile-d_3): δ 7.90 (d, *J* =8.94 Hz, 2H), 7.43 (t, *J* =7.56 Hz , 2H), 7.27 (t, *J* =7.20 Hz , 1H), 7.18 (d, *J* =7.56 Hz , 2H), 6.70 (d, *J* =8.28 Hz , 2H), 4.89 (s, 2H); ^{13}C NMR (150.91 MHz, acetonitrile-d_3) δ 166.14, 154.41, 152.47, 132.96 (C×2), 130.37 (C×2), 126.49, 123.08 (C×2), 117.91, 114.22 (C×2) ; GC-MS m/e: 213.10.

Phenyl *p*-fluorobenzoate:[49]

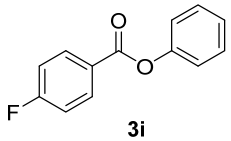

3i

^{1}H NMR (600.17 MHz, $CDCl_3$, TMS): δ 8.21 (d, *J* =8.94 Hz, 2H), 7.44 (t, *J* =7.56 Hz, 2H), 7.27 (t, *J* =7.56 Hz, 1H), 7.21-7.15 (m, 4H); ^{13}C NMR (150.92 MHz, $CDCl_3$, TMS) δ 166.09

(d, *J* =255.76 Hz), 164.15, 150.77, 132.74 (d, *J* =9.05 Hz; C×2), 129.48 (C×2), 125.94, 125.75, 121.61 (C×2), 115.74 (d, *J* =21.13 Hz; C×2) ; GC-MS m/e: 216.05.

Phenyl *p*-cholorobenzoate:[49]

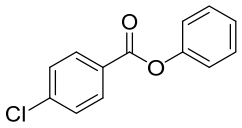

3j

^{1}H NMR (600.17 MHz, $CDCl_3$, TMS): δ 8.14 (d, *J* =8.22 Hz, 2H), 7.48 (d, *J* =8.22 Hz, 2H), 7.43 (t, *J* =7.92 Hz, 2H), 7.28 (t, *J* =7.56 Hz, 1H), 7.20 (d, *J* =8.22 Hz, 2H); ^{13}C NMR (150.92 MHz, $CDCl_3$, TMS) δ 164.32, 150.73, 140.09, 131.51 (C×2), 129.52 (C×2), 128.92 (C×2), 127.99, 126.02, 121.58 (C×2) ; GC-MS m/e: 232.05.

Phenyl *m*-fluorobenzoate:[46]

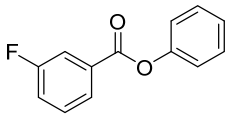

3k

^{1}H NMR (600.17 MHz, $CDCl_3$, TMS): δ 8.00 (d, *J* =8.94 Hz, 1H), 7.87 (d, *J* =8.94 Hz, 1H), 7.50-7.47(m, 1H), 7.43 (t, *J* =7.89 Hz, 2H), 7.33 (t, *J* =8.58 Hz, 1H), 7.28 (t, *J* =7.56 Hz, 1H), 7.20 (d, *J* =7.56 Hz, 2H); ^{13}C NMR (150.92 MHz, $CDCl_3$, TMS) δ 164.03, 162.58 (d, *J* =249.01 Hz) , 150.70, 131.70 (d, *J* =7.22 Hz), 130.22 (d, *J* =7.22 Hz), 129.53 (C×2), 126.08, 125.88, 121.55 (C×2), 120.67 (d, *J* =21.67 Hz), 117.01 (d, *J* =22.64 Hz); GC-MS m/e: 216.05.

Phenyl 1-naphthoate:[50]

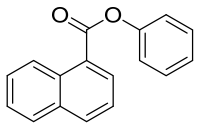

3l

^{1}H NMR (600.17 MHz, $CDCl_3$, TMS): δ 9.03 (d, *J* =8.88 Hz, 1H), 8.48 (d, *J* =6.18 Hz, 1H), 8.11 (d, *J* =7.56 Hz, 1H), 7.93 (d, *J* =7.56 Hz, 1H), 7.64 (t, *J* =7.23 Hz, 1H), 7.58 (t, *J* =7.89 Hz, 2H), 7.47 (t, *J* =9.00 Hz, 2H), 7.30 (t, *J* =7.20 Hz, 3H); ^{13}C NMR (150.92 MHz, $CDCl_3$, TMS) δ 165.82, 150.96, 134.31, 133.91, 131.68, 131.20, 129.55 (C×2), 128.67, 128.16, 126.40, 125.93, 125.84, 125.73, 124.51, 121.88 (C×2); GC-MS m/e: 248.10.

Phenyl 2-naphthoate:[49]

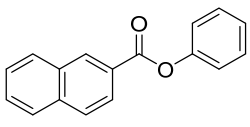

3m

^{1}H NMR (600.17 MHz, $CDCl_3$, TMS): δ 8.79 (s, 1H), 8.20 (d, *J* =10.32 Hz, 1H), 8.00 (d, *J*

=8.28 Hz, 1H), 7.95-7.91 (m, 2H), 7.63 (t, *J* =7.38 Hz, 1H), 7.57 (t, *J* =7.20 Hz, 1H), 7.45 (t, *J* =8.22 Hz, 2H), 57.30-7.24 (m, 3H); ^{13}C NMR (150.92 MHz, $CDCl_3$, TMS) δ 165.34, 151.02, 135.78, 132.47, 131.91, 129.51 (Cx2), 129.46, 128.60, 128.36, 127.82, 126.81, 126.74, 125.90, 125.44, 121.75 (Cx2); GC-MS m/e: 248.10.

Phenyl nicotinate:[51]

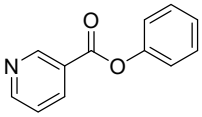

3n

^{1}H NMR (600.17 MHz, $CDCl_3$, TMS): δ 9.40 (s, 1H), 8.85 (t, *J* =6.84 Hz, 1H), 8.46-8.43 (m, 1H), 7.47-7.43 (m, 3H), 7.31-7.27 (m, 1H), 7.24 (d, *J* =7.56 Hz, 2H); ^{13}C NMR (150.92 MHz, $CDCl_3$, TMS) δ 163.79, 153.92, 151.30, 150.40, 137.48, 129.52 (C×2), 126.153, 125.49, 123.38, 121.46 (C×2) ; GC-MS m/e: 199.05.

Phenyl thiophene-2-carboxylate:[51]

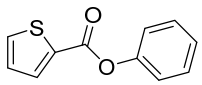

3o

^{1}H NMR (600.17 MHz, $CDCl_3$, TMS): δ 7.97 (d, *J* =3.42 Hz, 1H), 7.64 (d, *J* =6.00 Hz, 1H), 7.41 (t, *J* = 6.84 Hz, 2H), 7.26 (t, *J* = 7.56 Hz, 1H), 7.22 (d, *J* = 6.00 Hz, 2H), 7.16 (t, *J* = 6.18 Hz, 1H); ^{13}C NMR (150.92 MHz, $CDCl_3$, TMS) δ 160.55, 150.51, 134.63, 133.44, 132.85, 129.43 (C×2), 127.98, 125.94, 121.60 (C×2); GC-MS m/e: 204.05.

Phenyl furan-2-carboxylate:[4]

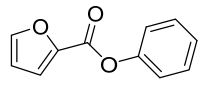

3p

^{1}H NMR (600.17 MHz, $CDCl_3$, TMS): δ 7.67 (s, 1H), 7.42 (t, *J* =7.56 Hz, 2H), 7.38 (d, *J* =3.48 Hz, 1H), 7.26 (t, *J* = 7.89 Hz, 1H), 7.21 (d, *J* = 8.22 Hz, 2H), 6.59 (d, *J* = 2.04 Hz, 1H); ^{13}C NMR (150.92 MHz, $CDCl_3$, TMS) δ 156.91, 150.14, 147.10, 143.97, 129.49 (C×2), 126.05, 121.57 (C×2), 119.40, 112.15; GC-MS m/e: 188.05.

Phenyl cinnamate:[51]

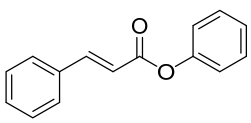

3q

^{1}H NMR (600.17 MHz, $CDCl_3$, TMS): δ 7.87 (d, *J* =18.01 Hz, 1H), 7.56 (t, *J* =4.71 Hz, 2H), 7.40-7.38 (m, 5H), 7.23 (t, *J* =7.56 Hz, 1H), 7.17 (d, *J* =8.28 Hz, 2H), 6.63 (d, *J* =15.78 Hz,

1H); ^{13}C NMR (150.92 MHz, $CDCl_3$, TMS) δ 165.31, 150.72, 146.49, 134.08, 130.63, 129.37 (C×2), 128.92 (C×2), 128.23 (C×2), 125.71, 121.58 (C×2), 117.22; GC-MS m/e: 224.10.

Phenyl (3r,5r,7r)-adamantane-1-carboxylate:[51]

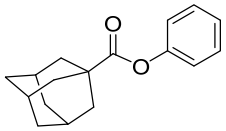

3r

^{1}H NMR (600.17 MHz, $CDCl_3$, TMS): δ 7.36 (t, *J* =7.89 Hz, 2H), 7.20 (t, *J* =7.20 Hz, 1H), 7.03 (d, *J* =7.56 Hz, 2H), 2.08-2.03 (m, 9H), 1.79-1.74 (m, 6H) ; ^{13}C NMR (150.92 MHz, $CDCl_3$, TMS) δ 165.82, 150.96, 134.31, 133.91, 131.68, 131.20, 129.55 (C×2), 128.67, 128.16, 126.40, 125.93, 125.84, 125.73, 124.51, 121.88 (C×2); GC-MS m/e: 256.15.

Phenyl pivalate:[4]

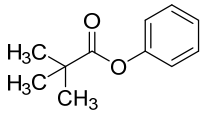

3s

^{1}H NMR (600.17 MHz, $CDCl_3$, TMS): δ 7.36 (t, *J* =7.92 Hz, 2H), 7.21 (t, *J* =7.56 Hz, 1H), 7.05 (d, *J* =7.56 Hz , 2H), 1.35 (s, 9H); ^{13}C NMR (150.92 MHz, $CDCl_3$, TMS) δ 177.07, 151.08, 129.31 (C×2), 125.53, 121.46 (C×2), 39.02, 27.11 (C×3) ; GC-MS m/e: 178.10.

Phenyl cyclohexanecarboxylate:[4]

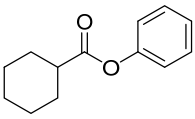

3t

^{1}H NMR (600.17 MHz, $CDCl_3$, TMS): δ 7.35 (t, *J* =8.94 Hz, 2H), 7.19 (t, *J* =7.56 Hz , 2H), 7.05 (d, *J* =7.56 Hz , 1H), 2.59-2.52 (m, 1H), 2.06 (d, *J* =10.98 Hz, 2H), 1.82-1.79 (m, 2H), 1.68 (d, *J* =12.0 Hz, 1H), 1.62-1.56 (m, 2H), 1.36 -1.28 (m, 3H); ^{13}C NMR (150.92 MHz, $CDCl_3$, TMS) δ 174.45, 150.82, 129.27 (C×2), 125.52, 121.59 (C×2), 43.11, 28.88, 25.66 (C×2), 25.29 (C×2); GC-MS m/e: 204.10.

Phenyl 2-(naphthalen-1-yl)acetate:[52]

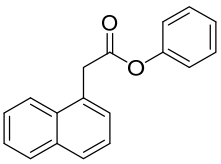

3u

^{1}H NMR (600.17 MHz, $CDCl_3$, TMS): δ 8.10 (d, *J* =8.28 Hz, 1H), 7.88 (t, *J* =7.56 Hz, 1H), 7.82 (d, *J* =8.28Hz, 1H), 7.57 (t, *J* =7.56 Hz, 1H), 7.51 (t, *J* =6.18 Hz, 2H), 7.46 (t, *J* =7.46 Hz, 1H), 7.31 (t, *J* =7.89 Hz, 2H), 7.18 (t, *J* =6.87 Hz, 1H), 7.091 (d, *J* =8.94 Hz, 2H), 4.30 (s, 2H);

^{13}C NMR (150.92 MHz, $CDCl_3$, TMS) δ 170.06, 150.69, 133.87, 132.07,130.02, 129.32, 128.81, 128.33, 128.17, 126.53 (Cx2), 125.87, 125.83, 125.52, 123.64, 121.39 (Cx2), 39.35; GC-MS m/e: 262.10.

Phenyl 2-phenylacetate:[52]

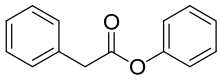

3v

^{1}H NMR (600.17 MHz, $CDCl_3$, 1 V/V% TMS): δ 7.41-7.33 (m, 6H), 7.30 (t, *J* =6.87 Hz , 1H), 7.21 (t, *J* =7.20 Hz , 1H), 7.05 (d, *J* =7.56 Hz , 2H), 3.86 (s, 2H); ^{13}C NMR (150.92 MHz, $CDCl_3$, TMS) δ 169.99, 150.70, 133.43, 129.36 (C×2), 129.28 (C×2), 128.71 (C×2), 127.31, 125.85, 121.42 (C×2), 41.42; GC-MS m/e: 212.08.

Phenyl stearate:[53]

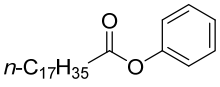

3w

^{1}H NMR (600.17 MHz, $CDCl_3$, TMS): δ 7.36 (t, *J* =7.89 Hz, 2H), 7.20 (t, *J* =7.56 Hz, 1H), 7.06 (d, *J* =8.22 Hz , 2H), 2.54 (t, *J* =7.56 Hz, 2H), 1.78-1.72 (m, 2H), 1.41-1.12 (m, 28H), 0.87 (t, *J* =6.87 Hz, 3H); ^{13}C NMR (150.92 MHz, $CDCl_3$, TMS) δ 172.26, 150.73, 129.33 (C×2), 125.63, 121.54 (C×2), 34.37, 31.91, 29.68, 29.64, 29.58 (C×2), 29.45 (C×2), 29.34 (C×2), 29.24 (C×2), 29.08 (C×2), 24.93, 22.67, 14.10 ; GC-MS m/e: 360.30.

Phenyl octanoate:[54]

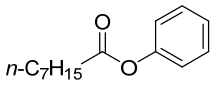

3x

^{1}H NMR (600.17 MHz, $CDCl_3$, 1 V/V %TMS): δ 7.35 (t, *J* =7.89 Hz, 2H), 7.20 (t, *J* =7.56 Hz, 1H), 7.06 (d, *J* =7.56 Hz , 2H), 2.53 (t, *J* =7.56 Hz, 2H), 1.77-1.70 (m, 2H), 1.43-1.28 (m, 8H), 0.89 (t, *J* =7.23 Hz, 3H); ^{13}C NMR (150.92 MHz, $CDCl_3$, TMS) δ 172.21, 150.70, 129.29 (C×2), 125.60, 121.51 (C×2), 34.32, 31.60, 29.00, 28.87, 24.88, 22.54, 14.00; GC-MS m/e: 220.15.

Phenyl butanoate:[55]

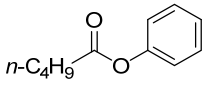

3y

^{1}H NMR (600.17 MHz, $CDCl_3$, 1 V/V %TMS): δ 7.35 (t, *J* =7.23 Hz, 2H), 7.20 (t, *J* =7.89 Hz, 1H), 7.06 (d, *J* =8.22 Hz , 2H), 2.54 (t, *J* =7.56 Hz, 2H), 1.74-1.70 (m, 2H), 1.45-1.42 (m, 2H), 0.96 (t, *J* =7.23 Hz, 3H); ^{13}C NMR (150.92 MHz, $CDCl_3$, TMS) δ 172.19, 150.68, 129.28 (C×2),

125.59, 121.49 (C×2), 34.01, 26.91, 22.15, 13.64; GC-MS m/e: 178.10.

Phenyl acetate:[56]

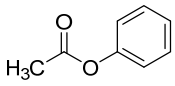

3z

^{1}H NMR (600.17 MHz, $CDCl_3$, TMS): δ 7.35 (t, *J* =8.92 Hz, 2H), 7.20 (t, *J* =7.56 Hz, 1H), 7.06 (d, *J* =7.56 Hz , 2H), 2.26 (s, 3H); ^{13}C NMR (150.92 MHz, $CDCl_3$, TMS) δ 169.33, 150.56, 129.29 (C×2), 125.69, 121.45 (C×2), 20.96; GC-MS m/e: 136.05.

***o*-Tolyl benzoate**:[46]

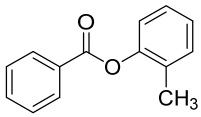

4a

^{1}H NMR (600.17 MHz, $CDCl_3$, TMS): δ 8.22 (d, *J* =6.90 Hz, 2H), 7.63 (t, *J* =8.25 Hz , 1H), 7.50 (t, *J* =7.92 Hz , 2H), 7.28-7.23 (m, 2H), 7.17 (t, *J* =6.63 Hz , 1H), 7.13 (d, *J* =8.22 Hz , 1H), 2.23 (s, 3H); ^{13}C NMR 150.92 MHz, $CDCl_3$, TMS) δ 164.80, 149.49, 133.52, 131.12, 130.25, 130.11 (C×2), 129.44, 128.56 (C×2), 126.94, 126.03, 121.95, 16.20 ; GC-MS m/e: 212.10.

***m*-Tolyl benzoate**:[18]

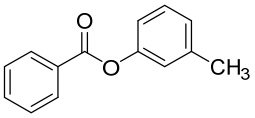

4b

^{1}H NMR (600.17 MHz, $CDCl_3$, TMS): δ 8.19 (d, *J* =7.56 Hz, 2H), 7.60 (t, *J* =7.56 Hz , 1H), 7.48 (t, *J* =7.89 Hz , 2H), 7.30-7.26 (m, 1H), 7.07 (d, *J* =7.56 Hz , 1H), 7.05 (t, *J* =7.23 Hz , 2H), 2.37 (s, 3H); ^{13}C NMR (150.92 MHz, $CDCl_3$, TMS) δ 165.20, 150.84, 139.59, 133.45, 130.07 (C×2), 129.58, 129.14, 128.48 (C×2), 126.62, 122.24, 118.58, 21.27 ; GC-MS m/e: 212.10.

***p*-Tolyl benzoate**[18]

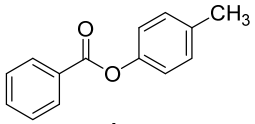

4c

^{1}H NMR (600.17 MHz, $CDCl_3$, TMS): δ 8.20 (d, *J* =6.84 Hz, 2H), 7.63 (t, *J* =7.56 Hz , 1H), 7.50 (t, *J* =7.89 Hz , 2H), 7.22 (d, *J* =8.28 Hz , 2H), 7.09 (d, *J* =8.28 Hz , 2H), 2.37 (s, 3H); ^{13}C NMR (150.92 MHz, $CDCl_3$, TMS) δ 165.37, 148.68, 135.50, 133.85, 130.14 (C×2), 129.98 (C×2), 129.66, 128.52 (C×2), 121.35 (C×2), 20.90; GC-MS m/e: 212.10.

***p*-Methoxyphenyl benzoate**:[4]

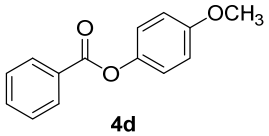

4d

^{1}H NMR (600.17 MHz, $CDCl_3$, TMS): δ 8.19 (d, *J* =6.90 Hz, 2H), 7.62 (t, *J* =7.56 Hz, 1H), 7.50 (t, *J* =7.92 Hz, 2H), 7.13 (d, *J* =9.60 Hz, 2H), 6.93 (d, *J* =8.88 Hz, 2H), 3.81 (s, 3H); ^{13}C NMR (150.92 MHz, $CDCl_3$, TMS) δ 165.51, 157.27, 144.36, 133.47, 130.10 (C×2), 129.59, 128.50 (C×2), 122.41 (C×2), 114.48 (C×2), 55.58; GC-MS m/e: 228.10.

4-Heptylphenyl benzoate:[57]

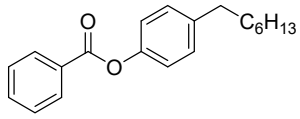

4e

^{1}H NMR (600.17 MHz, $CDCl_3$, TMS): δ 8.20 (d, *J* =13.02 Hz, 2H), 7.62 (t, *J* =9.27 Hz , 1H), 7.50 (t, *J* =11.67 Hz , 2H), 7.22 (d, *J* =12.36 Hz , 2H), 7.10 (d, *J* =13.08 Hz , 2H), 2.62 (t, *J* =11.67 Hz , 2H), 1.66-1.58 (m, 2H), 1.34-1.28 (t, *J* =10.65 Hz , 8H), 0.88 (t, *J* =10.32 Hz, 3H);^{13}C NMR (150.92 MHz, $CDCl_3$, TMS) δ 165.56, 148.73, 140.54, 133.46, 129.52, 130.12 (C×2), 129.31 (C×2), 128.51 (C×2), 121.28(C×2), 35.37, 31.80, 31.48, 29.23, 29.16, 22.66, 14.09; GC-MS m/e: 296.20.

4-(*tert*-Butyl)phenyl benzoate:[49]

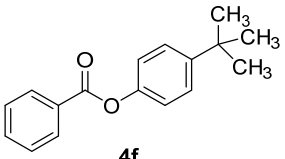

4f

^{1}H NMR (600.17 MHz, $CDCl_3$, TMS): δ 8.20 (d, *J* =7.56 Hz, 2H), 7.62 (t, *J* =7.56 Hz, 1H), 7.512 (t, *J* =7.56 Hz, 2H), 7.43 (d, *J* =8.22 Hz, 2H), 7.13 (d, *J* =8.28 Hz, 2H), 1.34 (s, 9H); ^{13}C NMR (150.92 MHz, $CDCl_3$, TMS) δ 165.33, 148.68, 148.56, 133.48, 130.14 (C×2), 129.68, 128.52 (C×2), 126.38 (C×2), 120.97 (C×2), 34.49, 31.42 (Cx3); GC-MS m/e: 254.05.

***p*-Phenylphenyl benzoate:**[47]

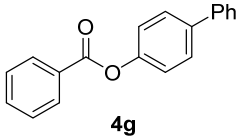

4g

^{1}H NMR (600.17 MHz, $CDCl_3$, TMS): δ 8.23 (d, *J* =6.90 Hz, 2H), 7.64 (d, *J* =8.28 Hz, 3H), 7.59 (d, *J* =7.56 Hz, 2H), 7.52 (t, *J* =7.56 Hz, 2H), 7.45 (t, *J* =7.56 Hz, 2H),7.36 (t, *J* =7.20 Hz, 1H), 7.29 (d, *J* =8.94 Hz, 2H); ^{13}C NMR (150.92 MHz, $CDCl_3$, TMS) δ 165.16, 150.01, 140.39, 139.01, 133.63, 130.19 (C×2), 129.49, 128.79 (C×2), 128.58 (C×2), 128.22 (C×2), 127.34,

127.13 (C×2), 121.97 (C×2); GC-MS m/e: 274.10.

***p*-Aminophenyl benzoate:**[58]

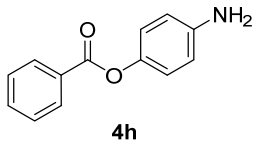

4h

^{1}H NMR (600.17 MHz, Methanol-D3, TMS): δ 7.90 (d, *J* =7.56 Hz, 2H), 7.55 (t, *J* =7.56 Hz, 1H), 7.49 (t, *J* =7.56 Hz, 2H), 7.44 (d, *J* =8.94 Hz, 2H), 6.78 (d, *J* =8.94 Hz, 2H), 4.88 (s, 2H); ^{13}C NMR (150.92 MHz, Methanol-D3) δ 167.73, 154.81, 135.36, 131.71, 130.55, 128.60 (C×2), 127.50 (C×2), 123.41(C×2), 115.23 (C×2); GC-MS m/e: 213.10.

***m*-Aminophenyl benzoate:**[58]

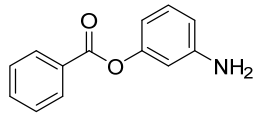

4i

^{1}H NMR (600.17 MHz, Methanol-D3, TMS): δ 7.90 (d, *J* =8.28 Hz, 2H), 7.56 (t, *J* =7.20 Hz, 1H), 7.50 (t, *J* =7.23 Hz, 2H), 7.30 (s, 1H), 7.15 (t, *J* =8.58 Hz, 1H), 7.09 (d, *J* =8.28 Hz, 1H), 6.59 (d, *J* =9.60 Hz, 1H), 4.89 (s, 2H); ^{13}C NMR (150.92 MHz, Methanol-D3, TMS) δ 167.93, 157.93, 140.11, 135.44, 131.81, 129.49, 128.61(C×2), 127.60(C×2), 112.39, 111.61, 108.43; GC-MS m/e: 213.10.

***p*-Fluorophenyl benzoate:**[22]

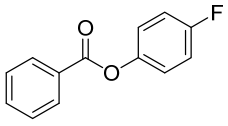

4j

^{1}H NMR (600.17 MHz, $CDCl_3$, TMS): δ 8.20 (d, *J* =8.22 Hz, 2H), 7.64 (t, *J* =6.87 Hz, 1H), 7.51 (t, *J* =7.56 Hz, 2H), 7.17 (t, *J* =7.92 Hz, 2H), 7.11 (t, *J* =7.12 Hz, 2H), ^{13}C NMR (150.92 MHz, $CDCl_3$, TMS) δ 165.19, 161.28 (d, *J* =244.48 Hz), 146.71, 133.71, 130.15 (C×3), 129.25, 128.59 (C×3), 123.10 (d, *J* =9.05 Hz), 116.13 (d, *J* =22.64 Hz); GC-MS m/e: 216.05.

***m*-Chlorophenyl benzoate:**[59]

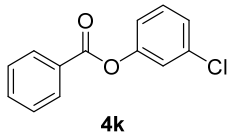

4k

^{1}H NMR (600.17 MHz, $CDCl_3$, TMS): δ 8.18 (d, *J* =8.22 Hz, 2H), 77.64 (t, *J* =6.87 Hz, 1H), 7.51 (t, *J* =7.92 Hz, 2H), 7.35 (t, *J* =8.31 Hz, 1H), 7.26 (d, *J* =6.90 Hz, 1H), 7.25 (s, 1H), 7.13 (d, *J* =6.84 Hz, 1H);^{13}C NMR (150.92 MHz, $CDCl_3$, TMS) δ 164.74, 151.38, 134.72, 133.81,

130.17 (C×3), 129.04, 128.61 (C×2), 126.15, 122.41, 120.12; GC-MS m/e: 232.05.

***p*-Bromophenyl benzoate:**[4]

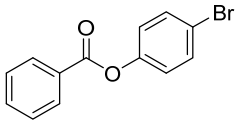

4l

^{1}H NMR (600.17 MHz, $CDCl_3$, TMS): δ 8.19 (d, *J* =7.56 Hz, 2H), 7.65 (t, *J* =7.20 Hz, 1H), 7.55-7.50 (m, 4H), 7.11 (d, *J* =6.84 Hz, 2H), ^{13}C NMR (150.92 MHz, $CDCl_3$, TMS) δ 164.86, 150.08, 133.80, 132.53 (C×2), 130.19 (C×2), 129.15, 128.63 (C×2), 123.53 (C×2), 118.98; GC-MS m/e: 276.0.

***p*-Acetylphenyl benzoate:**[60]

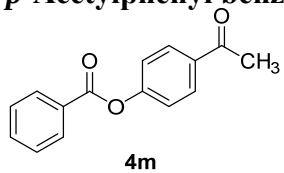

4m

^{1}H NMR (600.17 MHz, $CDCl_3$, TMS): δ 8.21 (d, *J* =6.90 Hz, 2H), 8.05 (d, *J* =8.28 Hz, 2H), 7.66 (t, *J* =8.22 Hz, 1H), 7.53 (t, *J* =7.56 Hz, 2H), 7.33 (d, *J* =8.94 Hz, 2H), 2.69 (s, 3H); ^{13}C NMR (150.92 MHz, $CDCl_3$, TMS) δ 190.90, 164.16, 154.66, 134.76, 133.92, 130.23 (C×2), 130.00 (C×2), 129.00, 128.66 (C×2), 121.92 (C×2), 26.63; GC-MS m/e: 240.10.

***p*-Trifluoromethylphenyl benzoate:**[4]

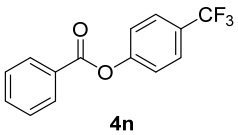

4n

^{1}H NMR (600.17 MHz, $CDCl_3$, TMS): δ 8.20 (d, *J* =8.22 Hz, 2H), 7.71 (d, *J* =8.94 Hz, 2H), 7.66 (t, *J* =7.56 Hz, 1H), 7.53 (t, *J* =8.58 Hz, 2H), 7.35 (d, *J* =8.94 Hz, 2H), ^{13}C NMR (150.92 MHz, $CDCl_3$, TMS) δ 164.65, 153.45, 133.96, 130.26 (C×2), 128.94, 128.69 (C×2), 128.17 (q, *J* =31.79 Hz), 126.86 (C×2) (q, *J* =4.34 Hz), 123.88 (q, *J* =271.65 Hz), 122.25 (C×2); GC-MS m/e: 266.05.

***p*-Nitrophenyl benzoate:**[18]

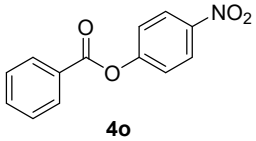

4o

^{1}H NMR (600.17 MHz, $CDCl_3$, TMS): δ 8.33 (d, *J* =8.94 Hz, 2H), 8.20 (d, *J* =8.28 Hz, 2H), 7.69 (t, *J* =7.56 Hz, 1H), 7.55 (t, *J* =7.89 Hz, 2H), 7.42 (d, *J* =8.94 Hz, 2H); ^{13}C NMR (150.92 MHz, $CDCl_3$, TMS) δ 164.24, 155.72, 145.41, 134.25, 130.34 (C×2), 128.79 (C×2), 128.52, 125.29 (C×2), 122.64 (C×2); GC-MS m/e: 243.10.

Naphthalen-1-yl benzoate:[22]

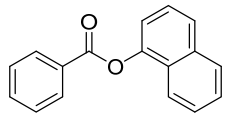

4p

^{1}H NMR (600.17 MHz, $CDCl_3$, TMS): δ 8.33 (d, *J* =6.84 Hz, 2H), 7.93 (d, *J* =8.28 Hz, 1H), 7.89 (d, *J* =8.94 Hz, 1H), 7.78 (d, *J* =8.22 Hz, 1H), 7.67 (t, *J* =6.08 Hz, 1H), 7.56 (t, *J* =7.89 Hz, 2H), 7.52-7.476 (m, 3H), 7.37 (d, *J* =7.56 Hz, 1H) ; ^{13}C NMR (150.92 MHz, $CDCl_3$, TMS) δ 165.17, 146.80, 134.68, 133.75, 130.29 (C×2), 129.36, 128.71 (C×2), 128.04, 126.96, 126.48, 126.45, 126.06, 125.45, 121.23, 118.22; GC-MS m/e: 248.10.

Naphthalen-2-yl benzoate:[22]

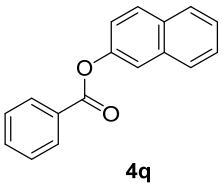

4q

^{1}H NMR (600.17 MHz, $CDCl_3$, TMS): δ 8.25 (d, *J* =8.22 Hz, 2H), 7.89 (d, *J* =8.94 Hz, 1H), 7.86 (d, *J* =7.56 Hz, 1H), 7.82 (d, *J* =7.56 Hz, 1H), 7.69 (s,1H), 7.64 (t, *J* =6.87 Hz, 2H), 7.54-7.46 (m, 3H), 7.36 (d, *J* =8.94 Hz, 1H) ; ^{13}C NMR (150.92 MHz, $CDCl_3$, TMS) δ 165.34, 148.57, 133.79, 133.63, 131.49, 130.19 (C×2), 129.53, 129.45, 128.58 (C×2), 127.78, 127.66, 126.55, 125.71, 121.22, 118.67; GC-MS m/e: 248.10.

Pyridin-4-yl benzoate:[61]

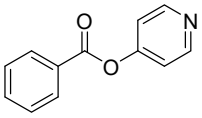

4r

^{1}H NMR (600.17 MHz, Methanol-D3, TMS): δ 8.44 (s, 2H), 7.95 (d, *J* =7.56 Hz, 2H), 7.84 (d, *J* =5.52 Hz, 2H), 7.61 (t, *J* =7.20 Hz, 1H), 7.53 (d, *J* =6.54 Hz, 2H); ^{13}C NMR (150.92 MHz, Methanol-D3, TMS) δ 168.27, 149.65 (C×2), 147.52, 134.66, 132.44 (C×2), 128.73 (C×2), 127.83 (C×2), 114.80; GC-MS m/e: 199.05.

2,6-Dimethylphenyl benzoate:[4]

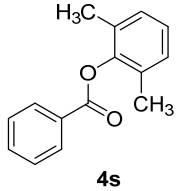

4s

^{1}H NMR (600.17 MHz, $CDCl_3$, TMS): δ 8.25 (d, *J* =6.90 Hz, 2H), 7.65 (t, *J* =7.89 Hz, 1H),

7.53 (t, *J* =8.25 Hz, 2H), 7.12-7.09 (m, 3H), 2.19 (s, 6H) ^{13}C NMR (150.92 MHz, $CDCl_3$, TMS) δ 164.41, 148.31, 133.55, 130.38, 130.15 (C×2), 129.28, 128.62 (C×3), 123.58 (C×2), 125.89, 16.37 (C×2); GC-MS m/e: 226.10.

3,5-Dimethylphenyl benzoate:[49]

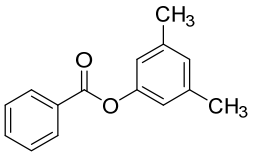

4t

^{1}H NMR (600.17 MHz, $CDCl_3$, TMS): δ 8.19 (d, *J* =7.56 Hz, 2H), 7.61 (t, *J* =7.23 Hz , 1H), 7.20 (t, *J* =7.20 Hz , 2H), 6.90 (s, 1H), 6.83 (s, 2H), 2.34 (s, 6H); ^{13}C NMR (150.92 MHz, $CDCl_3$, TMS) δ 165.35, 150.80, 139.30 (C×2), 133.43, 130.09 (C×2), 129.68, 128.49 (C×2), 127.60, 119.23 (C×2), 21.23 (C×2); GC-MS m/e: 226.10.

Mesityl benzoate:[51]

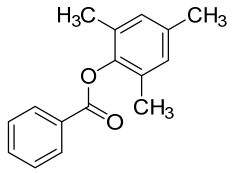

4u

^{1}H NMR (600.17 MHz, $CDCl_3$, TMS): δ 8.23 (d, *J* =7.56 Hz, 2H), 7.64 (t, *J* =7.56 Hz, 1H), 7.52 (t, *J* =7.56 Hz, 2H), 6.91 (s, 2H), 2.29 (s, 3H), 2.14 (s, 6H); ^{13}C NMR (150.92 MHz, $CDCl_3$, TMS) δ 164.53, 146.03, 135.32, 133.47, 130.13 (C×2) , 129.86 (C×2), 129.38, 129.23 (C×2), 128.56 (C×2), 20.78, 16.28 (Cx2); GC-MS m/e: 240.10.

2,4,6-Trichlorophenyl benzoate:[62]

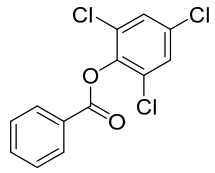

4v

^{1}H NMR (600.17 MHz, $CDCl_3$, TMS): δ 8.24 (d, *J* =8.22 Hz, 2H), 7.685 (t, *J* =7.56 Hz, 1H), 7.54 (t, *J* =7.89 Hz, 2H), 7.42 (s, 2H); ^{13}C NMR (150.92 MHz, $CDCl_3$, TMS) δ 162.95, 143.20, 134.26 (C×2),, 132.03, 130.56 (C×2), 129.79, 128.75 (C×2), 128.61 (C×2), 127.85; GC-MS m/e: 300.0.

4-Chloro-3,5-dimethylphenyl benzoate:

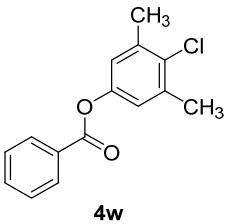

4w

^{1}H NMR (600.17 MHz, $CDCl_3$, TMS): δ 8.17 (d, *J* =13.08 Hz, 2H), 7.63 (t, *J* =11.34 Hz , 1H), 7.50 (t, *J* =11.70 Hz , 2H), 6.95 (s, 2H), 2.39 (s, 6H); ^{13}C NMR (150.92 MHz, $CDCl_3$, TMS) δ 165.14, 148.50, 137.52 (C×2), 133.64, 131.74, 130.14 (C×2), 129.41, 128.57 (C×2), 121.47 (C×2), 20.89 (C×2); GC-MS m/e: 260.05.

1,4-Phenylene dibenzoate:[63]

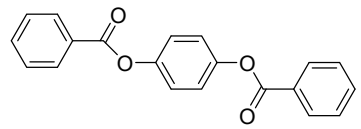

4x

^{1}H NMR (600.17 MHz, $CDCl_3$, TMS): δ 8.22 (d, *J* =8.22 Hz, 4H), 7.65 (t, *J* =7.20 Hz, 2H), 7.53 (t, *J* = 7.53 Hz, 4H), 2.19 (s, 4H); ^{13}C NMR (150.92 MHz, $CDCl_3$, TMS) δ 165.06(C×2), 148.51(C×2), 133.69 (C×2), 130.20 (C×4), 129.36(C×2), 128.52(C×4), 122.71(C×4); GC-MS m/e: 318.10.

5.5 Conclusion

In summary, we have developed a reusable catalytic method for the phenolysis of unactivated amides into the corresponding phenolic esters using CeO_2 as a catalyst. This catalytic system overcomes the typical stability issue of amides and phenols and thus offers a straightforward route to phenolic esters. This method is compatible with a wide range of substrates including various functionalized amides and phenols. A plausible mechanistic study suggests that the rate-determining step of the reaction proceeds via a negatively charged transition state, in which the phenoxide engages in a nucleophilic addition to the carboxylate species, followed by the transformation into the ester. Compared to previously reported catalytic methods for the phenolysis of activated amides, our method offers the following advantages: 1) catalyst reusability and easy catalyst/product separation, 2) a wide substrate scope including aryl, heteroaryl, ally, and alkyl amides as well as different homologues of phenols, and 3) a higher TON compared to those of the corresponding activated amides.

References

[1] A. Radzicka, R. Wolfenden, *J. Am. Chem. Soc.* **1996**, *118*, 6105–6109.

[2] H. Lundberg, F. Tinnis, N. Selander, H. Adolfsson, *Chem. Soc. Rev.* **2014**, *43*, 2714–2742.

[3] Y. Nishii, T. Hirai, S. Fernandez, P. Knochel, K. Mashima, *European J. Org. Chem.* **2017**, *2017*, 5010–5014.

[4] G. Li, P. Lei, M. Szostak, *Org. Lett.* **2018**, *20*, 5622–5625.

[5] D. M. Shendage, R. Fröhlich, G. Haufe, *Org. Lett.* **2004**, *6*, 3675–3678.

[6] P. L. Anelli, M. Brocchetta, D. Palano, M. Visigalli, *Tetrahedron Lett.* **1997**, *38*, 2367–2368.

[7] M. C. Bröhmer, S. Mundinger, S. Bräse, W. Bannwarth, *Angew. Chemie Int. Ed.* **2011**, *50*, 6175–6177.

[8] R. Karaman, *Comput. Theor. Chem.* **2011**, *963*, 427–434.

[9] L. Hie, N. F. Fine Nathel, T. K. Shah, E. L. Baker, X. Hong, Y.-F. Yang, P. Liu, K. N. Houk, N. K. Garg, *Nature* **2015**, *524*, 79–83.

[10] L. Hie, E. L. Baker, S. M. Anthony, J.-N. Desrosiers, C. Senanayake, N. K. Garg, *Angew. Chemie Int. Ed.* **2016**, *55*, 15129–15132.

[11] Y. Kita, Y. Nishii, T. Higuchi, K. Mashima, *Angew. Chemie Int. Ed.* **2012**, *51*, 5723–5726.

[12] Y. Kita, Y. Nishii, A. Onoue, K. Mashima, *Adv. Synth. Catal.* **2013**, *355*, 3391–3395.

[13] S. M. A. H. Siddiki, A. S. Touchy, M. Tamura, K. Shimizu, *RSC Adv.* **2014**, *4*, 35803–35807.

[14] T. Toyao, M. Nurnobi Rashed, Y. Morita, T. Kamachi, S. M. A. Hakim Siddiki, M. A. Ali, A. S. Touchy, K. Kon, Z. Maeno, K. Yoshizawa, et al., *ChemCatChem* **2019**, *11*, 449–456.

[15] H. Nagae, T. Hirai, D. Kato, S. Soma, S. Akebi, K. Mashima, *Chem. Sci.* **2019**, *10*, 2860–2868.

[16] P. Gautam, P. Kathe, B. M. Bhanage, *Green Chem.* **2017**, *19*, 823–830.

[17] P. J. Silva, *J. Org. Chem.* **2009**, *74*, 914–916.

[18] K. Subramanian, S. L. Yedage, B. M. Bhanage, *Adv. Synth. Catal.* **2018**, *360*, 2511–2521.

[19] A. A. Gami, M. Y. Shukor, K. A. Khalil, F. A. Dahalan, A. Khalid, S. A. Ahmad, *J. Environ. Microbiol. Toxicol.* **2014**, *2*, 11–24.

[20] M. Kumar, S. Bagchi, A. Sharma, *New J. Chem.* **2015**, *39*, 8329–8336.

[21] L. Zhang, G. Zhang, M. Zhang, J. Cheng, *J. Org. Chem.* **2010**, *75*, 7472–7474.

[22] Y. Tu, L. Yuan, T. Wang, C. Wang, J. Ke, J. Zhao, *J. Org. Chem.* **2017**, *82*, 4970–4976.

[23] W. Ren, A. Emi, M. Yamane, *Synthesis (Stuttg).* **2011**, *2011*, 2303–2309.

[24] L. Y. C. Xiuling, S. Shaofa, W. Minghu, W. Jian, G. Haibing, *Hubei Institute of Science And*, **2017**.

[25] Y. Bourne-Branchu, C. Gosmini, G. Danoun, *Chem. - A Eur. J.* **2017**, *23*, 10043–10047.

[26] L. Vivier, D. Duprez, *ChemSusChem* **2010**, *3*, 654–678.

[27] M. Tamura, K. Shimizu, A. Satsuma, *Chem. Lett.* **2012**, *41*, 1397–1405.

[28] M. Tamura, K. Tomishige, *Angew. Chemie - Int. Ed.* **2015**, *54*, 864–867.

[29] J. Paier, C. Penschke, J. Sauer, *Chem. Rev.* **2013**, *113*, 3949–3985.

[30] C. Yang, X. Yu, S. Heißler, P. G. Weidler, A. Nefedov, Y. Wang, C. Wöll, T. Kropp, J. Paier, J. Sauer, *Angew. Chemie - Int. Ed.* **2017**, *56*, 16399–16404.

[31] M. Kobune, S. Sato, R. Takahashi, *J. Mol. Catal. A Chem.* **2008**, *279*, 10–19.

[32] M. Honda, A. Suzuki, B. Noorjahan, K. I. Fujimoto, K. Suzuki, K. Tomishige, *Chem. Commun.* **2009**, 4596–4598.

[33] K. Tomishige, M. Tamura, Y. Nakagawa, *Chem. Rec.* **2018**, DOI 10.1002/tcr.201800117.

[34] S. Agarwal, X. Zhu, E. J. M. Hensen, B. L. Mojet, L. Lefferts, *J. Phys. Chem. C* **2015**, *119*, 12423–12433.

[35] T. Montini, M. Melchionna, M. Monai, P. Fornasiero, *Chem. Rev.* **2016**, *116*, 5987–6041.

[36] A. Rapeyko, M. J. Climent, A. Corma, P. Concepción, S. Iborra, *ACS Catal.* **2016**, *6*, 4564−4575.

[37] G. Vilé, D. Teschner, J. Pérez-ramírez, N. López, *Appl. Catal. B Environ.* **2016**, *197*, 299–312.

[38] A. Trovarelli, J. Llorca, *ACS Catal.* **2017**, *7*, 4716–4735.

[39] K. Werner, X. Weng, F. Calaza, M. Sterrer, T. Kropp, J. Paier, J. Sauer, M. Wilde, K. Fukutani, S. Shaikhutdinov, et al., *J. Am. Chem. Soc.* **2017**, *139*, 17608–17616.

[40] Z. Zhang, Y. Wang, J. Lu, J. Zhang, M. Li, X. Liu, F. Wang, *ACS Catal.* **2018**, *8*, 2635−2644.

[41] D. Stoian, F. Medina, A. Urakawa, *ACS Catal.* **2018**, *8*, 3181–3193.

[42] Y. Inamoto, Y. Kaga, Y. Nishimoto, M. Yasuda, A. Baba, *Org. Lett.* **2013**, *15*, 3452–3455.

[43] M. Tamura, S. M. A. Hakim Siddiki, K. Shimizu, *Green Chem.* **2013**, *15*, 1641.

[44] A. Popov, E. Kondratieva, J.-P. Gilson, L. Mariey, A. Travert, F. Maugé, *Catal. Today* **2011**, *172*, 132–135.

[45] T. Kamachi, S. M. A. H. Siddiki, Y. Morita, M. N. Rashed, K. Kon, T. Toyao, K. Shimizu, K. Yoshizawa, *Catal. Today* **2018**, *303*, 256–262.

[46] J. Chen, Y. Peng, M. Liu, J. Ding, W. Su, H. Wu, *Adv. Synth. Catal.* **2012**, *354*, 2117–2122.

[47] J. S. Ruso, N. Rajendiran, R. S. Kumaran, *Tetrahedron Lett.* **2014**, *55*, 2345–2347.

[48] H. N. Roy, A. H. Al Mamun, *Synth. Commun.* **2006**, *36*, 2975–2981.

[49] S. Chun, Y. K. Chung, *Org. Lett.* **2017**, *19*, 3787–3790.

[50] S. R. Joo, Y. J. Youn, Y. R. Hwang, S. H. Kim, *Synlett* **2017**, *28*, 2665–2669.

[51] T. Dohi, D. Koseki, K. Sumida, K. Okada, S. Mizuno, A. Kato, K. Morimoto, Y. Kita, *Adv. Synth. Catal.* **2017**, *359*, 3503–3508.

[52] J. X. Xu, X. F. Wu, *Org. Lett.* **2018**, *20*, 5938–5941.

[53] O. Kreye, M. A. R. Meier, *RSC Adv.* **2015**, *5*, 53155–53160.

[54] J. E. Won, H. K. Kim, J. J. Kim, H. S. Yim, M. J. Kim, S. B. Kang, H. A. Chung, S. G. Lee, Y. J. Yoon, *Tetrahedron* **2007**, *63*, 12720–12730.

[55] R. Murashige, Y. Hayashi, S. Ohmori, A. Torii, Y. Aizu, Y. Muto, Y. Murai, Y. Oda, M. Hashimoto, *Tetrahedron* **2011**, *67*, 641–649.

[56] F. Rajabi, R. Luque, *Catal. Commun.* **2014**, *45*, 129–132.

[57] L. E. E. Pyman, **1926**, 280–291.

[58] R. Horikawa, C. Fujimoto, R. Yazaki, T. Ohshima, *Chem. - A Eur. J.* **2016**, *22*, 12278–12281.

[59] C. K. Lee, J. S. Yu, H. J. Lee, *J. Heterocycl. Chem.* **2002**, *39*, 1207–1217.

[60] H. X. Liu, Y. Q. Dang, Y. F. Yuan, Z. F. Xu, S. X. Qiu, H. B. Tan, *Org. Lett.* **2016**, *18*, 5584–5587.

[61] F. Effenberger, A. O. Mück, E. Bessey, *Chem. Ber.* **1980**, *113*, 2086–2099.

[62] Z. Liu, Q. Ma, Y. Liu, Q. Wang, *Org. Lett.* **2014**, *16*, 236–239.

[63] W. Ren, A. Emi, M. Yamane, *Synthesis (Stuttg).* **2011**, 2303–2309.

Chapter 6

General Conclusions

In this research, I have invented the reason, for which the Lewis acid-base catalyzed transformations of carboxylic acid derivatives support the hypothesis and showed that water and base tolerant truly Lewis acid catalyst is more effective to overcome the drawbacks for transformation of carboxylic acid derivatives in presence of hard bases. So, a new water and base tolerant heterogeneous Lewis acidic catalytic system with different Nb_2O_5 catalysts is developed for this transformation. Additionally, CeO_2 acid-base catalysis has been found more effective for amide's transformation instead of only Lewis acid catalyst. The present catalytic system does not require high catalyst loading which increases the atom economy and showed higher turnover numbers than previous Lewis acid-base catalytic methods for these reactions. These newly developed simple, atom-efficient and environmentally benign method provide a practical and convenient route to synthesize various acid derivatives from readily available starting materials carboxylic acids and amides with a broad range of substrate scopes.

Chapters 2, 3 conclude that a solid Lewis acid, Nb_2O_5, effectively catalyzes three challenging reactions of carboxyl acids derivatives: 1) direct intramolecular dehydration of dicarboxylic acids, 2) hydrolysis of amides to carboxylic acids, 3) amidation of carboxylic acids with NH_3. The key feature in these catalytic systems is the activation of carbonyl group (soft base) even in presence of hard bases (H_2O and NH_3). Moreover, during preparation of different the Nb_2O_5 catalysts, the Lewis acid (LA) sites of Nb_2O_5 catalysts and interaction between LA sites and carbonyl group decreased with the calcination temperature. Low temperature calcined Nb_2O_5 (TT and/or T-Nb_2O_5 phases) are more reactive than that of high temperature calcined M- and/or H-Nb_2O_5 phases.

Chapters 4, 5 conclude that CeO_2 promotes two catalytic transformation of amides, 1) esterification reaction of tertiary amides by alcohols and 2) phenolysis of amides, which have been unprecedented by previous heterogeneous catalysts. The key step in these catalytic systems is cooperation of Ce (IV) Lewis acid sites (for coordination of carbonyl oxygen) and adjacent basic oxygen (nucleophilic oxygen).

Mechanistic and kinetic studies have been performed for CeO_2 catalyzed reactions which suggested that the Lewis acid-base sites of CeO_2 is more efficient than that of truly Lewis acid catalyst Nb_2O_5 in the transformation of amides. These heterogeneous Lewis acid-base catalysts can be applied to other reactions involving activation of carbonyl groups in the presence of hard bases.

Acknowledgements

Firstly, I would like to express my sincere gratitude to my advisor Professor Kenichi Shimizu for the continuous support of my PhD study and related research, for his patience, motivation, and immense knowledge. His guidance helped me in all the time of research and writing of this thesis. I could not have imagined having a better advisor and mentor for my PhD study. I am truly thankful for his constant enthusiasm with the various projects I have been involved in during my PhD and for giving me the opportunity to pursue the areas of chemistry that have taken my interest over the course of the whole time.

I also would like to thank Specially appointed Asst. Prof. S.M.A. Hakim Siddiki and Asst. Prof. Takashi Toyao for their kind assistance on experiments and discussion and their insightful comments and encouragement throughout. My Thankfulness also extended to Professor Junya Hasegawa, Associate Professor Shinya Furukawa and specially appointed Lecturer Maeno Zen for their kind help and co-operation. Their help has made my research work more understandable.

I would like to remember the kind assistance of all our technical staffs in ICAT, Hokkaido University during handling of analytical instruments and thankful for their continuous help.

I am also grateful to Dr. Abeda Sultana Touchy, and Dr. Ken-ichi Kon & Mr. Wataru Onodera for their kind support and co-operation.

I thank my fellow lab mates for the stimulating discussions, for the sleepless nights we were working together before deadlines, and for all the fun we have had in the last three years.

Finally, a huge thanks to my parents and my family, without their love and dedication I would not be where I am or who I am today.

Md. Nurnobi Rashed